

THE EFFECT OF ALCOHOLIC SOLUTIONS ON THE THERMO-MECHANICAL
PROPERTIES OF POLY (LACTIC ACID)

By

Dian Xu

A THESIS

Submitted to
Michigan State University
in partial fulfillment of the requirements
for the degree of

Packaging—Master of Science

2021

ABSTRACT

THE EFFECT OF ALCOHOLIC SOLUTIONS ON THE THERMO-MECHANICAL PROPERTIES OF POLY (LACTIC ACID)

By

Dian Xu

The effects of aqueous and deuterium oxide solutions of straight-chain alcohols with one to four carbon atoms on the thermo-mechanical properties of poly(lactic acid) – PLA – films were assessed by dynamic mechanical analysis (DMA). The glass transition temperature (T_g) of PLA films immersed in 25%, 50%, 75%, and 100% (v/v) alcoholic solutions were compared with the T_g 's of films immersed in 100% HPLC water and deuterium oxide. The T_g 's of PLA films immersed in methanol and ethanol (one to two carbon atoms) aqueous solutions decreased as the concentration of the alcohol solutions increased. For methanol and ethanol, the T_g 's decreased by 8.6 °C and 7.6 °C per every 25% (v/v) increase of alcohol, respectively. When the PLA films were immersed in alcohol solutions with three to four carbon atoms, the T_g 's reduced until 75% (v/v). T_g 's of PLA films immersed in 1-propanol and 2-propanol decreased by 8.6 °C and 8.9 °C for every 25% increase of propanol, respectively. Aqueous and deuterium oxide solutions had similar effects on T_g . The sorption amount of ethanol in PLA films at 40 °C was measured by quantitative proton nuclear magnetic resonance (^1H -qNMR). PLA films experienced the most significant sorption amount of ethanol (9.16%) at 4 h of immersion. The crystallinity (X_c) of PLA immersed in ethanol in the first 12 h, was less than 3%. When the time reached 24 h, the X_c exceeded 20%, and after 48 h stabilized at about 30% meanwhile the ethanol sorption stabilized at around 5%. The results of this work help in the development of PLA films needed to be in contact with aqueous-alcoholic solutions.

Copyright by
DIAN XU
2021

This thesis is dedicated to my family and friends.

ACKNOWLEDGMENTS

Throughout the process of writing this thesis, I received a lot of support and guidance from the people below.

I would first like to thank my advisor, Dr. Rafael Auras, who taught me a lot of research knowledge and allowed me to be more rigorous in studying and writing, which is very helpful for maintaining a good learning attitude. I want to extend my sincere thanks to my committee member, Dr. Maria Rubino; her courses are very enlightening, primarily instrumental analysis; that course was beneficial to my experiment. Anytime when I have questions, she would be very patient in answering them. I would also like to thank Dr. Loong-Tak Lim; he gave many great suggestions for my research, which were very helpful. I am grateful for all their help. Besides, I also wish to thank Dr. Uruchaya Sonchaeng. She taught me to do experiments in my first year of graduate school. She was very meticulous and patient. She always followed my research progress and gave many suggestions for my thesis. Many thanks to Wan, who has provided me with a lot of help in experiments and made my writing process more enjoyable. I also enjoyed working with the RAA research group members, Narisara, Anibal, Pooja, and Carlos. I would also like to present my thanks to Shiyuan, Kexin, Haoyang, Hailin, Shoue, and Heyu; they are all very kind. I gratefully acknowledge the assistance of Aaron; he helped me adjust the equipment many times and taught me how to use them patiently. Finally, I would like to express my most profound appreciation to my parents, cousins, and grandma. Without their support, I would not be able to complete this thesis. I am very grateful for their encouragement and trust.

TABLE OF CONTENTS

LIST OF TABLES	viii
LIST OF FIGURES	x
KEY TO ABBREVIATIONS	xiv
CHAPTER 1 Introduction	1
1.1 Background and motivation	1
1.2 Overall goal and objectives	4
REFERENCES	5
CHAPTER 2 Literature Review	9
2.1 Introduction of PLA	9
2.2 Production of PLA	11
2.3 PLA properties	13
2.3.1 Structure-property relationship PLA	13
2.3.1.1 Chain and nanophase structure	13
2.3.1.2 Crystal structure	15
2.3.1.3 Glass transition temperature	17
2.3.2 Properties of PLA affected by alcohol exposure	19
2.3.2.1 Solubility	19
2.3.2.2 Degree of swelling	23
2.3.2.3 Diffusion and permeation	26
2.3.2.4 Crystal structure and crystallinity	28
2.3.3 Factors affecting changes of thermo-mechanical properties during <i>in-situ</i> immersion	33
2.3.3.1 Solvent molecular sizes	33
2.3.3.2 Solvent concentration	34
2.3.3.3 Branching of molecules	35
2.4 Applications of PLA in packaging	36
REFERENCES	38
CHAPTER 3 Experimental	51
3.1 Materials	51
3.2 Methods	54
3.2.1 PLA film production	54
3.2.1.1 Cast film	54
3.2.1.2 Production of PLA amorphous film	55
3.2.2 Thermo-mechanical property measurements	56
3.2.2.1 Dynamic mechanical analysis (DMA)	56
3.2.2.2 Parameter estimation: Flory-Huggins (FH) model	59
3.2.2.3 Differential scanning calorimeter (DSC)	63

3.2.3 Sorption of alcohol solvents	65
3.2.3.1 Nuclear magnetic resonance (NMR).....	65
3.2.3.2 Vapor sorption analysis.....	68
3.2.4 Statistical analysis.....	68
REFERENCES.....	69
CHAPTER 4 Results and Discussion.....	72
4.1 Thermal properties of pre-immersion PLA film	72
4.2 Thermal properties of immersed PLA film	76
4.2.1 T_g reduction of PLA immersed in pure alcohols	76
4.2.2 Modeling relationship between pure alcohols and T_g changes of PLA.....	80
4.2.3 Effect of alcohol solution concentrations on T_g	82
4.2.4 Solubility of PLA in alcohols determined by HSP	92
4.3 Sorption amounts of alcohols in PLA films.....	99
4.3.1 Basic information about $^1\text{H-NMR}$ spectrum of PLA	99
4.3.2 Sorption amount of pure ethanol in PLA films	101
4.3.3 Sorption isotherm of PLA with water and D_2O	106
APPENDICES	109
APPENDIX A: One-way ANOVA results of T_g of PLA immersed in pure alcohols.....	110
APPENDIX B: T1 measurement for quantitative NMR test.....	116
APPENDIX C: Sorption isotherm for H_2O vapor in PLA films.....	117
REFERENCES.....	118
CHAPTER 5 Conclusions	121
5.1 Overall conclusions	121
5.2 Future work	123
REFERENCES.....	124

LIST OF TABLES

Table 2.1 Crystal forms and chain conformations of PLA.	16
Table 2.2 Crystal forms, size of lattice, crystallization temperature and melting temperature of PLA.	17
Table 3.1 Properties of alcohols used for immersion tests.....	51
Table 3.2 Product information of solvents used for immersion tests.....	52
Table 3.3 HSP (δ) and adjusted HSP (δ^*) of PLA and alcohols.....	60
Table 3.4 The mix HSP (δ') of alcohol-aqueous solution for PLA. The HSP parameters of PLA (target materials) was [$\delta_d = 17.4$, $\delta_h = 5.9$, $\delta_p = 6.1$]; adapted from [3,9,10].....	62
Table 3.5 Quantitative NMR parameters.....	66
Table 3.6 Chemical shifts in $^1\text{H-NMR}$ spectrum (Solvent: CDCl_3).....	67
Table 4.1 Thermal parameters of original and hot-pressed PLA films.	75
Table 4.2 T_g of PLA films immersed in different solvents as tested by DMA.....	77
Table 4.3 Fox equation parameters and estimate solvent weight fraction.	81
Table 4.4 Hansen solubility parameters and interaction parameters at 25 °C.	93
Table 4.5 Hansen solubility parameters and interaction parameters at T_g	94
Table 4.6 Hansen solubility parameters of mixture at T_g	95
Table 4.7 $^1\text{H-qNMR}$ compound group and chemical shifts of ethanol in PLA.	100
Table 4.8 Results of melting, crystallization and glass transition temperature of PLA film immersed in pure ethanol from DSC tests.....	104
Table A1 One-way ANOVA table (The GLM Procedure).....	110

Table A2 LS-means of T_g of PLA immersed in pure alcohols.....	110
Table A3 Tukey grouping results.....	111
Table A4 Differences of alcohol least square means table.....	112

LIST OF FIGURES

Figure 2.1 Life cycle of PLA and its products, adapted from [2,6,12].....	10
Figure 2.2 The synthesis routes of high molecular weight PLA, adapted from [12,18,23].	13
Figure 2.3 Schematic representation of crystalline lamella, rigid amorphous fraction, and mobile amorphous fractions in spherulite, adapted from [32–36].	14
Figure 2.4 Polymer solubility graph based on the Hansen parameter system. RED represents the relative energy difference, R_p is the interaction radius. Adapted from [64,68,69].	22
Figure 2.5 The molecular interaction between hydroxyl groups in alcohol-aqueous solution, adapted from [77,78]......	25
Figure 2.6 Difference between vapor-induced and solvent-induced crystallization, figure adapted from [43].	29
Figure 2.7 Schematic diagram of the structural evolution of solvent-induced PLA films, adapted from [90,91].	31
Figure 2.8 The stages of solvent-induced crystallization in polymers, adapted from [91,94,97].	33
Figure 2.9 Hydrolysis of PLA, adapted from [103].	35
Figure 2.10 The chemical structures of 1-propanol and 2-propanol.	36
Figure 3.1 Structure of alcohols used in immersion tests.	52
Figure 3.2 Structure of hexamethylcyclotrisiloxane, (a) chemical structure (b) 3-D chemical structure, adapted from [4].	53
Figure 3.3 Production of PLA film.	54
Figure 3.4 Hot pressing process of PLA film.	55

Figure 3.5 Dry system and immersion system of DMA. (a) Dry system, (b) Immersion system.....	57
Figure 3.6 Typical pre-immersion (dry) test results of PLA film from DMA, adapted from [3]. T_g is the glass transition temperature of PLA film. The scaling type of $\tan(\delta)$ and dynamic modulus are linear and log base 10, respectively.	58
Figure 3.7 HSP of solvents mixture. R_{a1} is the HSP distance between solvent 1 and polymer, R_{a2} is the HSP distance between solvent 2 and polymer, and R_a' is the HSP distance of the mixture.	60
Figure 3.8 A typical pre-immersion (dry) test result of PLA film from DSC, adapted from [3]. T_g denotes glass transition temperature, T_c is crystallization temperature, T_m is melting point.....	64
Figure 4.1 DMA test results of PLA pre-immersion samples: (a) $\tan \delta$ curves; (b) Storage modulus curves.	73
Figure 4.2 DSC test results of original PLA sample (i.e., without hot pressing).....	74
Figure 4.3 DSC test results of pre-immersion hot-pressed PLA sample (control).	76
Figure 4.4 $\tan \delta$ (bottom) and storage modulus (top) of the PLA films immersed in different alcohols as a function of temperature.....	78
Figure 4.5 Changes in the T_g values of the <i>in-situ</i> immersed PLA films in aliphatic (circle markers, showing average values and standard deviation bars) from the T_g of dry PLA (horizontal dash line) as a function of number of carbons of the solvent chains. Values shown above the circle markers are percent T_g reduction in Celsius from the T_g of dry PLA.	79
Figure 4.6 Predicted T_g of PLA film immersed in pure alcohols and water versus solvent weight fraction [6]. C1-C4 denote the carbon number in the main chain of alcohols and C3b indicates 2-propanol.	80
Figure 4.7 (a) $\tan \delta$ of PLA film in methanol-aqueous solution as a function of temperature (b) T_g of immersed PLA versus the concentration of methanol-aqueous solution.....	82
Figure 4.8 (a) $\tan \delta$ of PLA film in ethanol-aqueous solution as a function of temperature (b) T_g of immersed PLA versus the concentration of ethanol-aqueous solution.....	83

Figure 4.9 (a) $\tan \delta$ of PLA film in 1-propanol-aqueous solution as a function of temperature (b) T_g of immersed PLA versus the concentration of 1-propanol-aqueous solution..... 84

Figure 4.10 (a) $\tan \delta$ of PLA film in 2-propanol-aqueous solution as a function of temperature (b) T_g of immersed PLA versus the concentration of 2-propanol-aqueous solution..... 85

Figure 4.11 (a) $\tan \delta$ of PLA film in 1-butanol-aqueous solution as a function of temperature (b) T_g of immersed PLA versus the concentration of 1-butanol-aqueous solution..... 85

Figure 4.12 Reduction of T_g of PLA immersed in different alcohol-aqueous solutions. 86

Figure 4.13 (a) $\tan \delta$ of PLA film in methanol-D₂O solution as a function of temperature (b) T_g of immersed PLA versus the concentration of methanol-D₂O solution. 87

Figure 4.14 (a) $\tan \delta$ of PLA film in ethanol-D₂O solution as a function of temperature (b) T_g of immersed PLA versus the concentration of ethanol-D₂O solution. 87

Figure 4.15 (a) $\tan \delta$ of PLA film in propanol-D₂O solution as a function of temperature (b) T_g of immersed PLA versus the concentration of 1-propanol-D₂O solution..... 88

Figure 4.16 (a) $\tan \delta$ of PLA film in 2-propanol-D₂O solution as a function of temperature (b) T_g of immersed PLA versus the concentration of 2-propanol-D₂O solution..... 88

Figure 4.17 (a) $\tan \delta$ of PLA film in 1-butanol-D₂O solution as a function of temperature (b) T_g of immersed PLA versus the concentration of 1-butanol-D₂O solution..... 89

Figure 4.18 T_g of PLA immersed in alcohol-aqueous solutions as a function of alcohol concentration..... 90

Figure 4.19 T_g of PLA immersed in alcohol-D₂O solutions as a function of alcohol concentration..... 91

Figure 4.20 Hansen solubility parameters 3D plot of PLA, water and alcohols (C1-C4) at T_g . PLA HSP data adapted from reference [9]. The x-axis, y-axis, and z-axis represent the dispersion (δ_d), polar (δ_p), and hydrogen bonding (δ_h), respectively. The light blue square represents the 75% (v/v) methanol-aqueous solution, and red squares denote the water (1% soluble) and alcohols. Letter a, b and c indicate 1-propanol, 2-propanol and 1-butanol, respectively. The green dash line indicates the HSP distance. The original HSP data of PLA is from reference [9], and it was adjusted

to the temperature where the T_g of PLA was observed in the <i>in-situ</i> immersion DMA test by using Eq. (3.3) – (3.5).....	92
Figure 4.21 T_g of PLA film as a function of Flory-Huggins interaction parameter.	97
Figure 4.22 The ^1H -qNMR result of the PLA film immersed in pure ethanol (Immersion time: 72h).	99
Figure 4.23 ^1H -qNMR results of PLA immersed in pure ethanol for 0h to144h.	100
Figure 4.24 Commonly observed splitting patterns in ^1H -NMR spectrum. J denotes coupling constant.	101
Figure 4.25 Ethanol sorption in PLA samples as a function of immersion time at 25 °C.	102
Figure 4.26 Percent crystallinity of PLA film immersed in ethanol versus immersion time at 25 °C.	102
Figure 4.27 Relationship between ethanol sorption amount (left y-axis), percent crystallinity (right y-axis) and the immersion time.	103
Figure 4.28 DSC results for amorphous PLA with different immersion time in pure ethanol at 25 °C (first heat run).	105
Figure 4.29 Sorption isotherm curve of PLA film in H_2O at 25 °C.	107
Figure 4.30 Sorption isotherm curve of PLA film in D_2O at 25 °C.	108
Figure A1 Distribution plot of T_g of PLA.	113
Figure A2 Fit diagnostics plots for T_g of PLA.	114
Figure A3 The differences comparisons of T_g for alcohol.	115
Figure B1 T1 measurement for quantitative NMR experiment.	116
Figure C1 Sorption isotherm for water vapor in PLA films at 40 °C.	117

KEY TO ABBREVIATIONS

ANOVA	Analysis of variance
DMA	Dynamic mechanical analysis
DSC	Differential scanning calorimeter
EFPs	Environmental footprints
FTIR-ATR	Fourier transform infrared-attenuated total reflectance
HDPE	High-density polyethylene
¹ H-qNMR	Proton quantitative nuclear magnetic resonance
HSP	Hansen solubility parameter
LA	Lactic acid
LCA	Life cycle assessment
LDPE	Low-density polyethylene
MAF	Mobile amorphous fraction
M_n	Number average molecular weight
NMR	Nuclear magnetic resonance
PC	Polycarbonate
PET	Polyethylene terephthalate
PLA	Poly(lactic acid)
PP	Polypropylene
PS	Polystyrene
QAC	Organomodifier, surfactant
RAF	Rigid amorphous fraction

ROP	Ring-opening polymerization
T_c	Cold crystallization temperature
T_g	Glass transition temperature
T_m	Melting temperature
X_c	Degree of crystallinity
ΔH_m	Heat of fusion

CHAPTER 1 Introduction

1.1 Background and motivation

During the last several decades, to achieve energy saving, environmental footprint reduction, and increase the recycling rate of plastic products, the research of bio-based polymers has been gradually developed. Focusing on the packaging field, not only the effective re-using or recycling of plastics, such as polyolefins (high-density polyethylene (HDPE), low-density polyethylene (LDPE), and polypropylene (PP)) and poly(ethylene terephthalate) (PET) but also the use of novel renewable materials can play a significant role in reducing the burden of plastics on the environment [1–6].

Among these renewable and biodegradable polymers, poly(lactic acid) -PLA- has become a highly sought and widely used material able to be recycled to its monomers and reduce the consumption of non-renewable resources [7,8]. As a compostable polymer with one of the lowest environmental footprints per kilogram of resin, PLA can be completely industrial composted to CO₂ and water by the action of microorganisms in the environment [9–11]. PLA has been used in many fields including food packaging, biomedicine, and agriculture. But its properties are easily affected by environmental conditions such as temperature and humidity. To expand PLA's potential applications, research on PLA has been focused on areas such as the synthesis and characterization of PLA's blends or composites as they can present better thermal stability, higher mechanical strength, and be more resistant to hydrolysis compared to the neat PLA [12–16].

Furthermore, in the field of food packaging, some studies have shown that organic substances such as aroma compounds can interact with food packaging materials such

as polyolefins, polycarbonate (PC), and PET as well as PLA and change their properties and performance. These interactions can cause the swelling or plasticization of polymers, thereby reducing the performance of the packaging and affecting the shelf life of the product [17–20]. Similarly, the sorption of organic vapors (ethanol, 1-propanol, and 2-propanol) on the PLA film can cause vapor-induced crystallization [21]. In addition, solvent-induced crystallization can also be observed on PLA film immersed in a liquid organic solvent. For example, Sato et al. [22] investigated the effects of organic solvents on PLA film by using the Hansen solubility parameter (HSP) and found that PLA films immersed in some organic solvents such as methanol, ethanol, and 1-propanol became cloudy without the change of chemical structure, and instead of depending on the type of solvents, their crystalline structure depends on the degree of swelling. By using *in-situ* time-resolved Fourier transform infrared-attenuated total reflectance (FTIR-ATR) spectroscopy, Davis et al. [23] found that with the increase of water vapor activities, the water inside PLA form larger water cluster.

The interaction of a mixture of organic solvents and water with PLA film during immersion can affect the hydrolytic degradation and the thermal properties of PLA during its service life. The different concentrations of ethanol-aqueous solution can affect the hydrolytic degradation of PLA and further affect the release of an organic compound from the PLA matrix. Compared with unsubmerged PLA, Sonchaeng et al. reported that the glass transition temperature (T_g) of PLA film in a mixed solution of organic compounds and water decreases, and the concentration of the solution affects the reduction of T_g [24]. However, this study did not quantify the amount of solution absorbed in the PLA films. Furthermore, Iñiguez-Franco et al. studied the hydrolytic degradation of PLA-

nanocomposite produced with organomodified montmorillonite at 5 wt% (PLA-OMMT) in ethanol solutions at 40 °C. They found that when PLA-OMMT is immersed in a higher concentration of an ethanol-aqueous solution, the release of organomodifier (QAC) is higher than that in a lower concentration solution during the early stage. But later the release is higher in a lower concentration solution. The release increases exponentially due to faster hydrolysis making it easier for the QAC molecules to diffuse out of the film [25]. However, so far, there is limited information regarding the effects of immersion of PLA in various concentrations of organic compounds, such as alcohol-aqueous solutions, on the thermal properties of PLA films.

In addition, because the OH/OD bond length and the hydrogen bond length between water and deuterium oxide (D₂O) are different, it is essential to compare the effect of water and D₂O on the thermo-properties of PLA. Also, when conducting NMR experiments, water from the environment can interfere with the experimental results, thereby hindering the quantification of water and alcohol sorption in PLA, but using D₂O can avoid this problem [25].

Thus, it is necessary to accurately measure the sorption capacity of PLA film to alcohol solutions and the change in its thermo-mechanical properties to fully develop PLA applications. By detecting the thermo-mechanical properties of PLA, including the dynamic modulus and T_g , the changes in the chemical structure of PLA films immersed in alcohol-aqueous solutions can be analyzed. Understanding the principle of the interaction of PLA with organic compounds can help to design better packaging systems based on PLA.

1.2 Overall goal and objectives

The overall goal of this thesis is to determine the effect of alcohol-aqueous and deuterium oxide solutions on the thermo-mechanical properties of PLA. To achieve this goal, this thesis aims to address two specific objectives, which are:

Objective 1: To understand the effect of alcohol-aqueous solution exposure on the thermo-mechanical properties of PLA films.

Objective 2: To quantify the sorption of alcohols and water and D₂O in PLA films.

REFERENCES

REFERENCES

- [1] Achilias D. S., Roupakias C., Megalokonomos P., *et al.*, Chemical recycling of plastic wastes made from polyethylene (LDPE and HDPE) and polypropylene (PP), *Journal of Hazardous Materials*, vol. 149, no. 3, pp. 536–542, 2007, doi: 10.1016/j.jhazmat.2007.06.076.
- [2] Bahlouli N., Pessey D., Raveyre C., *et al.*, Recycling effects on the rheological and thermomechanical properties of polypropylene-based composites, *Materials & Design*, vol. 33, pp. 451–458, 2012, doi: 10.1016/j.matdes.2011.04.049.
- [3] Lemos Junior W. J. F., do Amaral dos Reis L. P., *et al.*, Reuse of refillable PET packaging : Approaches to safety and quality in soft drink processing, *Food Control*, vol. 100, pp. 329–334, 2019, doi: 10.1016/j.foodcont.2019.02.008.
- [4] Karayannidis G. P. and Achilias D. S., Chemical Recycling of Poly (ethylene terephthalate), *Macromolecular Materials and Engineering*, vol. 292, no.2, pp. 128–146, 2007, doi: 10.1002/mame.200600341.
- [5] Nikles D. E. and Farahat M. S., New Motivation for the Depolymerization Products Derived from Poly (Ethylene Terephthalate) (PET) Waste : a Review, *Macromolecular Materials and Engineering*, vol. 290, no. 1, pp. 13–30, 2005, doi: 10.1002/mame.200400186.
- [6] Silvestre C., Duraccio D., and Cimmino S., Progress in Polymer Science Food packaging based on polymer nanomaterials, *Progress in Polymer Science*, vol. 36, no. 12, pp. 1766–1782, 2011, doi: 10.1016/j.progpolymsci.2011.02.003.
- [7] Piemonte V. and Gironi F., Kinetics of Hydrolytic Degradation of PLA, *Journal of Polymers and the Environment*, vol. 21, no. 2, pp. 313–318, 2013, doi: 10.1007/s10924-012-0547-x.
- [8] Gironi F., Frattari S., and Piemonte V., PLA Chemical Recycling Process Optimization : PLA Solubilization in Organic Solvents, *Journal of Polymers and the Environment*, vol. 24, no. 4, 2016, doi: 10.1007/s10924-016-0777-4.
- [9] Lee S. H., Kim I. Y., and Song W. S., Biodegradation of Polylactic Acid (PLA) Fibers Using Different Enzymes, *Macromolecular Research*, vol. 22, no. 6, pp. 657–663, 2014, doi: 10.1007/s13233-014-2107-9.

- [10] Li G., Sarazin P., Orts W. J., *et al.*, Biodegradation of Thermoplastic Starch and its Blends with Poly (lactic acid) and Polyethylene: Influence of Morphology, *Macromolecular Chemistry and Physics*, vol. 212, no. 11, pp. 1147–1154, doi: 10.1002/macp.201100090.
- [11] Lunt J., Large-scale production, properties and commercial applications of poly lactic acid polymers, *Polymer Degradation and Stability*, vol. 59, no. 1–3, pp. 145–152, 1998, doi: 10.1016/s0141-3910(97)00148-1.
- [12] Lim D. W. and Park T. G., Stereocomplex Formation between Enantiomeric PLA – PEG – PLA Triblock Copolymers: Characterization and Use as Protein-Delivery Microparticulate Carriers. *Journal of Applied Polymer Science*, vol. 75, no. 13, pp. 1615–1623, 2000, doi: 10.1002/(sici)1097-4628(20000328)75:13<1615::aid-app7>3.0.co;2-1.
- [13] Farah S., Anderson D. G., and Langer R., Physical and mechanical properties of PLA , and their functions in widespread applications — A comprehensive review, *Advanced Drug Delivery Reviews*, vol. 107, 2016, doi: 10.1016/j.addr.2016.06.012.
- [14] Hughes J., Thomas R., Byun Y., and Whiteside S., Improved flexibility of thermally stable poly-lactic acid (PLA), *Carbohydrate Polymers*, vol. 88, no. 1, pp. 165–172, 2012, doi: 10.1016/j.carbpol.2011.11.078.
- [15] Ho C. H., Wang C. H., Lin C. I., and Lee Y. Der, Synthesis and characterization of TPO-PLA copolymer and its behavior as compatibilizer for PLA/TPO blends, *Polymer*, vol. 49, no. 18, pp. 3902–3910, 2008, doi: 10.1016/j.polymer.2008.06.054.
- [16] Nofar M., Tabatabaei A., and Park C. B., Effects of nano-/micro-sized additives on the crystallization behaviors of PLA and PLA/CO₂ mixtures, *Polymer*, vol. 54, no. 9, pp. 2382–2391, 2013, doi: 10.1016/j.polymer.2013.02.049.
- [17] Salazar R., Domenek S., Courgneau C., and Ducruet V., Plasticization of poly (lactide) by sorption of volatile organic compounds at low concentration, *Polymer Degradation and Stability*, vol. 97, 2012, doi: 10.1016/j.polymdegradstab.2012.03.047.
- [18] Willige R. W. G. Van, Linssen J. P. H., Meinders M. B. J., *et al.*, Influence of flavour absorption on oxygen permeation through LDPE , PP , PC and PET plastics food packaging, *Food Additives and Contaminants*, vol. 19, no. 3, 2010, doi: 10.1080/0265203011008114.

- [19] Hernandez-mun P., Gavara R. and Hernandez R. J., Evaluation of solubility and diffusion coefficients in polymer film - vapor systems by sorption experiments, *Journal of Membrane Science*, vol. 154, no. 2, pp. 195–204, 1999, doi: 10.1016/s0376-7388(98)00276-2.
- [20] Samus M. A. and Rossi G., Methanol Absorption in Ethylene - Vinyl Alcohol Copolymers : Relation between Solvent Diffusion and Changes in Glass Transition Temperature in Glassy Polymeric Materials, *Macromolecules*, vol. 29, no. 6, pp. 2275–2288, 1996, doi: 10.1021/ma950767p.
- [21] Moriizumi Y. and Nagai K., Vapor-induced Crystallization in Alcoholic Sorption using Poly (lactic acid) Films, *Journal of Applied Membrane Science & Amp; Technology*, vol. 22, no. 2, pp. 65–84, 2018, doi: 10.11113/amst.v22n2.125.
- [22] Sato S., Gondo D., Wada T., *et al.*, Effects of Various Liquid Organic Solvents on Solvent-Induced Crystallization of Amorphous Poly (lactic acid) Film, *Journal of Applied Polymer Science*, vol. 129, no. 3, 2013, doi: 10.1002/app.38833.
- [23] Davis E. M., Minelli M., Baschetti M. G., *et al.*, Nonequilibrium Sorption of Water in Polylactide, *Macromolecules*, vol. 45, no. 18, pp. 7486–7497, 2012, doi: 10.1021/ma301484u.
- [24] Sonchaeng U., Auras R., Selke S., *et al.*, *In-situ* changes of thermo-mechanical properties of poly (lactic acid) film immersed in alcohol solutions, *Polymer Testing*, vol. 82, 2020, doi: 10.1016/j.polymertesting.2019.106320.
- [25] Iñiguez-franco F., Auras R., Rubino M., *et al.*, Effect of nanoparticles on the hydrolytic degradation of PLA- nanocomposites by water-ethanol solutions, *Polymer Degradation and Stability*, vol. 146, pp. 287–297, 2017, doi: 10.1016/j.polymdegradstab.2017.11.004.

CHAPTER 2 Literature Review

2.1 Introduction of PLA

Due to the exploitation and consumption of fossil fuels during the last century, the concentration of methane (CH₄) and carbon dioxide (CO₂) in the atmosphere has far exceeded natural levels forcing people to pay more attention to using sustainable resources [1,2]. The CO₂ produced by the burning of fossil fuels is one of the main factors contributing to global warming [3,4]. To slow this trend, people have begun to search for new materials that can replace unsustainable fossil-derived materials such as plastics [1]. Among the wide variety of plastics, most of them are derived from fossil fuels. Although plastic production only accounts for about 4% to 5% of global crude oil consumption, the development of plastics derived from renewable resources can open the path for a new circular plastic economy [3]. Some biopolymers with lower environmental footprints (EFPs) than fossil-based polymers have been gradually developed, and poly(lactic acid) -PLA is one of them. A life cycle assessment (LCA) study – a method to determine the EFPs of a product or system – of the PLA production process found that in the long run, the PLA production process can not only get rid of the dependence on fossil energy but also become a source of carbon credits [5]. **Figure 2.1** shows the cradle-to-cradle life cycle of PLA products. Initially, starch is extracted from corn or other grains, then fermented into lactic acid (LA) and processed into PLA. PLA resins can be used to develop products for industries such as packaging, medical and agriculture [6]. At the end of their useful life, the products can be completely hydrolyzed and chemically recycled or recovered

through composting. The degradation time of PLA in an industrial compost environment is about 6 months and in the environment around 2 years, while the degradation time of traditional plastics such as polystyrene (PS) and polyethylene (PE) is 500 to 1000 years [7–9]. Unlike PS, which needs to be degraded to the parts per million (ppm) level to avoid toxicity, the hydrolysate byproducts of PLA are LA, which is an inherent benign substance in the human body and food [10]. Therefore, improving the production and performance of PLA is of positive significance for increasing its use and protecting the environment [11].

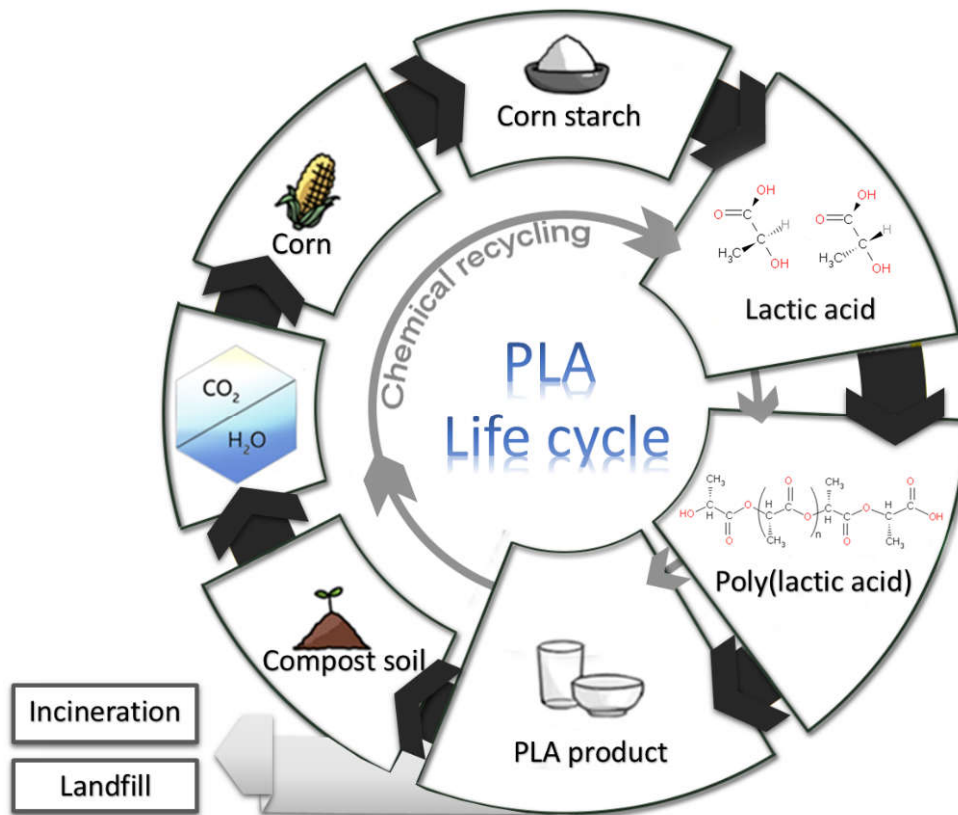


Figure 2.1 Life cycle of PLA and its products, adapted from [2,6,12].

2.2 Production of PLA

PLA is a linear aliphatic thermoplastic polyester with a chemical basic structure as $-(\text{CH}_2\text{CHO}-\text{CO})_n-$ [13]. In 1845, the French chemist Théophile-Jules Pelouze synthesized it for the first time through the condensation reaction of LA [14,15]. Since then, many efforts have been made to reduce the synthesis cost and increase the molecular weight of the synthesized PLA. Nowadays, PLA can be obtained by two major routes, which are the ring-opening polymerization (ROP) of lactide and the direct condensation polymerization of LA. By using a stannous octoate-based catalyst, the ROP route provides easy access to high molecular weight PLA. As a form of chain-growth polymerization, the principle of ROP is the terminal end of a chain acting as a reactive center and other cyclic monomers can react by opening PLA's ring system to form a longer chain [16,17]. Because ROP does not require high temperature and long reaction time, it is also the most commonly used commercial production method [5,18,19].

Compared with the first route, because of the difficulty of removing water and impurities from viscous polymer, direct condensation polymerization can only produce low to intermediate molecular weight PLA [18,20]. The LA monomer used in the second route is obtained from the fermentation of sugar raw materials including starch, glucose, lactose, and maltose from corn or potatoes [21,22]. The use of renewable raw materials has become one major advantage of PLA over fossil-based plastics. In addition to the above routes, an azeotropic dehydration condensation route, which is a biosynthesis method using enzyme-catalyzed processes can also be used to produce PLA [18,23–25].

During the production process, three forms of PLA can be formed, including poly-L-lactic acid (PLLA), poly-D-lactic acid (PDLA), and poly-D,L-lactic acid (PDLLA). This is because LA, the basic building block of PLA, is a chiral molecule with L-type and D-type isomers [18,21]. LA can be produced through microbial fermentation through chemical or biological routes. The chemical synthesis is based on the hydrolysis of lactonitrile by strong acids and is not conducive to producing a mixture of levorotatory L(+) and dextrorotatory D(-) lactic acid. The production of PLA requires LA with high optical purity of L(+) or D(-), which can be achieved well through biosynthesis [26]. The different synthesis methods for producing PLA are shown in **Figure 2.2**.

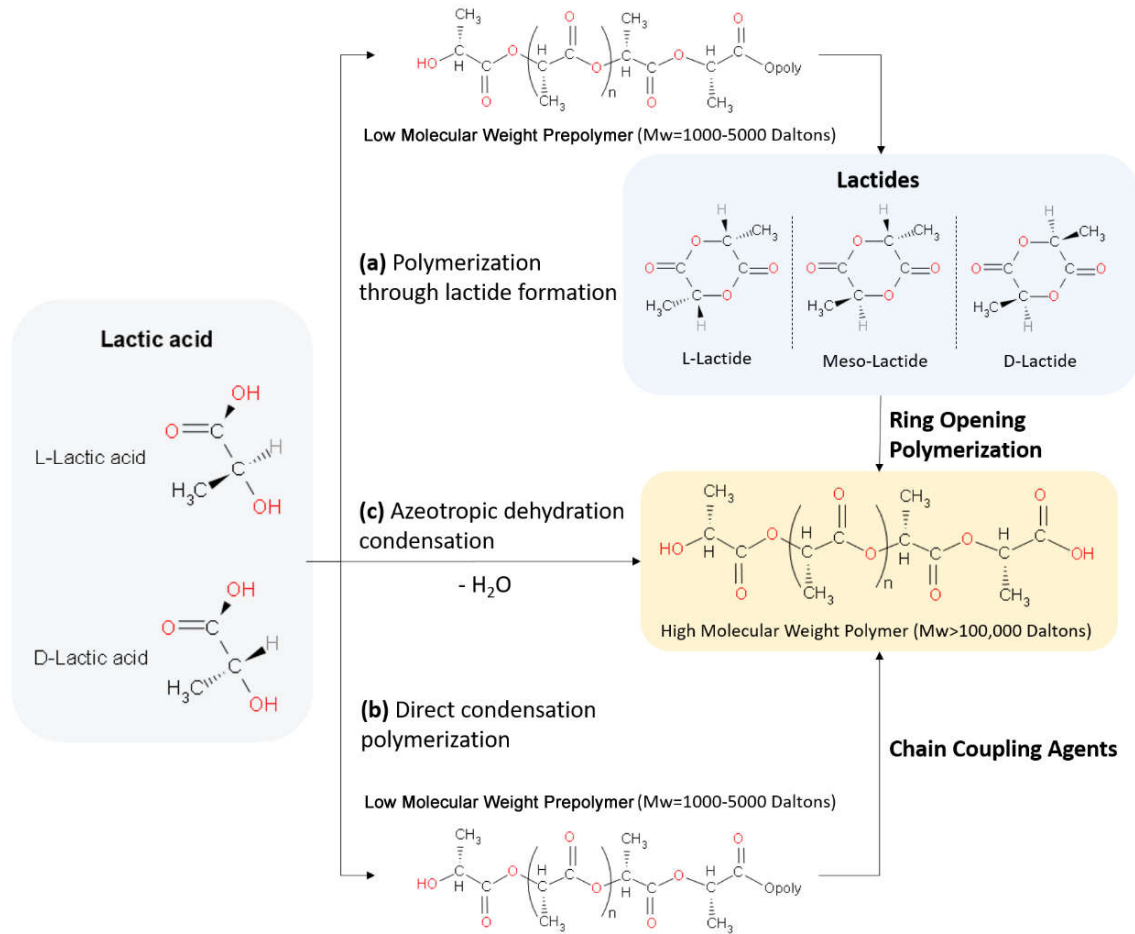


Figure 2.2 The synthesis routes of high molecular weight PLA, adapted from [12,18,23].

2.3 PLA properties

2.3.1 Structure-property relationship PLA

2.3.1.1 Chain and nanophase structure

Since the basic monomer to produce PLA is LA, four different atoms and groups are attached to its α carbon atom with optical activity. The optical isomers are L-lactic acid and D-lactic acid, thus producing PDLA, PLLA, and PDLLA. PDLLA can be amorphous or semi-crystalline, if PLA synthesized from LA contains $\geq 8\%$

D-lactide (DLA) and/or meso-lactide, it will be amorphous because the PLA molecules cannot be arranged regularly, while PLLA and PDLA are both thermoplastic crystalline polymers and semi-crystalline polymers [27,28]. The thermo-mechanical properties of PLA change according to its structural phases [29]. The general description of semi-crystalline polymers such as PLA is composed of two separate phases, one is the amorphous phase and the other is the crystalline phase. A more complete description proposed by Wunderlich [30] shows that it also contains intermediate nanophases that exist at the interface between the crystal and the surrounding melt. Since the length of the polymer molecule is much higher than the size of the crystalline phase in at least one direction, the decoupling between the crystalline phase and the amorphous phase is incomplete [31].

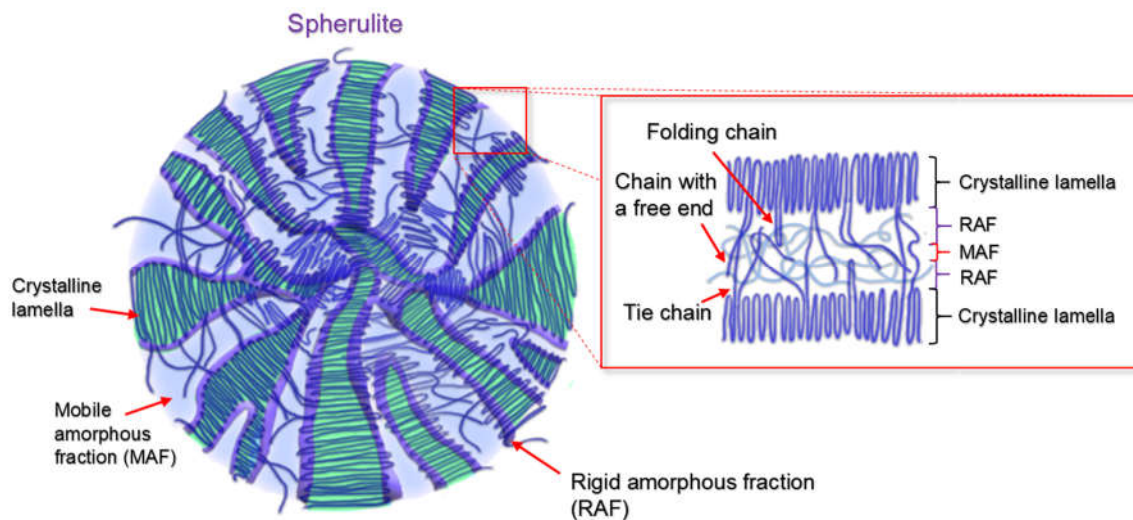


Figure 2.3 Schematic representation of crystalline lamella, rigid amorphous fraction, and mobile amorphous fractions in spherulite of a semi-crystalline polymer, adapted from [32–36].

According to the degree of coupling with the crystalline phase, the amorphous part can be subdivided into a mobile amorphous fraction (MAF) and a rigid amorphous fraction (RAF) as shown in **Figure 2.3** [30,35]. MAF consists of the polymer chains that are decoupled from the crystals and mobilize at T_g [35]. RAF is attributed to the area where the chain is constrained at the boundary of the crystalline fraction [36,37]. There are some studies indicated that the RAF has an effect on mechanical behavior and gas permeability of the semi-crystalline PLA [38–40].

2.3.1.2 Crystal structure

Under different crystallization conditions or external field induction, PLA will form different types of spherulites. The crystal forms of PLA include α crystal form, β crystal form, γ crystal form, and δ (or α' or disordered α) crystal form, which have different spiral structures and unit symmetry [41,42]. In addition to the limiting disordered modifications such as α' and β' , there are also some limiting ordered modifications such as α'' and β'' as described in some studies [43–45]. The α crystal form (pseudo-orthorhombic or orthorhombic unit cell) is formed when PLA is crystallized from a melt or solution [41,46,47], and it is also the most common and stable polymorph. The β crystal form (trigonal or orthorhombic unit cell) is obtained by applying stretching at high draw-ratio and high-temperature conditions to the α crystal form, and its thermal stability is poorer than that of the α crystal form since the melting temperature (T_m) is relatively low [47]. In addition, γ form (orthorhombic unit cell) can be obtained by epitaxial crystallization [47,48].

Compared with the α form, the chain packing of the δ form is looser and less ordered [49]. Also, PLLA and PDLA could be mixed at a 1:1 molar ratio to form the PLA stereocomplex crystal (SC) [42]. Compared with the α form, PLA SC has better thermal properties. The T_m of SC is higher than that of the α form, which makes it attractive for being used in various areas [50].

Table 2.1 Crystal forms and chain conformations of PLA.

Crystal form	Growth condition	Chain conformation	Crystal system
α	Melt/cold-crystallization, or solution	10_3 helical	Pseudo-orthorhombic
			Orthorhombic
$\alpha'(\delta)$	Melt/cold-crystallization	N/A	Pseudo-hexagonal
β	Stretching under high temperature and high draw-ratio, melt-spun, and solution-spun	3_1 helical	Orthorhombic
			Trigonal
γ	epitaxial crystallization	3_1 helical	Orthorhombic
SC	Blend of PLLA and PDLA	3_1 helical	Triclinic
		3_1 helical	Trigonal

Note: N/A denotes not available.

Table 2.2 Crystal forms, size of lattice, crystallization temperature, and melting temperature of PLA.

Crystal form	size of lattice			Crystallization temperature (T_c) °C	Melting temperature (T_m) °C	Ref.
	a, Å	b, Å	c, Å			
α	10.3-10.7	5.9-6.4	27.8-28.8	~130	~180	[52]
	10.5-10.7	6.0-6.1	28.7-28.8	-	(Pseudo-orthorhombic)	
$\alpha'(\delta)$	10.8	6.2	28.8	Below 110°	-	
β	10.3-10.4	17.7-18.2	9	-	-	[33]
	10.5	10.5	8.8	-	-	
γ	9.9	6.2	8.8	-	-	
SC	9.16	9.16	8.7	-	~230 (Triclinic)	[49]
	14.98	14.98	8.7	-	~230 (Trigonal)	

2.3.1.3 Glass transition temperature

The glass transition temperature (T_g) of PLA is in the range of 58-65 °C [51–53]. Because the mobility of polymer chains is related to T_g , the T_g is very important in determining the crystallization window of PLA [49]. The T_g can be affected by different chain architectures, the minor unit concentration of additives, molecular weight, and external condition such as pressure. Due to the higher free volume caused by more chain ends, the T_g value of branched PLA is lower than that of linear structure [49,54,55]. Saeidlou et al. [49] indicated that under a given molecular weight, the increase in optical impurities reduces PLA's T_g . The minor

unit concentration is defined as D -lactate in the case of an L -lactide rich PLA and as L -lactate for a D -lactide rich PLA. And for PLA with different D -lactate concentrations, the T_g increases rapidly before the molecular weight increases to 80-100 kg/mol , but then reaches a constant value. In this case, the T_g can be predicted by using the Flory–Fox equation given by

$$T_g = T_g^\infty - \frac{K}{M_n} \quad (2.1)$$

in which T_g^∞ is the glass transition temperature for infinite molecular weight, K is a constant expressed in $^\circ C \text{ kg/mol}$ and M_n is the number- average molecular weight.

In addition to the internal structure of the polymer, external conditions may also affect the T_g of PLA. But in fact, these external conditions, such as exposure to organic solvents, also change the thermo-mechanical properties by changing the matrix structure. Sato et al. [56] found that the T_g of PLA film not immersed in organic solvent was 60.3 ± 2.1 $^\circ C$, but when PLA film was immersed in different organic solvents at 35 $^\circ C$ for 24 h, there would be slight changes in T_g . For example, T_g became 57.5 ± 1.8 $^\circ C$ after being immersed in 1-butanol. Also, in the study of Sonchaeng et al. [57], when PLA was immersed in alcohol and alcohol aqueous solution, the T_g of PLA was lower than that of dry PLA. Sonchaeng et al. [57] also reported that for the smallest and lowest molecular weight aliphatic alcohol – methanol, the T_g reduced the most. For larger, higher molecular weight aliphatic alcohols, the change in T_g became smaller. In their work, the decrease in the T_g of PLA in alcohol was attributed to the interaction between alcohol and PLA, in which small molecular weight alcohols can plasticize the PLA matrix leading to

the movement of PLA segmental chains, and therefore has a lower T_g , but this hypothesis needs further verification.

2.3.2 Properties of PLA affected by alcohol exposure

2.3.2.1 Solubility

Hildebrand et al. [58–60] first proposed the concept of the solubility parameter and cohesive energy only produced by dispersion. The solubility parameter in Eq. 2.2 is called the Hildebrand solubility parameter or Hildebrand parameter [60].

$$\delta = (CED)^{1/2} = [\Delta H - \left(\frac{RT}{V_m}\right)]^{1/2} = \left(\frac{\Delta E}{V_m}\right)^{1/2} \quad (2.2)$$

where δ denotes the solubility parameter, CED is the cohesive energy density, ΔH is the enthalpy of vaporization, R is gas constant, T is temperature, V_m is molar volume, ΔE is the free energy of vaporization.

Also, the Hildebrand solubility parameter is related to the heat or enthalpy of mixing. The relationship between them is shown in the following equations [61,62]:

$$\Delta H_m = n_s V_s \Phi_p (\delta_s - \delta_p)^2 \quad (2.3)$$

$$\Delta G_m = \Delta H_m - T \Delta S_m \quad (2.4)$$

where ΔH_m is the heat of mixing, n_s and V_s denote the moles and molar volume of the solvent, Φ_p is the volume fraction of polymer. δ_s and δ_p are the solubility

parameters of solvent and polymer, respectively. ΔG_m is Gibb's free energy and ΔS_m is the entropy of mixing at temperature T .

When the solubility parameters of a solvent and polymer are similar, the polymer will be more soluble in the solvent. According to the equation above, the greater the difference in solubility parameters, the greater the value of the heat of mixing, then the higher the temperature at which the polymer to be soluble [58].

To further improve this concept, polar and hydrogen bonding forces were also taken into consideration, Hansen [63] proposed an extended system, treating cohesive energy as the sum of contributions from dispersive (E_d), polar (E_p), and hydrogen bonding (E_h), as shown in the formulas below [60,64,65]:

$$E_{coh} = E_d + E_p + E_h \quad (2.5)$$

$$E_{coh}/V_m = E_d/V_m + E_p/V_m + E_h/V_m \quad (2.6)$$

$$\delta_d = (E_d/V_m)^{1/2}, \delta_p = (E_p/V_m)^{1/2}, \delta_h = (E_h/V_m)^{1/2}, \quad (2.7)$$

$$\delta^2 = \delta_d^2 + \delta_p^2 + \delta_h^2 \quad (2.8)$$

where E_{coh} denotes the total cohesion energy, V_m is molar volume, δ is the total solubility parameter, δ_d , δ_p , δ_h are the dispersive, the polar, and the hydrogen bonding contributions respectively.

The three solubility parameters are related to each other. Sato et al. [56] indicated that δ_h depends on the hydrogen bonding as well as δ_d and δ_p , and based on the three cohesive parameters, δ_h reflects the solubility of PLA more effectively.

For the polymer in organic solvents, an equation to predict the solubility of the polymer has been proposed. The equation is shown below [64,65]:

$$(R_a)^2 = 4(\delta_{d2} - \delta_{d1})^2 + (\delta_{p2} - \delta_{p1})^2 + (\delta_{h2} - \delta_{h1})^2 \quad (2.9)$$

where R_a is the solubility parameter “distance”, and has a unit of $(MPa)^{1/2}$; 1 represents the polymer, 2 represents the solvent (i.e., δ_{d2} is the dispersive solubility parameter for the solvent, and δ_{p1} is the polar solubility parameter for the polymer). The constant “4” was predicted by the Prigogine corresponding state theory (CST) of polymer solutions for representing the solubility data as a sphere encompassing the solvent correctly [65].

If the R_a value is small, it indicates that the solubility of the solute polymer in the solvent is high, because the interaction forces between the solute molecules and the solvent molecules are similar. In contrast, a large R_a indicates that the solubility of the polymer in the solvent is low [64]. Specifically, if the radius of polymer’s solubility parameters in the three-dimensional space R_1 is greater than R_a , then this polymer is soluble in the solvent, and if $R_1 < R_a$, then the polymer is insoluble. In other words, when the solubility parameter distance increases, the solubility will decrease [66].

In some other cases, it is also necessary to calculate the change of the δ_d , δ_p and δ_h parameters of the liquids with the temperature, for example, Sonchaeng et al. [67] calculated the temperature of PLA *in-situ* immersion T_g by using the following formulas [65]:

$$\frac{d\delta_d}{dT} = -1.25\alpha\delta_d \quad (2.10)$$

$$\frac{d\delta_p}{dT} = -0.5\alpha\delta_p \quad (2.11)$$

$$\frac{d\delta_h}{dT} = -\delta_h(1.22 \times 10^{-3} + 0.5\alpha) \quad (2.12)$$

where T is temperature, α is the coefficient of thermal expansion.

Figure 2.4 shows the polymer solubility graph based on the Hansen parameter system. When the relative energy difference (RED) between the polymer and solvent is greater than 1, the polymer is not soluble in the solvent. If RED is lower than 1, then the polymer is soluble in the solvent.

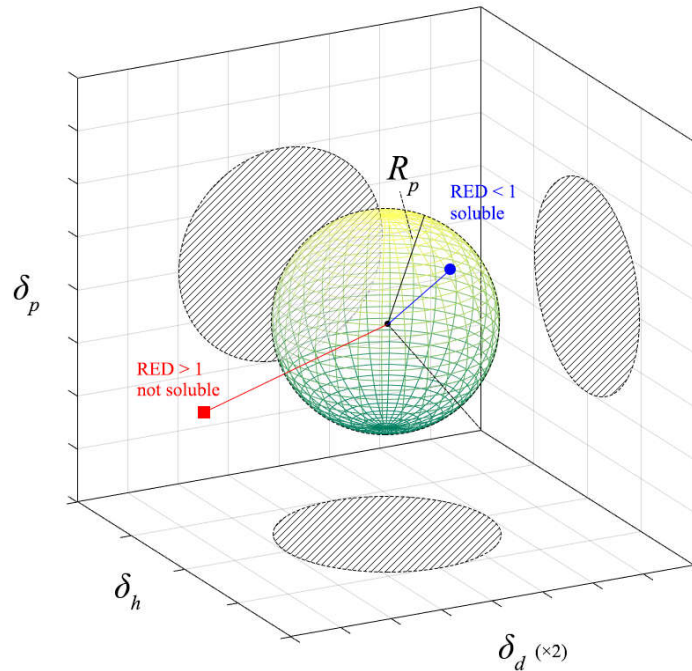


Figure 2.4 Polymer solubility graph based on the Hansen parameter system. RED represents the relative energy difference, R_p is the interaction radius. Adapted from [64,68,69].

In addition, if the solubility parameter value is known, there is another method called the group contribution method proposed by Hoftyzer and Van Krevelen that can be used to measure the degree of swelling of the polymer in the solvent [60,70]. However, compared with using the solubility parameter calculated by the group contribution method to estimate the solubility of the PLA film, using the Hansen solubility parameter (HSP) to analyze the solubility is more accurate [56].

Based on the HSP, Lindvig et al. [71] presented the estimation of the Flory–Huggins coefficient to predict the coefficients of solvent activity at infinite dilution in several polymers. The lower the Flory-Huggins interaction parameter (FH parameter, χ_{12}) value ($\chi_{12} \leq 0.5$), the greater the miscibility. χ_{12} can be predicted as follows:

$$\chi_{12} = \alpha \frac{V_1}{RT} ((\delta_{d2} - \delta_{d1})^2 + 0.25(\delta_{p2} - \delta_{p1})^2 + 0.25(\delta_{h2} - \delta_{h1})^2) \quad (2.13)$$

where α is the Lindvig's coefficient ($\alpha = 0-1$), V_1 is the molar volume of the solvent, R denotes the gas constant, T is the temperature [60,65].

2.3.2.2 Degree of swelling

Swelling is one of the structural changes that PLA may undergo when it comes into contact with organic solvents. The degree of swelling of PLA is affected by the solubility parameters. By immersing the PLA films in different organic solvents, Sato et al. [56] found that there is a relationship between the degree of swelling and the total HSP, that is, compared with other values, when the total

solubility parameter of the solvent is close to $21.2 \text{ MPa}^{1/2}$, which is the total HSP of PLA, greater swelling would occur. In addition, Gee et al. [72] indicated that the swelling of rubber is maximum when $(\delta_{d2} - \delta_{d1})^2 = 0$. Udayakumar et al. [73] also got a similar conclusion about PLLA in organic solvents such as ethyl acetate (EA), o-dichlorobenzene (ODCB), and nitrobenzene (NB). The degree of swelling can be obtained by the following equation [74]:

$$\text{Degree of swelling (\%)} = \frac{W_S W_D}{W_D} \times 100 \quad (2.14)$$

where W_S (g) is the weight of the swollen film, W_D is the weight of the dry film.

The degree of swelling was reported to be related to the concentration of the organic solution. Shinkawa et al. [74] studied the swelling behavior of PLA in ethanol solution and found that the sorption amount of ethanol and water on the PLA film is proportional to the feed concentration. In the ethanol solution, hydrogen bonds are formed between water molecules, and the water molecules are connected to ethanol molecules through hydrogen bonds to form hydrates [75]. The molecular interaction in the alcohol solution is illustrated in **Figure 2.5**. Usually, it can be suggested that the interaction between PLA and ethanol is stronger than the interaction between PLA and water. When the concentration of ethanol increased from 10 wt% to 50 wt%, the swelling degree of water for PLA film increased by about 4 times, and the swelling degree of ethanol for PLA film increased by 11 times. When the feed concentration was 10 wt%, the concentration of ethanol in the PLA film was 11 wt% ethanol/PLA, and when the feed concentration was 50 wt%, the concentration of ethanol in the film reached

almost 20 wt% ethanol/PLA. At different concentrations, because the sorption and diffusion mechanisms were different, the permeation mechanisms of ethanol and water were also different [76].

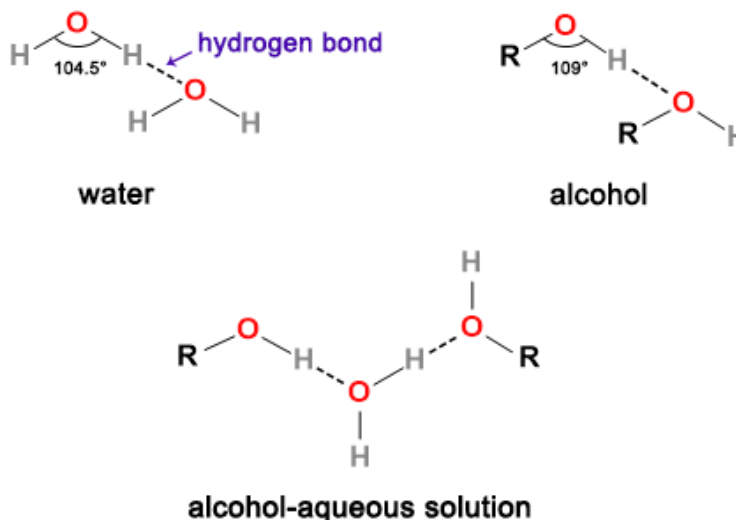


Figure 2.5 The molecular interaction between hydroxyl groups in alcohol-aqueous solution, adapted from [77,78].

The swelling behavior could also be affected by the *pH* of the aqueous solutions and the molecular weight of polymers [79,80]. An aqueous solution with a higher *pH* value can promote the swelling of PLA, which may be related to the degradation rate, and PLA can exhibit better stability under a higher *pH* condition [79]. Andreopoulos et al. [80] immersed amorphous PLA in the buffer solution with a *pH* of 7.2. They found that compared with low molecular weight PLA, the degradation of high molecular weight PLA would lead to a modified product that swell more easily. They also reported that for low molecular weight polymers, hydrolytic degradation would start in a few days, while for high molecular weight polymers, it takes longer and may require a two-stage mechanism. They concluded that the reason for this phenomenon is the random depolymerization

reactions that occur with the condensation of PLA produce diverse lengths of chain fragments. Thus, the polydispersity of the swollen sample is different from that of the original sample, and its molecular weight distribution changed, leading to changes in the swelling behavior of the sample. So, when studying the swelling behavior of PLA in organic solvents, the molecular weight of the PLA samples must be controlled.

2.3.2.3 Diffusion and permeation

The transmission behavior of the alcohol solution can be detected by using the pervaporation (PV) studies [74,81], and the diffusion behavior can be estimated by studying the separation factors (i.e., permselective separation factor α_P , solubility selectivity α_S , and the diffusion selectivity α_D) for the organic solution through PLA film. Shinkawa et al. [74] reported that the permeability of alcohol (such as ethanol) will be affected by the crystalline state of the PLA film because during the permeation process, the feed solution can be dissolved and diffused only in the amorphous regions of the film. Also, the total flux of ethanol solution through PLA film mainly depends on the flux of water. In the PV method, the permeate flux [$kg/(m^2h)$] and permselective separation factor α_P can be obtained by the following equations:

$$J = \frac{Q}{A \times t} \quad (2.15)$$

$$\alpha_P = \frac{P_{water}/P_{ethanol}}{F_{water}/F_{ethanol}} \quad (2.16)$$

where J is the diffusive flux, Q is the permeate weight (kg), A is the area of PLA film (m^2), t is the operating time (h). P represents the weight fraction in permeate phase, F is the weight fraction in the feed phase [74,82,83].

To estimate the solubility selectivity α_S (water/ethanol), Eq. 2.17 was used:

$$\alpha_S = \frac{M_{water}/M_{ethanol}}{F_{water}/F_{ethanol}} \quad (2.17)$$

where M represents the weight fractions of water or ethanol in the PLA film, F denotes the weight fractions of water or ethanol in the solution.

In addition, Fick's first law can be used for calculating the diffusion selectivity α_D , the equations are shown below [74,84,85]:

$$J_x = -D \frac{d\varphi}{dx} \quad (2.18)$$

$$J = \frac{D_0}{\gamma l} (e^{\gamma\varphi_l} - 1) \quad (2.19)$$

$$\varphi_x = kS_x \quad (2.20)$$

$$\frac{1}{k} = \frac{S}{d_s} + \frac{100}{d_f} \quad (2.21)$$

$$\bar{D} = \frac{D_l - D_0}{\ln D_l/D_0} \quad (2.22)$$

$$D_l = D_0 e^{\gamma\varphi_l} \quad (2.23)$$

$$J = \frac{\bar{D}\varphi_l}{l} = \frac{\bar{D}kS}{l} \quad (2.24)$$

$$\alpha_D = \frac{\bar{D}_{water}}{\bar{D}_{ethanol}} \quad (2.25)$$

where J_x is the diffusion flux in the x -direction, D is the diffusion coefficient, φ is the liquid concentration per unit area in the film, x denotes the position, which is the distance along the direction of permeation. The parameter γ is the characteristic of the influence of solvent concentration on the movement of polymer chain segments. \bar{D} is the apparent diffusion coefficient, l is the thickness of the film, k is a coefficient that controls the conversion of concentration units. S is the swelling ratio of the film in the solution, d_s and d_f are the densities of the sorbed solution and the film, respectively.

PLA was found to have water permselective properties by analyzing the separation factor. The water molecule with a smaller molecular size (0.311 nm) is easier to diffuse than the ethanol molecule with a larger size (0.460 nm) [74]. When the solution concentration increased, the diffusion coefficient of ethanol was almost constant, while the diffusion coefficient of water decreased. The reason for this phenomenon was considered to be the interaction between ethanol molecules and water molecules or the interaction between ethanol molecules and PLA [74,86]. It was presumed that the dissolution of ethanol may cause the chain gap of PLA to increase and the hydration between water and ethanol molecules may also reduce the diffusivity of the water molecules.

2.3.2.4 Crystal structure and crystallinity

The effect of alcohol on the crystallization of PLA film has been examined in many studies. These studies are mainly divided into two types, the study of vapor-induced crystallization and the study of solvent-induced crystallization. In

vapor-induced crystallization, the amount of the crystal nucleus increased because the organic vapor was dispersed throughout the film. In solvent-induced crystallization, the crystal developed from the nucleus, and the size of the crystal nucleus changed. The solvent-induced crystallization is caused by the dissolution of high polarity organic solvents in the interstices of polymer chains [43,56,87]. The difference between vapor-induced and solvent-induced crystallization is shown in

Figure 2.6.

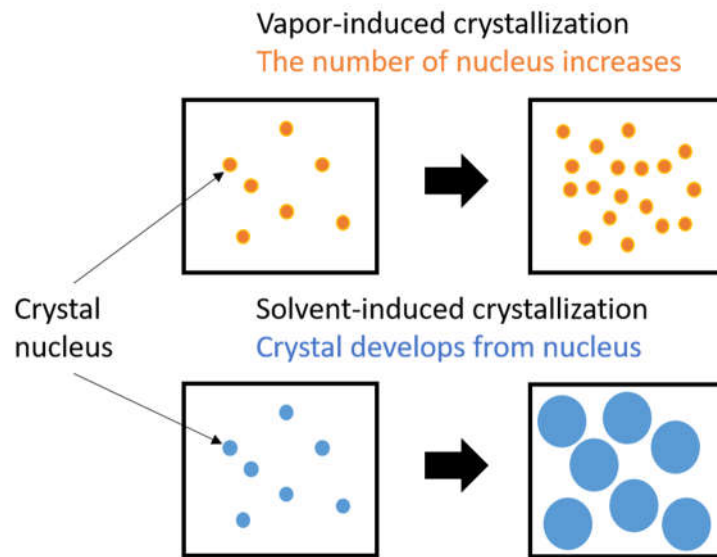


Figure 2.6 Difference between vapor-induced and solvent-induced crystallization, figure adapted from [43].

Generally, the dissolution of vapor molecules relative to macromolecules is explained by sorption, which includes the adsorption on the surface of polymer film and the absorption inside the film. The sorption amount means the amount of gaseous molecules dissolved in the film [43,88]. Sato et al. [87] investigated the effect of methanol and ethanol vapor-induced crystallization on the structure of PLA. The α -crystal was formed in the vapor-induced crystallization. The dissolution

of these organic solvents with high polarity in the chain interstitial spaces of PLA can cause slight cloudiness, but no chemical structure changes of PLA. Moriizumi et al. [43] measured the organic vapor sorption to PLA and found that the alcohol vapors sorbed in the PLA film caused vapor-induced crystallization, and formed different crystal modifications. In addition, in the low-pressure region, as the amount of alcohol vapor volume decreased, the sorption amount of alcohols increased. Compared with molecules without side chains (linear 1-propanol), the sorption amount of the molecules containing side chains (branched 2-propanol) was reduced. In the high-pressure area, as the cluster size increased, the PLA film tended to swell and be plasticized, and the rate of sorption further increased. Besides, after sorption of ethanol vapor, the crystal structure of PLA film has higher thermal stability than that after sorption of 1-propanol and 2-propanol vapors. Under the treatment of alcohols with different carbon numbers, the crystal structure of PLA was positioned as an intermediate product during the rearrangement of the chain from amorphous to thermally stable α -crystal.

Similar to the vapor-induced situation, immersing PLA film in an organic solvent can also make it cloudy which indicates the occurrence of crystallization but would not change its chemical structure. Unlike vapor-induced crystallization, organic solvent-induced crystallization forms a mixture of α -crystal and β -crystal [73]. The crystal structure formed does not depend on the organic solvent but on the degree of swelling [43,56,89]. For the molecular mechanism of solvent-Induced crystallization, according to Tashiro and Yoshioka [90], the difference in the interaction strength between the polymer and organic solvent depends on the type

of solvent. The interaction between the random coil and the organic solvent causes the micro-Brownian motion of the amorphous chain. It accelerates the regularization of the random coil into a helical conformation. The short helical segments thus produced grow longer and gather to form crystal domains [96–98] as shown in **Figure 2.7**.

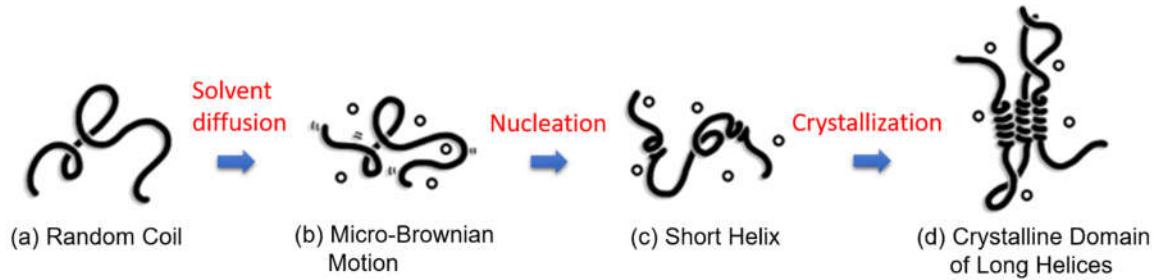


Figure 2.7 Schematic diagram of the structural evolution of solvent-induced PLA films, adapted from [90,91].

In addition to the crystal structure of PLA immersed in the organic solvents, the crystallinity also changes due to the degree of swelling. The crystallinity of polymer can be estimated by using the following equation:

$$X_c = \frac{\Delta H_m + \Delta H_c}{\Delta H_m^0} \times 100 \quad (2.26)$$

where ΔH_m is the melting enthalpy of polymer and ΔH_c is the crystallization enthalpy of polymer, and $\Delta H_m^0 = 93 \text{ J/g}$, it represents the enthalpy of the PLA crystal (L-donor 100%), which has an infinite crystal thickness [56,93].

There are also some studies on whether organic solvents such as alcohols can produce crystalline structure, thereby changing the X_c of PLA films. Sato et al. [56] found that compared with the original amorphous PLA film, the film immersed in the alcohols created a crystalline structure. Besides, as the X_c increases, the

crystal growth of the film gradually branches in a radial pattern. Iñiguez-Franco et al. [94] studied the solvent-induced crystallization and hydrolytic degradation of PLA in 50% and 95% water-ethanol solutions. They found that after immersion in the ethanol solutions at 40 °C for 15 days, the X_c increased to about 26% for both concentrations. And in 50% solution, PLA started to show higher X_c after one month due to the higher solubility of water molecules in the amorphous area of the PLA film. They reported that the changes of X_c were related to the decrease of T_g . If the T_g is lower than 40 °C, the polymer chain has sufficient mobility and tends to rearrange into a more stable crystal structure.

Figure 2.8 shows the first stage of transport of water-ethanol solution in the PLA film as the occurrence of primary crystallization. In this stage, as the release of the internal stress, the chains of PLA start to fold and form large amounts of crystallites. In the second stage, the crystallization speed becomes slow, and the chains can form small crystals dispersed in the amorphous region. In the third stage, the remaining amorphous area can be preferentially hydrolyzed, and as the degradation progresses, the net crystalline area increases [94–97]. In addition, the time and temperature of the PLA film immersing in the solution also have a certain effect on the X_c . Gao et al. [89] found that short time (50 minutes) immersion in pure ethanol at room temperature did not cause crystallization of PLA film. However, when mixed ethanol in different volume ratios with acetone, which is the most effective solvent for crystallization of amorphous PLA [98], different shapes of crystals would be produced, such as bundled spherulite and chrysanthemums-like spherulite. Besides, Naga et al. [98] found that after amorphous PLA was

immersed in methanol for 24 h, its X_c would increase to 40.3%. They also found that compared with other organic solvents such as acetone (ketone), ethyl acetate (ester), and toluene (aromatic hydrocarbon), methanol (alcohol) induces crystallization at a slower rate.

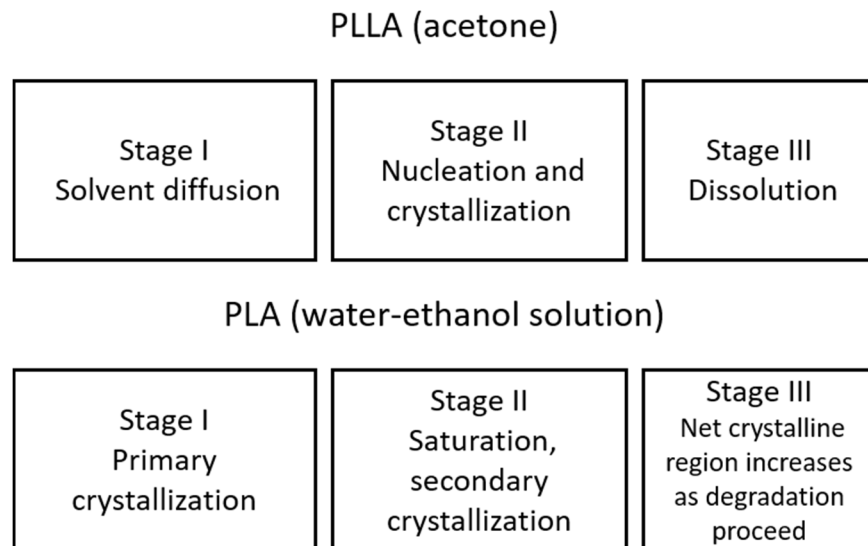


Figure 2.8 The stages of solvent-induced crystallization in polymers, adapted from [91,94,97].

2.3.3 Factors affecting changes of thermo-mechanical properties during in-situ immersion

2.3.3.1 Solvent molecular sizes

The number of carbon atoms in the main chain of straight-chain alcohols may affect the T_g of PLA immersed in the alcohol solutions. Sonchaeng et al. [67] reported that when immersed in alcohols with smaller number of carbon atoms in the main chain, the T_g 's of PLA films are lower than T_g 's of PLA films immersed in alcohols with greater number of carbon atoms, which means that smaller alcohol

molecules can diffuse faster through the free volume region. This is consistent with the general observation that the size of the penetrant in the chemically similar series is inversely proportional to the diffusion coefficient through the polymer matrix [99]. In other words, when the number of carbon atoms in the main chain of the alcohol increases, its diffusion coefficient will decrease. The decrease in the diffusion coefficient reflects the need to create a critical activation volume in the polymer that is proportional to the penetrant molecules. Moreover, some studies have shown that the activation energy of diffusion is proportional to the molecular size of the penetrant molecules [99–102].

2.3.3.2 Solvent concentration

The concentration of the alcohol solution has an effect on the X_c and T_g of the PLA film. As mentioned before, Iñiguez-Franco et al. [94] indicated that the X_c of the PLA film immersed in the 50% ethanol solution is higher than that of 95% ethanol solution, because water molecules have a higher solubility in the amorphous region thus PLA can be hydrolyzed quickly. Then, because the hydrolysis will reduce the amorphous area of PLA, the X_c will increase even if the crystalline area may remain unchanged. The hydrolysis process of PLA is shown in **Figure 2.9**. Sonchaeng et al. [67] studied the T_g changes of PLA film when immersed in different concentrations of 2-propanol /water solutions. Compared with the original T_g of PLA, the T_g of the immersed film decreased the most in pure 2-propanol. As 2-propanol concentration decreases, the reduction in T_g becomes

smaller, which shows that the mass transfer of 2-propanol in PLA is related to the concentration of the solution.

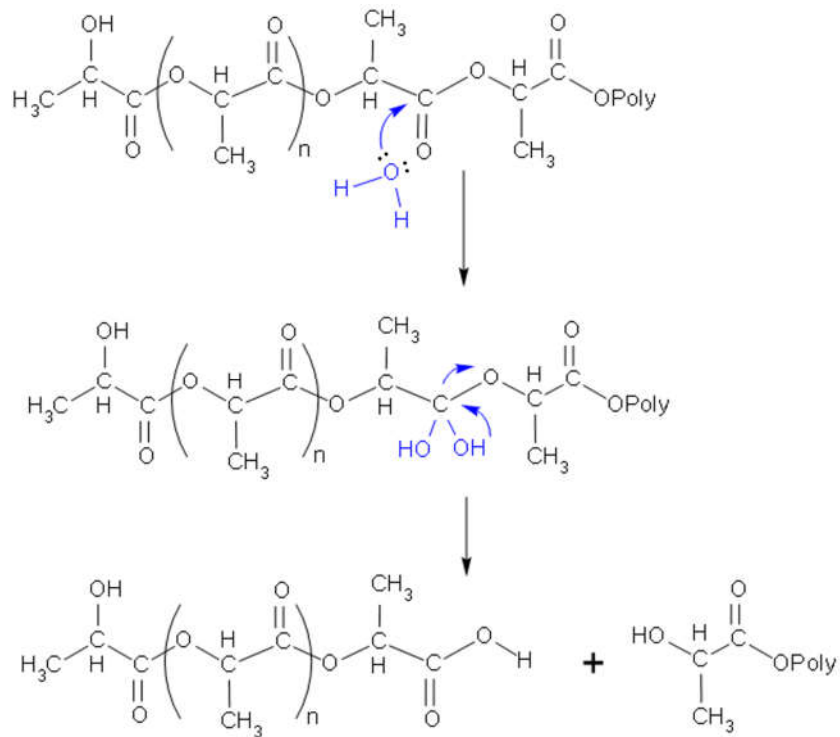


Figure 2.9 Hydrolysis of PLA, adapted from [103].

2.3.3.3 Branching of molecules

Some studies have explored the influence of the chemical structure of the solvent on the performance of PLA. As structural isomers with the same chemical formula, 1-propanol (straight-chain alcohol) and 2-propanol (branched-chain alcohol) are often selected as experimental subjects. **Figure 2.10** shows the chemical structures of 1-propanol and 2-propanol. For alcohols with a small amount of carbon, straight-chain alcohols pack more tightly than their branched isomers, but the difference in their molecular volume is not large, which is about 1.8 mL/mol [104]. Sonchaeng et al. [67] found that there was no significant

difference in the effect of immersion in 1-propanol and 2-propanol on the T_g value of PLA. However, Moriizumi et al. [43] showed that after sorption of 1-propanol and 2-propanol, PLA film formed different crystal forms during the vapor-induced crystallization process. The α and β crystal forms were formed in the PLA after sorption of 1-propanol. Only α -crystal was formed in the PLA after sorption of 2-propanol. Also, the sorption amount of 2-propanol (branched) was lower than 1-propanol (linear).

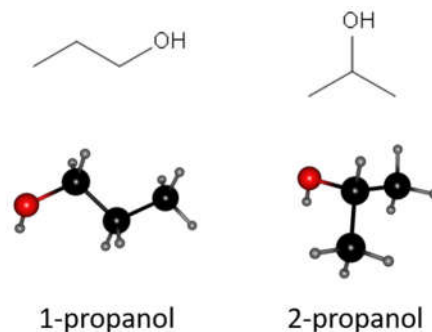


Figure 2.10 The chemical structures of 1-propanol and 2-propanol.

2.4 Applications of PLA in packaging

Since PLA has excellent biodegradability, biocompatibility, low energy consumption for production, low toxicity, good moldability due to a T_m as low as 150 °C, and mechanical properties equivalent to traditional petroleum-based polymers, it has significant advantages in commercially available bio-based thermoplastic polymers [17,74,85,105–108]. In addition, with the development of synthesis technology, routes for obtaining high molecular weight PLA have become more mature, making it easy to process and to apply in many fields including packaging. PLA has been approved for use in food packaging [17].

Currently, the main thermoforming or extrusion packaging applications of PLA include films, blister packaging, thermoforming food and beverage containers, loose-fill packaging, and compostable bags [17,23,109]. In addition, lunch boxes and fresh food packaging, as well as bottled water, juice, and yogurt packaging, are also examples of PLA packaging applications. Specifically, a Danish dairy company has used biodegradable PLA materials as their yogurt cups. The potential of PLA in antibacterial packaging applications has also been explored, such as composite films of PLA with nanoclay or other added biopolymers [17,110–113]. PLA has also some shortcomings which limit its application, such as its high brittleness, low thermal stability, low melt strength, low crystallization rate, and poor rheological properties. So, mixing PLA with cheaper fillers has become a common way to reduce costs and improve its properties [106]. For example, to improve the foam-ability of foam packaging, Liu et al. [114] found that the addition of a multi-epoxide chain extender (CE) improves the overall X_c of PLA during cooling, which has a major impact on the foam-ability. In addition, there are some other methods to modify PLA's properties, such as copolymerization and multicomponent polymer blending [115–119].

REFERENCES

REFERENCES

- [1] Sukan A., Roy I., and Keshavarz T., Dual production of biopolymers from bacteria, *Carbohydrate Polymers*, vol. 126, pp. 47–51, 2015, doi: 10.1016/j.carbpol.2015.03.001.
- [2] Ingrao C., Tricase C., Cholewa-Wójcik A., *et al.*, Polylactic acid trays for fresh-food packaging: A Carbon Footprint assessment, *Science of the Total Environment*, vol. 537, pp. 385–398, 2015, doi: 10.1016/j.scitotenv.2015.08.023.
- [3] Colwill J. A., Wright E. I., and Rahimifard S., A Holistic Approach to Design Support for Bio-polymer Based Packaging, *Journal of Polymers and the Environment*, vol. 20, no. 4, pp. 1112–1123, 2012, doi: 10.1007/s10924-012-0545-z.
- [4] Queiroz A. U. B. and Collares-Queiroz F. P., Innovation and industrial trends in bioplastics, *Polymer Reviews*, vol. 49, no. 2, pp. 65–78, 2009, doi: 10.1080/15583720902834759.
- [5] Vink E. T. H., Rabago K. R., Glassner D. A., *et al.*, Applications of life cycle assessment to NatureWorks™ polylactide (PLA) production, *Polymer Degradation and Stability*, vol. 80, pp. 403–419, 2003, doi: 10.1016/S0141-3910(02)00372-5.
- [6] Peng T., Energy Modelling for FDM 3D Printing from a Life Cycle Perspective Energy modelling for FDM 3D printing from a life cycle perspective, *International Journal of Manufacturing Research*, vol. 12, no. 1, 2017, doi: 10.1504/IJMR.2017.10003722.
- [7] Barbosa D. V and Silva W. S., Avaliação da Biodegradação em Compósitos com Fibras Naturais através de Perda de Massa e Produção de CO₂, *Revista virtual de Química*, vol. 8, no. 4, pp. 1115–1129, 2016, doi: 10.21577/1984-6835.20160080.
- [8] Kumar N., Kaur P., and Bhatia S., Advances in bio-nanocomposite materials for food packaging : a review, *Nutrition & Food Science*, vol. 47, no. 4, pp. 591–606, 2017, doi: 10.1108/NFS-11-2016-0176.
- [9] Ferreira T., Menezes F., Montagna L. S., *et al.*, Effect of lignin as accelerator of the biodegradation process of poly (lactic acid)/ lignin composites, *Materials Science and Engineering: B*, vol. 251, p. 114441, 2019, doi: 10.1016/j.mseb.2019.114441.

- [10] Sinclair R. G. and Sinclair R. G., The Case for Polylactic Acid as a Commodity Packaging Plastic, *Journal of Macromolecular Science, Part A*, vol. 33, no. 5, pp. 585–597, 1996, doi: 10.1080/10601329608010880.
- [11] Lee S. H., Kim I. Y., and Song W. S., Biodegradation of Polylactic Acid (PLA) Fibers Using Different Enzymes, *Macromolecular Research*, vol. 22, no. 6, pp. 657–663, 2014, doi: 10.1007/s13233-014-2107-9.
- [12] Auras R., Harte B., and Selke S., An overview of polylactides as packaging materials, *Macromolecular Bioscience*, vol. 4, no. 9, pp. 835–864, 2004, doi: 10.1002/mabi.200400043.
- [13] Liu X., Dever M., Fair N., and Benson R. S., Thermal and mechanical properties of poly(lactic acid) and poly(ethylene/butylene succinate) blends, *Journal of Environmental Polymer Degradation*, vol. 5, no. 4, pp. 225–235, 1997, doi: 10.1007/BF02763666.
- [14] Benninga, H., *A History of Lactic Acid Making: A Chapter in the History of Biotechnology*, 1st ed., vol. 11. Dordrecht Netherland: Kluwer Academic Publishers, 1990.
- [15] Peres C., Matos A. I., Conriot J., *et al.*, Poly (lactic acid)-based particulate systems are promising tools for immune modulation, *Acta Biomaterialia*, vol. 48, pp. 41–57, 2017, doi: 10.1016/j.actbio.2016.11.012.
- [16] Jacobsen S., Fritz H., Dege P., and Je R., New developments on the ring opening polymerisation of polylactide, *Industrial Crops and Products*, vol. 11, no. 2-3, pp. 265–275, 2000, doi: 10.1016/S0926-6690(99)00053-9.
- [17] Öz A. T., Poly (Lactic Acid) Films in Food Packaging Systems, *Food Science and Nutrition Technology*, vol. 2, no. 4, 2017, doi: 10.23880/FSNT-16000131.
- [18] Murariu M. and Dubois P., PLA composites : From production to properties, *Advanced Drug Delivery Reviews*, vol. 107, pp. 17–46, 2016, doi: 10.1016/j.addr.2016.04.003.
- [19] Vink E. T. H. and Davies S., Life Cycle Inventory and Impact Assessment Data for 2014 Ingeo™ Polylactide Production, *Industrial Biotechnology*, vol. 11, no. 3, pp. 167–180, 2015, doi: 10.1089/ind.2015.0003.
- [20] Slomkowski S., Penczek S., and Duda A., Polylactides — an overview, *Polymers for Advanced Technologies*, vol. 25, no. 5, 2014, doi: 10.1002/pat.3281.

- [21] Guo F., Li Q. and Zhou C., *et al.*, Synthesis and Biological Application of fluoro-modified nucleic acids, *Organic & Biomolecular Chemistry*, vol. 15, no. 45, pp. 9552–9565, 2020, doi: 10.1039/c7ob02094e.
- [22] Fukushima K. and Kimura Y., An Efficient Solid-State Polycondensation Method for Synthesizing Stereocomplexed Poly (Lactic Acid) s with High Molecular Weight, *Journal of Polymer Science Part A: Polymer Chemistry*, vol. 46, no. 11, pp. 3714–3722, 2008, doi: 10.1002/pola.22712.
- [23] Nampoothiri K. M., Nair N. R., and John R. P., Bioresource Technology An overview of the recent developments in polylactide (PLA) research, *Bioresource Technology*, vol. 101, no. 22, pp. 8493–8501, 2010, doi: 10.1016/j.biortech.2010.05.092.
- [24] Xiao L., Wang B., Yang G., and Gauthier M., Poly (Lactic Acid)-Based Biomaterials : Synthesis, Modification and Applications, *Biomedical Science, Engineering and Technology*, 2012, doi: 10.5772/23927.
- [25] Taguchi S., Current advances in microbial cell factories for lactate-based polyesters driven by lactate-polymerizing enzymes : Towards the further creation of new LA-based polyesters, *Polymer Degradation and Stability*, vol. 95, no. 8, pp. 1421–1428, 2010, doi: 10.1016/j.polymdegradstab.2010.01.004.
- [26] Msuya N., Poly (lactic-acid) Production_from Monomer to Polymer : A Review, *SciFed Journal of Polymer Science*, vol. 1, pp. 1–15, 2018.
- [27] Ribeiro C., Sencadas V., and miguel costa C., Tailoring the morphology and crystallinity of poly(L-lactide acid) electrospun membranes, *Science and Technology of Advanced Materials*, vol. 12, no. 1, pp. 015001, 2011, doi: 10.1088/1468-6996/12/1/11660947.
- [28] Kishida H., Hasegawa T. and Nomura N., *et al.*, "Method to produce semi-crystalline polylactides", U.S. Patent, 9284403B2, 2014.
- [29] Gnanou Y. and Fontanille M., Thermomechanical Properties of Polymers, *Organic and Physical Chemistry of Polymers.*, pp. 401–426, 2008, doi: 10.1002/9780470238127.ch11.
- [30] Wunderlich B., Reversible crystallization and the rigid-amorphous phase in semicrystalline macromolecules, *Progress in Polymer Science*, vol. 28, no. 3, pp. 383–450, 2003, doi: 10.1016/S0079-6700(02)00085-0.

- [31] Righetti M. C. and Tombari E., Thermochemical Acta Crystalline , mobile amorphous and rigid amorphous fractions in poly (L-lactic acid) by TMDSC, *Thermochemical Acta*, vol. 522, no. 1–2, pp. 118–127, 2011, doi: 10.1016/j.tca.2010.12.024.
- [32] Monnier X., Cavallo D., Righetti M. C., *et al.*, Physical Aging and Glass Transition of the Rigid Amorphous Fraction in Poly(L-Lactic acid), *Macromolecules*, 2020, doi: 10.1021/acs.macromol.0c01182.
- [33] Sonchaeng U., Iniguez-Franco F. and Auras R., *et al.*, Progress in Polymer Science Poly (lactic acid) mass transfer properties, *Progress in Polymer Science*, vol. 86, pp. 85–121, 2018, doi: 10.1016/j.progpolymsci.2018.06.008.
- [34] Iniguez-Franco F., Hydrolytic degradation of neat and modified poly(lactic acid) with nanoparticles and chain extenders by water-ethanol solutions, PhD thesis, Michigan State University, Michigan, 2018, doi:10.25335/M5SN01677.
- [35] Di Lorenzo M. L. and Righetti M. C., Crystallization-induced formation of rigid amorphous fraction, *Polymer Crystallization*, vol. 1, no. 2, pp. 1–14, 2018, doi: 10.1002/pcr2.10023.
- [36] Drive F. and States U., Direct Calorimetric Observation of the Rigid Amorphous Fraction in a Semiconducting Polymer, *The Journal of Physical Chemistry Letters*, vol. 9, no. 5, pp. 8–13, 2018, doi: 10.1021/acs.jpcllett.7b03110.
- [37] Suzuki H., Grebowicz J., and Wunderlich B., Glass Transition of Poly(oxymethylene), *British Polymer Journal*, vol. 17, no. 1, pp. 1–3, 1985, doi: 10.1002/pi.4980170101.
- [38] Martin S., Exposito M. T., Vega J. F. & Martinez-Salazar J., Microstructure and Properties of Branched Polyethylene : Application of a Three-Phase Structural Model, *Journal of Applied Polymer Science*, pp. 1–8, 2012, doi: 10.1002/app.38290.
- [39] Drieskens M., Peeters R., Mullens J., *et al.*, Structure Versus Properties Relationship of Poly (lactic acid). I . Effect of Crystallinity on Barrier Properties, *Journal of Polymer Science Part B: Polymer Physics*, vol. 47, no. 22, pp. 2247–2258, 2009, doi: 10.1002/polb.21822.
- [40] Guinault A., Sollogoub C., Ducruet V., *et al.*, Impact of Crystallinity of Poly (lactide) on Helium and Oxygen Barrier Properties, *European Polymer*

Journal, vol. 48, no. 4, pp. 779–788, doi: 10.1016/j.eurpolymj.2012.01.014.

- [41] Sasaki S. and Asakura T., Helix Distortion and Crystal Structure of the R - Form of Poly (L -lactide), *Macromoleculars*, vol. 36, no. 22, pp. 8385–8390, 2003, doi: 10.1021/ma0348674.
- [42] Tashiro K., Kouno N., Wang H. & Tsuji H., Crystal Structure of Poly(lactic acid) Stereocomplex: Random Packing Model of PDLA and PLLA Chains As Studied by X-ray Diffraction Analysis, *Macromoleculars*, vol. 50, no. 20, pp. 8048–8065, 2017, doi: 10.1021/acs.macromol.7b01468.
- [43] Moriizumi Y. and Nagai K., Vapor-induced Crystallization in Alcoholic Sorption using Poly (lactic acid) Films, *Journal of Applied Membrane Science & Amp; Technology*, vol. 22, no. 2, pp. 65–84, 2018, doi: 10.11113/amst.v22n2.125.
- [44] De Rosa C., Guerra G., Petraccone V., and Corradini P., Crystal Structure of the Emptied Clathrate Form (δ_e Form) of Syndiotactic Polystyrene, *Macromolecules*, vol. 30, no. 14, pp. 4147–4152, 1997, doi: 10.1021/ma970061q.
- [45] Puiggali J., Ikada Y., Tsuji H., *et al.*, The Frustrated Structure of Poly (L-lactide), *Polymer*, vol. 41, no. 25, pp. 8921–8930, 2000, doi: 10.1016/s0032-3861(00)00235-4.
- [46] Hoogsteen W., Postema A. R., Pennings A. J., and Brinke G., Crystal Structure, Conformation, and Morphology of Solution-Spun Poly (L-lactide) Fibers, *Macromoleculars*, vol. 23, no. 2, pp. 634–642, 1990, doi: 10.1021/ma00204a041.
- [47] Tábi T., Hajba S., and Kovács J. G., Effect of crystalline forms (α' and α) of poly(lactic acid) on its mechanical, thermo-mechanical, heat deflection temperature and creep properties, *European Polymer Journal*, vol. 82, pp. 232–243, 2016, doi: 10.1016/j.eurpolymj.2016.07.024.
- [48] Cartier L., Okihara T., Ikada Y., *et al.*, Epitaxial crystallization and crystalline polymorphism of polylactides, *Polymer*, vol. 41, no. 25, pp. 8909–8919, 2000, doi: 10.1016/s0032-3861(00)00234-2.
- [49] Saeidlou S., Huneault M. A., Li H., and Park C. B., Progress in Polymer Science Poly (lactic acid) crystallization, *Progress in Polymer Science*, vol. 37, no. 12, pp. 1657–1677, 2012, doi: 10.1016/j.progpolymsci.2012.07.005.

- [50] Zhou W., Stoichiometry and crystal structure of poly(lactic acid) (PLA) stereocomplex (SC) in cold-crystallization and solution-grown crystals as studied by solid-state NMR and ¹³C isotope labeling, Master thesis, The University of Akron, Ohio, 2018.
- [51] Lunt J., Large-scale production, properties and commercial applications of poly lactic acid polymers, *Polymer Degradation and Stability*, vol. 59, no. 1–3, pp. 145–152, 1998, doi: 10.1016/s0141-3910(97)00148-1.
- [52] Middleton J. C. and Tipton A. J., Synthetic biodegradable polymers as orthopedic devices, *Biomaterials*, vol. 21, no. 23, pp. 2335–2346, 2000, doi:10.1016/s0142-9612(00)00101-0.
- [53] Stolt M. and Södergård A., Properties of lactic acid based polymers and their correlation with composition, *Progress in Polymer Science*, vol. 27, no. 6, 2002.
- [54] Zhao Y. L., Cai Q., Jiang J., *et al.*, Synthesis and thermal properties of novel star-shaped poly(L-lactide)s with starburst PAMAM-OH dendrimer macroinitiator, *Polymer*, vol. 43, no. 22, pp. 5819–5825, 2002, doi: 10.1016/S0032-3861(02)00529-3.
- [55] Pitet L. M., Hait S. B., Lanyk T. J., and Knauss D. M., Linear and branched architectures from the polymerization of lactide with glycidol, *Macromolecules*, vol. 40, no. 7, pp. 2327–2334, 2007, doi: 10.1021/ma0618068.
- [56] Sato S., Gondo D., Wada T., *et al.*, Effects of various liquid organic solvents on solvent-induced crystallization of amorphous poly(lactic acid) film, *Journal of Applied Polymer Science*, vol. 129, no. 3, pp. 1607–1617, 2013, doi: 10.1002/app.38833.
- [57] Sonchaeng U., Iñiguez-Franco F., Auras R., *et al.*, Poly(lactic acid) mass transfer properties, *Progress in Polymer Science*, vol. 86, pp. 85–121, 2018, doi: 10.1016/j.progpolymsci.2018.06.008.
- [58] Vandenburg H. J., Clifford A. A., Bartle K. D., *et al.*, A simple solvent selection method for accelerated solvent extraction of additives from polymers, *The Analyst*, vol. 124, no. 11, pp. 1707–1710, 1999.
- [59] Barton A. F. M., *CRC Handbook of Solubility Parameters and Other Cohesion Parameters*. Boca Raton, Florida: CRC Press, Inc, 1983.

- [60] Adamska K., Voelkel A., and Berli A., The solubility parameter for biomedical polymers — Application of inverse gas chromatography, *Journal of Pharmaceutical and Biomedical Analysis*, vol. 127, pp. 202–206, 2016, doi: 10.1016/j.jpba.2016.04.014.
- [61] Fink J. K., *Reactive Polymers Fundamentals and Applications*, 2nd ed., William Andrew Publishing, 2017.
- [62] Chasib K. F. and Kadhim B. M., Prediction of The Behavior for Polymer Blends Using Thermodynamic Model, *Juniper Publishers*, vol. 6, no. 5, 2019, doi: 10.19080/RAPSCI.2019.06.555699.
- [63] Hansen C. M., Polymer additives and solubility parameters, *Progress in Organic Coatings*, vol. 51, no. 2, pp. 109–112, 2004, doi: 10.1016/j.porgcoat.2004.05.003.
- [64] Agata Y. and Yamamoto H., Determination of Hansen solubility parameters of ionic liquids using double-sphere type of Hansen solubility sphere method, *Chemical Physics*, vol. 513, pp. 165–173, 2018, doi: 10.1016/j.chemphys.2018.04.021.
- [65] Hansen C. M., *Hansen solubility parameters: a user's handbook.*, 2nd ed., Boca Raton: CRC Press, Taylor & Francis Group, 2018.
- [66] Terada M. and Marchessault R. H., Determination of solubility parameters for poly (3-hydroxyalkanoates), *International Journal of Biological Macromolecules*, vol. 25, pp. 207–215, 1999, doi: 10.1016/s0141-8130(99)00036-7.
- [67] Sonchaeng U., Critical and systematic review of poly (lactic acid) mass transfer and evaluation of the *in-situ* changes of its thermo-mechanical properties when immersed in alcohol solutions, PhD thesis, Michigan State University, Michigan, 2019, doi: 10.25335/76kp-yt65.
- [68] Strivens T. A. and Lambourne R., *Paint and Surface Coatings: Theory and Practice*, 2nd ed., Cambridge: Woodhead Publ. Ltd, 1999, pp. 166–184.
- [69] Sanchez-Lengeling B., Roch L. M., Perea J. D., *et al.*, A Bayesian Approach to Predict Solubility Parameters, *Advanced Theory Simulations*, vol. 2, no. 1, 2019, doi: 10.1002/adts.201800069.
- [70] Rowe R. C., White E. F. T., Division I. C. I. P., *et al.*, The solubility parameters of some cellulose derivatives and polyethylene glycols used in tablet film

coating, *International Journal of Pharmaceutics*, vol. 31, no. 1–2, pp. 175–177, 1986, doi: 10.1016/0378-5173(86)90229-2.

- [71] Lindvig T., Michelsen M. L., and Kontogeorgis G. M., A Flory-Huggins model based on the Hansen solubility parameters, *Fluid Phase Equilibria*, vol. 203, no. 1–2, pp. 247–260, 2002, doi: 10.1016/S0378-3812(02)00184-X.
- [72] Gee G., The interaction between rubber and liquids. IX. The elastic behaviour of dry and swollen rubbers, *Transactions of the Faraday Society*, vol. 42, pp. 585–598, 1946, doi: 10.1039/TF9464200585.
- [73] Udayakumar M., Kollár M., Kristály F., *et al.*, Temperature and time dependence of the solvent-induced crystallization of poly(L-lactide), *Polymers*, vol. 12, no. 5, pp. 1–16, 2020, doi: 10.3390/POLYM12051065.
- [74] Shinkawa Y., Hayashi Y., Sato S., and Nagai K., Permeability of ethanol solution through poly (lactic acid) film, *Applied Polymer Science*, vol. 132, no. 23, pp. 1–9, 2015, doi: 10.1002/app.42031.
- [75] Egashira K. AND Nishi N., Low-Frequency Raman Spectroscopy of Ethanol - Water Binary Solution : Evidence for Self-Association of Solute and Solvent Molecules, *The Journal of Physical Chemistry B*, vol. 102, no. 21, pp. 4054–4057, 1998, doi: 10.1021/jp9806359.
- [76] Radovanovic P., Thiel S. W. & Hwang S.-T., Transport of ethanol-water dimers in pervaporation through a silicone rubber membrane, *Journal of Membrane Science*, vol. 48, no. 1, pp. 55–65, 1990, doi: 10.1016/s0376-7388(00)80795-4.
- [77] Nose A. and Hojo M., Alcoholic Beverage Consumption and Health: Interaction between water and ethanol via hydrogen bonding in alcoholic beverages, *Nova Science Publishers*, 2009.
- [78] Patz C., Molecular level structure in water-alcohol mixtures ; from shots to pints : L' Chaim!, Master thesis, Iowa State University, Iowa, 2016.
- [79] Proikakis C. S., Mamouzelos N. J., Tarantili P. A., and Andreopoulos A. G., Swelling and hydrolytic degradation of poly(d,l-lactic acid) in aqueous solutions, *Polymer Degradation and Stability*, vol. 91, no. 3, pp. 614–619, 2006, doi: 10.1016/j.polymdegradstab.2005.01.060.
- [80] Andreopoulos A. G., Hatzi E., Doxastakis M., Synthesis and properties of poly (lactic acid), *Journal of Materials Science: Materials in Medicine*, vol. 10,

no. 1, pp. 29–33, 1999, doi: 10.1023/a:1008887910068.

- [81] Drioli E., Giorno L. and Fontananova E., *Comprehensive Membrane Science and Engineering*, 2nd ed, Amsterdam: Elsevier, 2017.
- [82] Kujawski W., Application of Pervaporation and Vapor Permeation in Environmental Protection, *Polish Journal of Environmental Studies*, vol. 9, no. 1, pp. 13–26, 2000.
- [83] Ulutan S. and Nakagawa T., Separability of ethanol and water mixtures through PTMSP–silica membranes in pervaporation, *Journal of Membrane Science*, vol. 143, no. 1–2, pp. 275–284, 1998, doi: 10.1016/s0376-7388(98)00022-2.
- [84] Aptel P., Cuny J., Jozefonvicz J., *et al.*, Liquid Transport Through Membranes Prepared by Grafting of Polar Monomers onto Distribution in Membrane During Pervaporation, *Journal of Applied Polymer Science*, vol. 18, pp. 365–378, 1974, doi: 10.1002/app.1974.070180205.
- [85] Komatsuka T., Kusakabe A., and Nagai K., Characterization and gas transport properties of poly (lactic acid) blend membranes, *DES*, vol. 234, no. 1–3, pp. 212–220, 2008, doi: 10.1016/j.desal.2007.09.088.
- [86] Goodrich T. B. F., Diffusion of Organic Vapors at Low Concentrations of Chemical [II], vol. 10, 1982.
- [87] Sato S., Wada T., Ido R., *et al.*, Dependence of alcohol vapor-induced crystallization on gas and vapor permeabilities of poly(lactic acid) films, *Journal of Applied Polymer Science*, vol. 131, no. 8, pp. 1–9, 2014, doi: 10.1002/app.40140.
- [88] Paksoy Halime Ö, Thermal energy storage for sustainable energy consumption: Fundamentals, case studies and design, Dordrecht: Springer, 2007.
- [89] Gao J., Duan L., Yang G., *et al.*, Applied Surface Science Manipulating poly (lactic acid) surface morphology by solvent-induced crystallization, *Applied Surface Science*, vol. 261, pp. 528–535, 2012, doi: 10.1016/j.apsusc.2012.08.050.
- [90] Tashiro K. and Yoshioka A., Molecular Mechanism of Solvent-Induced Crystallization of Syndiotactic Polystyrene Glass. 2. Detection of Enhanced Motion of the Amorphous Chains in the Induction Period of Crystallization,

Macromolecules, vol. 35, no. 2, pp. 410–414, 2002.

- [91] Wu N., Lang S., Zhang H., *et al.*, Solvent-Induced Crystallization Behaviors of PLLA Ultrathin Films Investigated by RAIR Spectroscopy and AFM Measurements, *The Journal of Physical Chemistry B*, vol. 118, no. 44, pp. 12652–12659, 2014, doi: 10.1021/jp506840e.
- [92] Yoshioka A. and Tashiro K., Solvent Effect on the Glass Transition Temperature of Syndiotactic Polystyrene Viewed from Time-Resolved Measurements of Infrared Spectra at the Various Temperatures and Its Simulation by Molecular Dynamics Calculation, *Macromolecules*, vol. 37, no.2, pp. 467–472, 2004, doi: 10.1021/ma035505z.
- [93] Fischer B. E. W., Sterzel H. J., and Wegner G., Investigation of the structure of solution grown crystals of lactide copolymers by means of chemical reactions, vol. 990, pp. 980–990, 1973.
- [94] Iñiguez-Franco F., Auras R., Burgess G., Holmes D., *et al.*, Concurrent solvent induced crystallization and hydrolytic degradation of PLA by water-ethanol solutions, *Polymer*, vol. 99, pp. 315–323, 2016, doi: 10.1016/j.polymer.2016.07.018.
- [95] Ouyang H., Lee W., Ouyang W., *et al.*, Solvent-Induced Crystallization in Poly (ethylene terephthalate) during Mass Transport: Mechanism and Boundary Condition, *Macromolecules*, vol. 37, no. 20, pp. 7719–7723, 2004, doi: 10.1021/ma0400416.
- [96] Lee W., Ouyang H., Shih M., and Wu M., Kinetics of Solvent-Induced Crystallization of Poly (ethylene terephthalate) at the Final Stage, *Journal of Polymer Research*, vol. 10, no. 2, pp. 133–137, 2003, doi: 10.1023/A:1024917228811.
- [97] Ouyang H., Lee W., and Shih M., Three Stages of Crystallization in Poly (ethylene terephthalate) during Mass Transport, *Macromolecules*, vol. 35, no. 22, pp. 8428–8432, 2002, doi: 10.1021/ma020851m.
- [98] Naga N., Yoshida Y., Inui M., *et al.*, Crystallization of Amorphous Poly (lactic acid) Induced by Organic Solvents, *Journal of Applied Polymer Science*, vol. 119, no. 4, pp. 2058–2064, 2011, doi: 10.1002/app.32890.
- [99] Rogers C. E., *Polymer Permeability*. Dordrecht: Springer Netherlands, 1985.
- [100] Crank J., *The mathematics of diffusion*, 2nd ed. Oxford: Clarendon Press,

1975.

- [101] Crank J. and Park G. S., *Diffusion in Polymers*. New York: Academic Press, 1968.
- [102] Fox D., Labes M. M., and Weissberger A., *Physics and Chemistry of the Organic Solid State (Volume 2)*, New York: Interscience, 1965.
- [103] Farah S., Anderson D. G., and Langer R., Physical and mechanical properties of PLA , and their functions in widespread applications — A comprehensive review, *Advanced Drug Delivery Reviews*, vol. 107, pp. 367–392, 2016, doi: 10.1016/j.addr.2016.06.012.
- [104] Walz M.-M., Werner J., Ekholm V., *et al.*, Alcohols at the aqueous surface: chain length and isomer effects, *Physical Chemistry Chemical Physics*, vol. 18, no. 9, pp. 6648–6656, 2016, doi: 10.1039/C5CP06463E.
- [105] Li F., Tan L., Zhang S., and Zhu B., Compatibility , steady and dynamic rheological behaviors of polylactide/poly (ethylene glycol) blends, *Journal of Applied Polymer Science*, vol. 133, no. 4, pp. 1–10, 2016, doi: 10.1002/app.42919.
- [106] Lagarón J. M., López-rubio A., and José Fabra M., Bio-based Packaging, *Journal of Applied Polymer Science*, vol. 133, no. 2, 2015, doi: 10.1002/app.42971.
- [107] Vert M., Dos Santos I., Ponsart S., *et al.*, Degradable polymers in a living environment: Where do you end up?, *Polymer International*, vol. 51, no. 10, pp. 840–844, 2002, doi: 10.1002/pi.903.
- [108] Yang H. S., Yoon J. S., and Kim M. N., Dependence of biodegradability of plastics in compost on the shape of specimens, *Polymer Degradation and Stability*, vol. 87, no. 1, pp. 131–135, 2005, doi: 10.1016/j.polymdegradstab.2004.07.016.
- [109] Tullo A., Plastic found at the end of the maize, *Chemical & Engineering News*, vol. 78, no. 3, p. 13, 2000, doi: 10.1021/cen-v078n003.p013.
- [110] Fei Y., Wang H., Gao W., *et al.*, Antimicrobial activity and mechanism of PLA / TP composite nanofibrous films, *The Journal of the Textile Institute*, vol. 105, no. 2, 2013, doi: 10.1080/00405000.2013.834573.
- [111] Li W., Coffin D. R., Jin T. Z., *et al.*, Biodegradable Composites from Polyester

and Sugar Beet Pulp with Antimicrobial Coating for Food Packaging, *Journal of Applied Polymer Science*, 2012, doi: 10.1002/app.

- [112] Rhim J., Hong S., and Ha C., Tensile , water vapor barrier and antimicrobial properties of PLA/nanoclay composite films, *LWT - Food Science and Technology*, vol. 42, no. 2, pp. 612–617, 2009, doi: 10.1016/j.lwt.2008.02.015.
- [113] Mustapha A., Ariyapitipun T. and Clarke A.D., Survival of Escherichia Coli 0157 : H7 on Vacuum-Packaged Raw Beef Treated with Polylactic Acid, Lactic Acid, and Nisin, *Journal of Food Science*, vol. 67, no. 1, pp. 262–267, doi: 10.1111/j.1365-2621.2002.tb11395.x
- [114] Liu B., Du Z., Wang X., *et al.*, Crystallization Kinetics of Chain Extended Poly (lactic acid)/ Clay Nanocomposites, *Polymer Composites*, vol. 36, no. 11, 2015, doi: 10.1002/pc.23123.
- [115] Tasaka F., Ohya Y., and Ouchi T., One-Pot Synthesis of Novel Branched Polylactide Through the Copolymerization of Lactide with Mevalonolactone, *Macromolecular Rapid Communication*, vol. 22, no. 11, pp. 820–824, 2001, doi: 10.1002/1521-3927(20010701)22:11<820::aid-marc820>3.0.co;2-7.
- [116] Zhang K., Mohanty A. K., and Misra M., Fully Biodegradable and Biorenewable Ternary Blends from Polylactide , Poly (3-hydroxybutyrate-co-hydroxyvalerate) and Poly (butylene succinate) with Balanced Properties, *ACS Applied Materials & Interfaces*, vol. 4, no. 6, pp. 3091–3101, 2012, doi: 10.1021/am3004522.
- [117] Kulinski Z., Piorkowska E., Gadzinowska K., and Stasiak M., Plasticization of Poly (L-lactide) with Poly (propylene glycol), *Biomacromolecules*, vol. 7, no. 7, pp. 2128–2135, 2006, doi: 10.1021/bm060089m.
- [118] Jing Z., Shi X., Zhang G., and Lei R., Investigation of poly (lactide) stereo-complexation between linear poly (L-lactide) and PDLA-PEG-PDLA tri-block copolymer, *Polymer International*, vol. 64, no. 10, 2015, doi: 10.1002/pi.4932.
- [119] Shi X., Qin J., Wang L., *et al.*, Introduction of stereocomplex crystallites of PLA for the solid and microcellular poly(lactide)/ poly(butylene adipate-co-terephthalate) blends, *RSC Advances*, vol. 8, no. 22, pp. 11850–11861, 2018, doi: 10.1039/C8RA01570H.

CHAPTER 3 Experimental

3.1 Materials

Poly(lactic acid) - PLA Ingeo™ 2003D resin supplied by NatureWorks LLC, (Minnetonka, MN, USA) was used to produce PLA cast film. Alcohols used as solvents in the immersion test were straight-chain alcohols with the number of carbon atoms C1–C4 in main chains (i.e., methanol, ethanol, 1-propanol, 1-butanol), branched-chain alcohol (2-propanol). All the alcohols were purchased from Sigma-Aldrich (St. Louis, MO, USA). **Table 3.1** shows alcohols used in this study. HPLC grade water (VWR, Radnor, PA, USA) and deuterium oxide (D₂O, 99.9 atom % D, Sigma-Aldrich) were used as solvent mixtures with the alcohols for the immersion test.

Table 3.1 Properties of alcohols used for immersion tests.

Alcohols	Linear Formula	Main chain #C	Boiling point (°C)	Molecular weight (g/mol)	T_g (°C)	ΔC_p (T_g) $J/(mol \cdot K)$
methanol	CH ₃ OH	1	65	32.04	-170.4	30.0
ethanol	CH ₃ CH ₂ OH	2	79	46.07	-176.1	35.3
1-propanol	CH ₃ CH ₂ CH ₂ OH	3	97	60.10	-173.3	45.0
2-propanol	(CH ₃) ₂ CHOH	3	82	60.10	-158.0	46.0
1-butanol	CH ₃ (CH ₂) ₃ OH	4	118	74.12	-161.5	48.0

Data adapted from manufacturers' data sheets [1–3].

Figure 3.1 shows the chemical structure of water and all the alcohols used in this study. **Table 3.2** shows the production information of the solvents used in the immersion test.

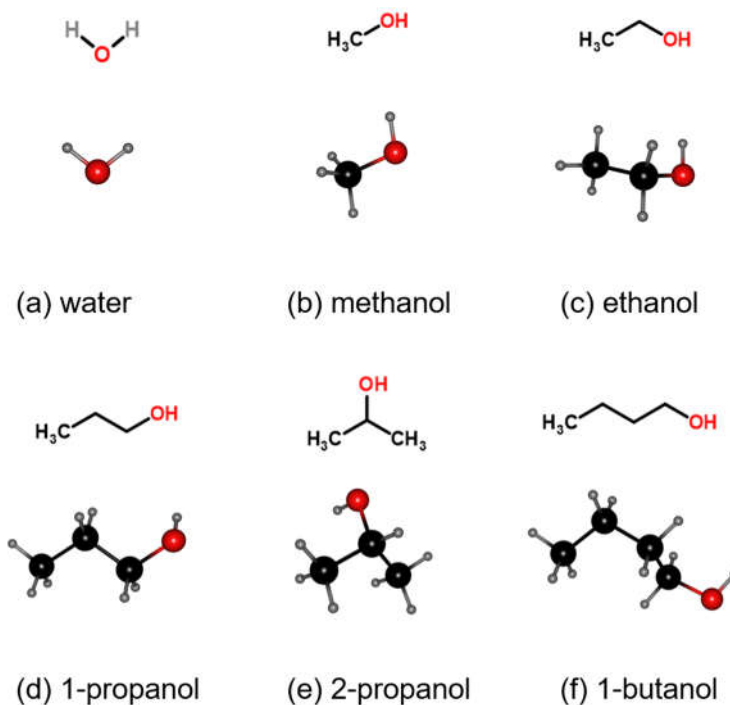


Figure 3.1 Structure of alcohols used in immersion tests.

Table 3.2 Product information of solvents used for immersion tests.

Solvents	Grade	Manufacturer	CAS
methanol	HPLC grade, $\geq 99.9\%$	Sigma-Aldrich	67-56-1
ethanol	200 proof, HPLC/spectrophotometric	Sigma-Aldrich	64-17-5
1-propanol	ACS reagent, $\geq 99.5\%$	Sigma-Aldrich	71-23-8
2-propanol	ACS reagent, $\geq 99.5\%$	Sigma-Aldrich	67-63-0

Table 3.2 (cont'd)

Solvents	Grade	Manufacturer	CAS
1-butanol	ACS reagent, $\geq 99.4\%$	Sigma-Aldrich	71-36-3
water (H ₂ O)	HPLC grade	VWR	7732-18-5
deuterium oxide (D ₂ O)	99.9 atom % D	Sigma-Aldrich	7789-20-0

Data adapted from manufacturers' datasheets [1–3].

Deuteriochloroform (CDCl₃, 99.8 atom % D) purchased from Sigma-Aldrich was used as a standard purity solvent for nuclear magnetic resonance (NMR) analyses. Hexamethylcyclotrisiloxane (C₆H₁₈O₃Si₃, 98%) was obtained from Sigma Aldrich and used as an internal standard in quantitative nuclear magnetic resonance (qNMR). The structure of C₆H₁₈O₃Si₃ is shown in **Figure 3.2**.

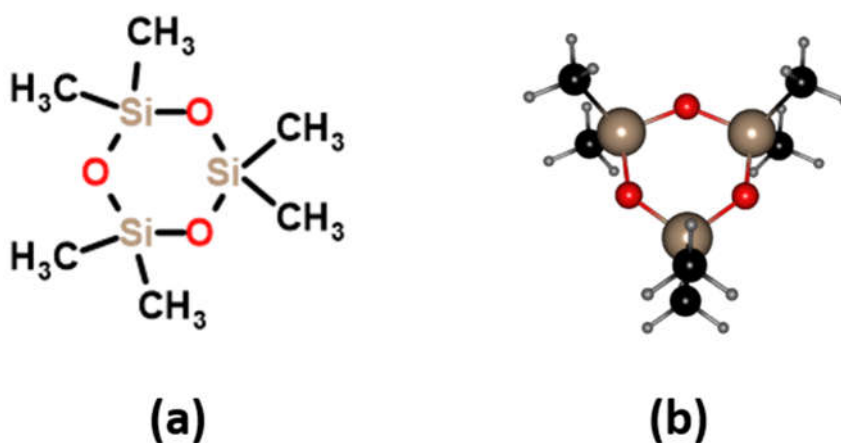


Figure 3.2 Structure of hexamethylcyclotrisiloxane, (a) chemical structure (b) 3-D chemical structure, adapted from [4].

3.2 Methods

3.2.1 PLA film production

3.2.1.1 Cast film

PLA cast film was produced by a micro extruder supplied by Randcastle Extrusion Systems, Inc. (Cedar Grove, NJ, USA) at 193–215 °C and 49 rpm. The volume of the instrument is 34 cc. The screw diameter and working L/D isomer ratio are 1.5875 cm and 24:1, respectively. PLA pellets were dried in a vacuum oven at 60 °C for 24 h before extruding the film. The thickness of the produced PLA film varied from 15 to 25 μm . PLA films were stored in a refrigerator (-20 °C) and conditioned at 23 °C (50% RH) for 24 h before use to minimize physical aging [3]. The production procedure of PLA films is shown in **Figure 3.3**.

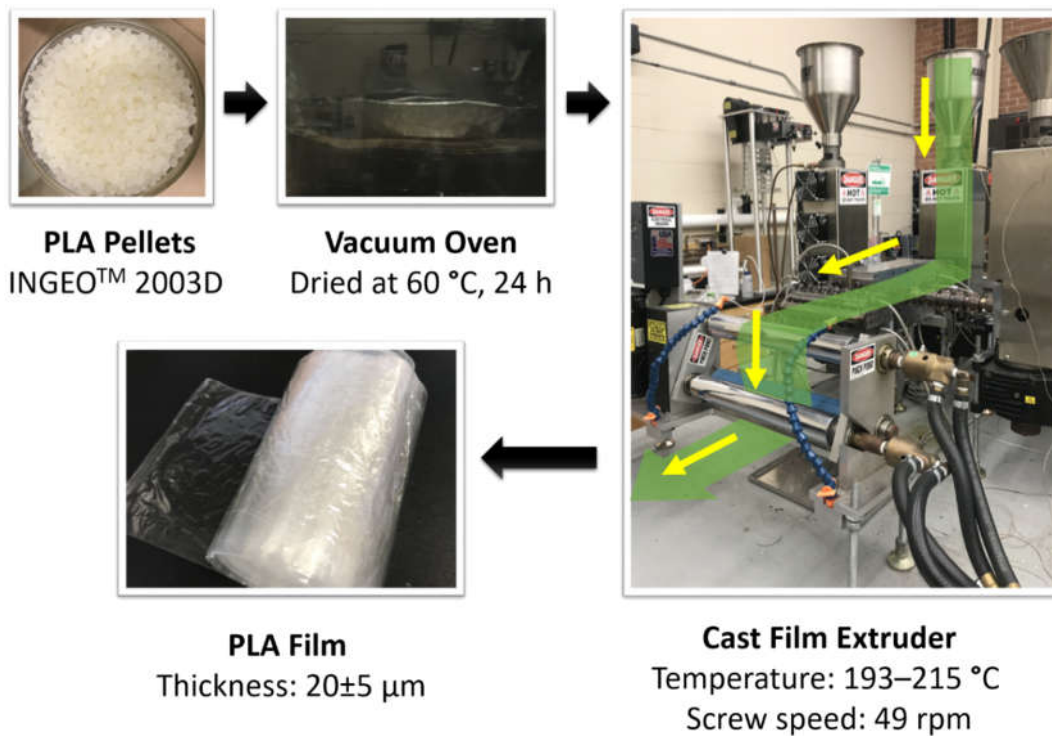


Figure 3.3 Production of PLA film.

3.2.1.2 Production of PLA amorphous film

To ensure that the PLA film was totally amorphous, a hot pressing process was performed on the PLA film by using manual hydraulic compression presses (PHI, City of Industry, CA, USA). The heating temperature was set as 160 °C which is higher than the T_m of the PLA samples (150 °C), and the heating time was 10 minutes.

Two layers of Teflon (polytetrafluoroethylene—PTFE) were used to clamp the original PLA film. After hot pressing, the film was cooled immediately to prevent crystallization during the cooling process. The cold platens were used to cool the hot PLA film. The hot-pressing process is shown in **Figure 3.4**.

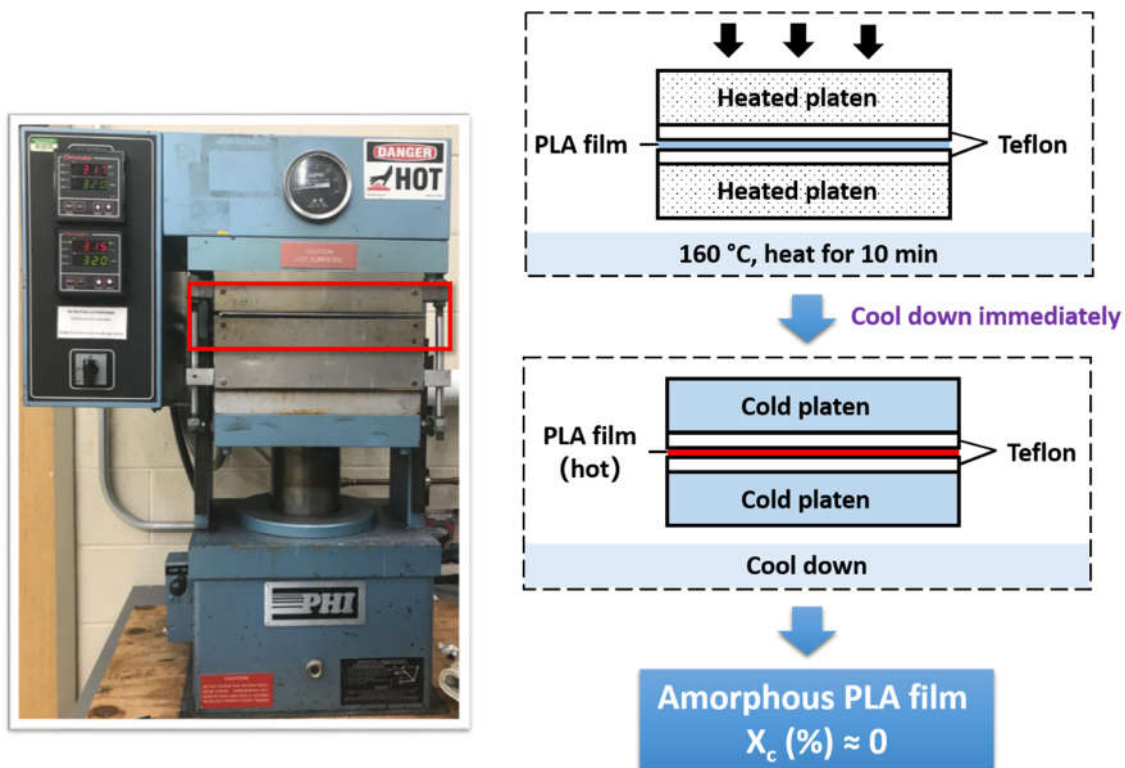


Figure 3.4 Hot pressing process of PLA film. X_c denotes percent crystallinity.

3.2.2 *Thermo-mechanical property measurements*

3.2.2.1 Dynamic mechanical analysis (DMA)

To measure the thermo-mechanical properties of the PLA films, an RSA-G2 Solids Analyzer (TA Instruments, New Castle, DE, USA) DMA instrument was used. The films were tested before and during the immersion process. Parameters of the DMA test were set as follows: preload force 100 g, strain 0.2%, loading gap 15 mm, max gap changes up 5–10 mm, max gap changes down 1 mm, frequency 1 Hz, temperature ramp rate 5 °C/min with the set temperature range -5 °C – 100 °C [3].

Figure 3.5 shows the dry system and immersion system of DMA test. The sample size of PLA films was 10 mm x 50 mm. The temperature ramp started at 25 °C for the dry environment and 5 °C for the immersions condition, respectively. Before starting each immersion test, the alcohol solvents were precooled to 5 °C. Liquid nitrogen was used to control the temperature.

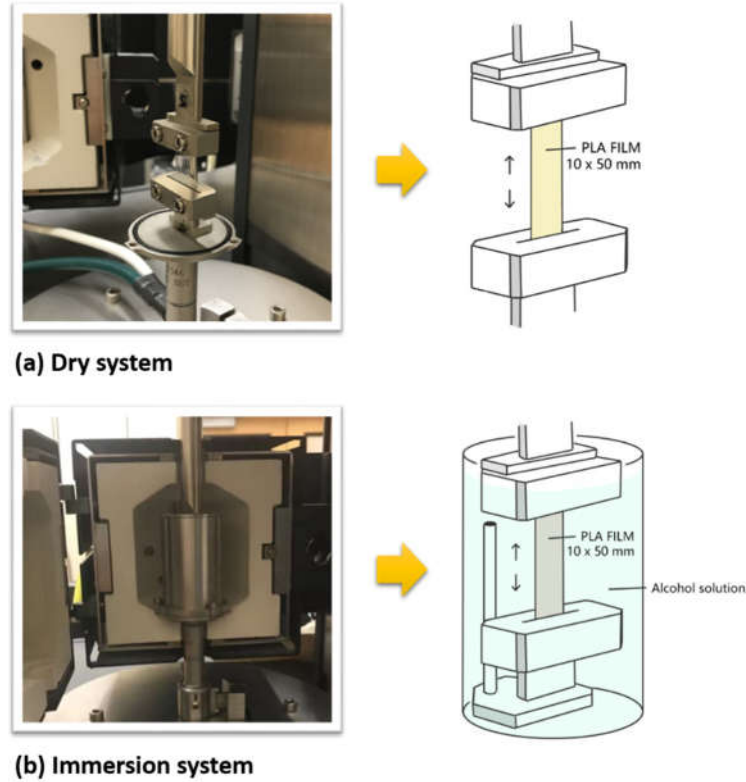


Figure 3.5 Dry system and immersion system of DMA. (a) Dry system, (b) Immersion system.

The thickness was measured in five different positions of the films using a digital micrometer (Testing Machines Inc., Ronkonkoma, NY, USA) with 120 V, 60 Hz and the readability of 0.001 mm. Three replicates were tested for each film. The immersion condition tests were conducted in alcohol-aqueous solution at 0, 25%, 50%, 75% and 100% (v/v) - volume ratio of alcohol to water (or D₂O) in the solution. The dynamic moduli (storage modulus and loss modulus) and $\tan \delta$ were obtained.

δ is the phase angle between the stress and strain, which is a parameter to characterize the viscoelastic behavior of a material, and $\tan \delta$ can be defined as follows:

$$\tan \delta = \frac{\text{energy loss}}{\text{energy stored}} = \frac{E''}{E'} \quad (3.1)$$

where E' is the tensile storage modulus, and E'' is the tensile loss modulus [5].

The maximum value of $\tan \delta$ – peak as shown in **Figure 3.6** – represents the glass transition temperature of the PLA films. The data were analyzed using the TRIOS software version 4.5.0 (TA Instruments).

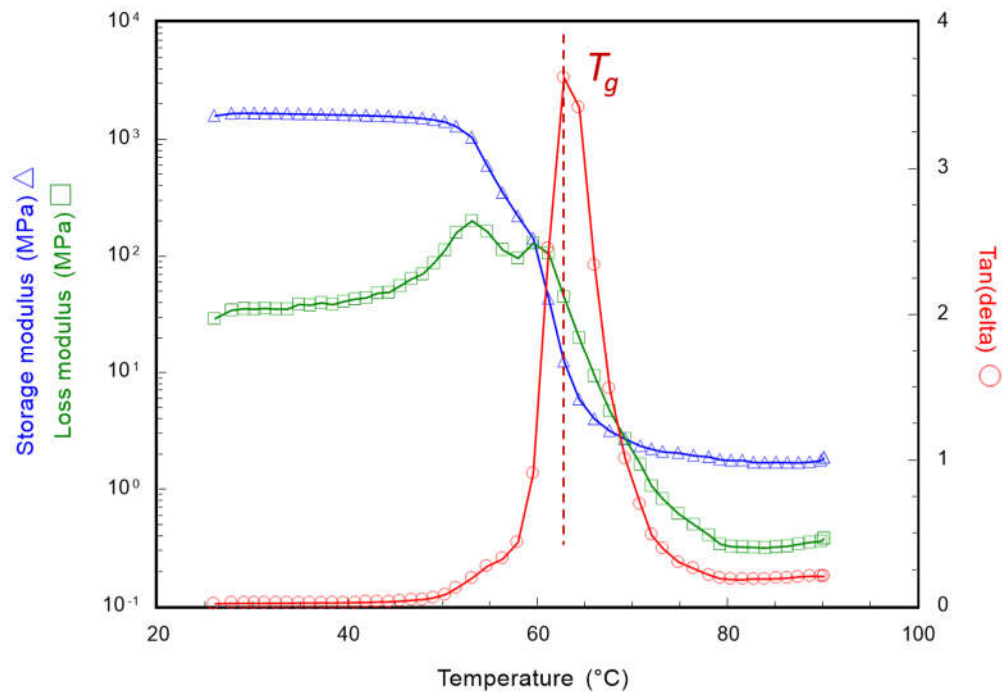


Figure 3.6 Typical pre-immersion (dry) test results of PLA film from DMA, adapted from [3]. T_g is the glass transition temperature of PLA film. The scaling type of $\tan \delta$ and dynamic moduli (storage modulus and loss modulus) are linear and log base 10, respectively.

3.2.2.2 Parameter estimation: Flory-Huggins (FH) model

To determine the effect of the alcohol-aqueous solution on the PLA films, the FH model based on the Hansen solubility parameters (HSP) was calculated to evaluate the changes of T_g . The interaction parameters χ_{12} can be obtained through the equation below:

$$\chi_{12} = \alpha' \frac{V_1}{RT} ((\delta_{d2} - \delta_{d1})^2 + 0.25(\delta_{p2} - \delta_{p1})^2 + 0.25(\delta_{h2} - \delta_{h1})^2) \quad (3.2)$$

where α' is the Lindvig's coefficient, and it was set to be 0.6 in this study according to the previous research [3,6], V_1 denotes the molar volume of the solvent, R represents the gas constant, and T is the temperature.

If the temperature is changed, the density will change and the HSP value will change accordingly. So, the adjusted HSP is adjusted to the T_g of PLA measured by DMA in this study. The adjusted HSP can be calculated by the following equations [3,7]:

$$\frac{d\delta_d}{dT} = -1.25\alpha\delta_d \quad (3.3)$$

$$\frac{d\delta_p}{dT} = -\alpha \frac{\delta_p}{2} \quad (3.4)$$

$$\frac{d\delta_h}{dT} = -(1.22 \times 10^{-3} + \frac{\alpha}{2})\delta_h \quad (3.5)$$

The adjusted HSP was calculated from HSP software (v5.3.06) under $T_g = 62.8$ °C instead of the normal temperature of 25 °C. The unadjusted and adjusted HSP values are shown in **Table 3.3**.

Table 3.3 HSP (δ) and adjusted HSP (δ^*) of PLA and alcohols.

Chemicals	δ_d (MPa ^{1/2})	δ_d^* (MPa ^{1/2})	δ_p (MPa ^{1/2})	δ_p^* (MPa ^{1/2})	δ_h (MPa ^{1/2})	δ_h^* (MPa ^{1/2})
methanol	14.7	13.9	12.3	12.0	22.3	20.8
ethanol	15.8	14.9	8.8	8.6	19.4	18.1
1-propanol	16.0	15.2	6.8	6.7	17.4	16.2
2-propanol	15.8	15.0	6.1	6.0	16.4	15.3
1-butanol	16.0	15.2	5.7	5.6	15.8	14.8
water (H ₂ O)	15.1	14.5	20.4	20.1	16.5	15.5
PLA	17.6	17.5	5.9	5.9	6.4	6.1

Data adapted from [2,3,8,9]. The adjusted HSP is adjusted to the PLA *in-situ* T_g .

As shown in **Figure 3.7**, the Hansen solubility parameter of solvents mixture can be calculated by the formulas below:

$$\delta_d' = \frac{a\delta_{d1} + b\delta_{d2}}{a + b} \quad (3.6)$$

$$\delta_p' = \frac{a\delta_{p1} + b\delta_{p2}}{a + b} \quad (3.7)$$

$$\delta_h' = \frac{a\delta_{h1} + b\delta_{h2}}{a + b} \quad (3.8)$$

where subscript 1 denotes solvent 1, and subscript 2 denotes solvent 2, a and b are the volume ratio of solvent 1 and solvent 2.

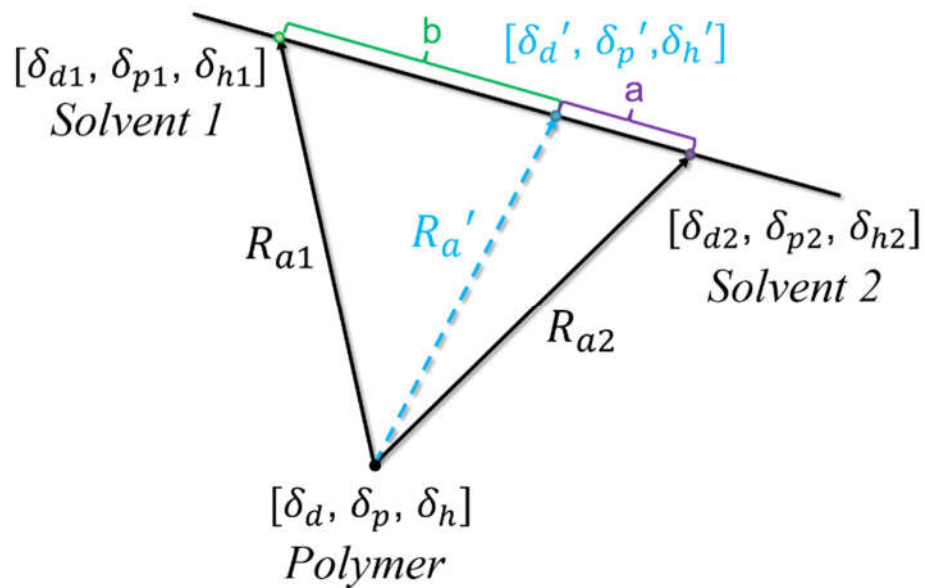


Figure 3.7 HSP of solvents mixture. R_{a1} is the HSP distance between solvent 1 and polymer, R_{a2} is the HSP distance between solvent 2 and polymer, and $R_{a'}$ is the HSP distance of the mixture.

The mix HSP values of alcohol-aqueous solution for PLA are shown in **Table 3.4**.

Table 3.4 The mix HSP (δ') of alcohol-aqueous solution for PLA. The HSP parameters of PLA (target materials) was [$\delta_d = 17.4$, $\delta_h = 5.9$, $\delta_p = 6.1$]; adapted from [3,9,10].

Solvent 1	Solvent 2	% of Solvent 1	δ_d' (MPa ^{1/2})	δ_h' (MPa ^{1/2})	δ_p' (MPa ^{1/2})
methanol	water	25%	14.4	18.1	16.8
		50%	14.2	16.1	18.2
		75%	14.1	14.0	19.5
ethanol	water	25%	14.6	17.2	16.2
		50%	14.7	14.4	16.8
		75%	14.8	11.5	17.5
1-propanol	water	25%	14.7	16.8	15.7
		50%	14.9	13.4	15.9
		75%	15.0	10.1	16.0
2-propanol	water	25%	14.6	16.6	15.5
		50%	14.8	13.1	15.4
		75%	14.9	9.5	15.4

According to the interaction parameters, the partition coefficient K can be calculated through the following equation:

$$\ln K_{i,L/P} = r_L^{-1} + \chi_{i,P} - \chi_{i,L} \quad (3.9)$$

where the subscript i denotes the solute, L denotes the liquid, P represents the PLA, and r_L denotes the ratio of the liquid volume to the solute volume.

In addition, to evaluate the T_g changes of PLA immersed in alcohol-aqueous solutions, the Fox equation was used. The T_g of the mixture can be calculated as follows:

$$\frac{1}{T_g^*} = \frac{w_1}{T_{g1}} + \frac{w_2}{T_{g2}} \quad (3.10)$$

where T_g^* denotes the T_g of the mixture, w_1 represents the weight fraction of component 1 (solvent), w_2 is the weight fraction of component 2 (polymer), and $w_1 + w_2 = 1$. T_{g1} is the T_g of the solvent and T_{g2} is the T_g of the polymer.

3.2.2.3 Differential scanning calorimeter (DSC)

To measure the degree of crystallinity of PLA samples after hot pressing, a differential scanning calorimeter DSC Q100 (TA Instruments) calibrated with indium standards was used. The weight of each sample was between 5 and 10 mg, and samples were sealed in the hermetic aluminum pans. There was one heating cycle from 0 °C to 210 °C with a flow rate of 70 mL/min. The temperature ramp rate was 10 °C/min, and each sample was tested on three replicates. The software for analyzing the data was TA Instruments Universal Analysis 2000 version 4.5A (TA Instruments). From the step change and integration of the curve obtained by the DSC instrument, the T_g and crystallinity of PLA films were obtained. In addition, for studying the effect of alcohols on the crystallinity of PLA, DSC was

also used to measure the crystallinity of PLA films after being immersed in the alcohol solvents. The degree of crystallinity can be obtained by the following equation:

$$\%X_c = \frac{\Delta H_m + \Delta H_c}{\Delta H_m^0} \times 100 \quad (3.11)$$

where ΔH_m is the melting enthalpy of polymer, ΔH_c is the crystallization enthalpy of polymer, and $\Delta H_m^0 = 93.7 \text{ J/g}$ represents the heat of fusion for 100% crystalline PLA [11].

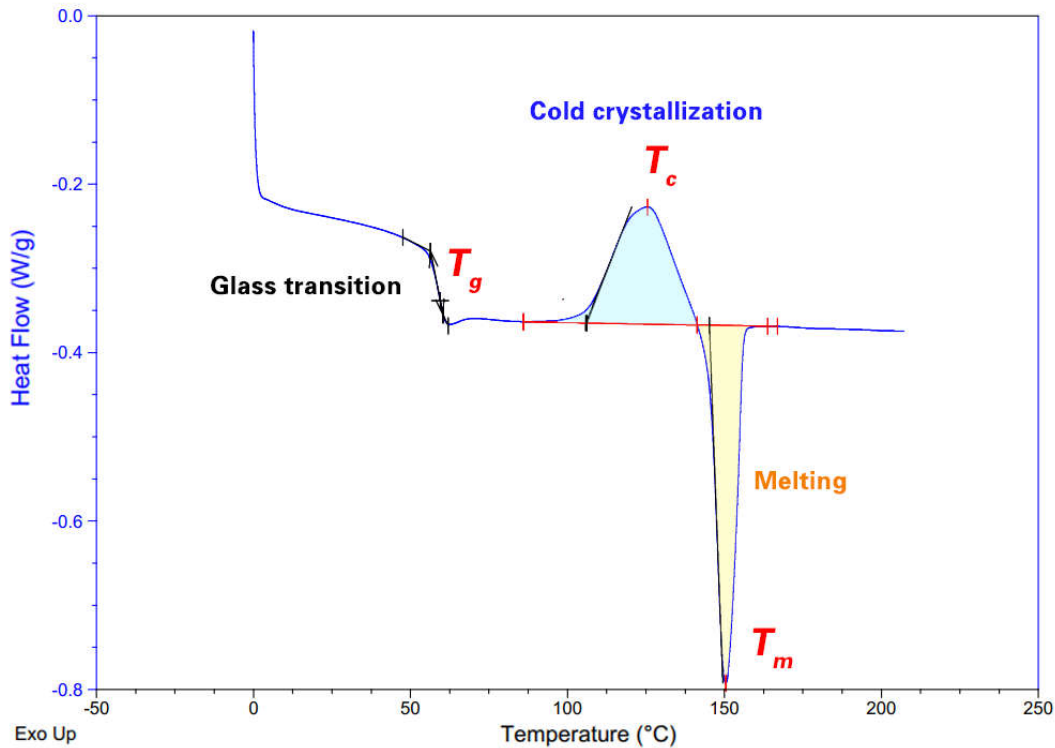


Figure 3.8 A typical pre-immersion (dry) test result of PLA film from DSC, adapted from [3]. T_g denotes glass transition temperature, T_c is crystallization temperature, T_m is melting temperature.

3.2.3 Sorption of alcohol solvents

3.2.3.1 Nuclear magnetic resonance (NMR)

To measure the amount of alcohol solvents absorbed into the PLA films, an Agilent DDR2 500 MHz NMR spectrometer (Agilent Scientific Instruments, Santa Clara, CA, USA) equipped with 7600AS 96 sample autosamplers and running a VnmrJ 3.2A software was used.

The PLA films were cut into circular disks with a diameter of 2 cm, threaded into the stainless-steel wire with alternating glass beads and stored in vials containing alcohol solvents. The samples were stored at 25 °C for different durations (i.e., 0.5 h-72 h) in a PTC-1 Peltier effect temperature-controlled portable cabinet (Sable System International, North Las Vegas, NV, USA). Samples immersed in alcohols were wiped dry with low-lint tissues (AccuWipe disposable delicate task wiper, Georgia-Pacific Consumer Products LP, Atlanta, GA, USA) before the NMR tests to ensure the alcohol remaining on the surface of the sample was removed.

For the preparation of the quantitative NMR (for proton) samples, the weight of PLA samples was between 10 and 15 mg. The solvent used to dissolve the samples was CDCl_3 , and the volume was in the range of 0.6 to 0.7 mL. CDCl_3 does not react with the PLA sample and can dissolve it quickly. For quantitative tests, the internal standard was hexamethylcyclotrisiloxane, with a chemical shift at 0.18 ppm. This internal standard does not react with samples, and the chemical shift of its chemical bond is different from that of the chemical bond of the analyte. The parameters for the quantitative NMR test are shown below in **Table 3.5**.

Table 3.5 Quantitative NMR parameters.

Parameters	Abbreviation	Calculation	Values	Ref.
Spectrometer frequency (MHz)	<i>sfrq</i>	-	499.905	
Pulse width (μ s)	<i>pw</i>	$\theta = \gamma B_1 t_p$	45°	[12]
Acquisition time (s)	<i>at</i>	$at = \frac{np}{2sw}$ $res = \frac{1}{at} = \frac{2sw}{np}$	4.000	[13]
Number of points	<i>np</i>	$np = \frac{2sw}{res}$	64102	[13]
Sweep/ Spectral width (ppm)	<i>sw</i>	$DigitizeRate = \frac{1}{2sw}$	8012.8	[12]
Recycle delay (s)	<i>d1</i>	$d1 = TT - at$ $TT = 5 \times T_1$	60	[13]
Number of scans	<i>nt</i>	-	64	

* θ is the angle through which the magnetization vector is rotated, γ represents the gyromagnetic ratio of perturbed nuclei, B_1 denotes the strength of applied field, t_p is the pulse width [12], res is the digital resolution of the spectrum, TT is the total time and $T_1=1/R$, where R is the rate of relaxation [13].

Table 3.6 shows the chemical shifts of functional groups for PLA, $CDCl_3$ and alcohols in the 1H -NMR spectrum.

Table 3.6 Chemical shifts in $^1\text{H-NMR}$ spectrum (Solvent: CDCl_3).

Chemicals	Structure	Chemical shifts δ (ppm)			Ref.
PLA		1.56 ^a	5.14 ^b		[14]
CDCl_3		7.26 ^a	-		[12,13]
methanol		3.49 ^a	-		[16]
ethanol		1.24 ^a	3.72 ^b		[16]
1-propanol		0.94 ^a	1.53 ^b	3.60 ^c	[17]
2-propanol		1.21–1.22 ^a	4.03–4.04 ^b		[15,16]
1-butanol		0.94 ^a	1.35 ^b	1.52 ^c 3.65 ^d	[16,18]

a, b, c, d represents different hydrogen types.

Quantification of sample content can be calculated by adding internal standards in the sample. The purity of the sample (% g/g) is obtained as follows:

$$P_{\text{sample}} = \frac{I_{\text{Analyte}}}{I_{\text{Cal}}} \cdot \frac{N_{\text{Cal}}}{N_{\text{Analyte}}} \cdot \frac{M_{\text{Analyte}}}{M_{\text{Cal}}} \cdot \frac{m_{\text{Cal}}}{m_{\text{Sample}}} \cdot P_{\text{Cal}} \quad (3.12)$$

where P_{sample} denotes the purity of the sample as mass fraction. $I_{Analyte}$ is the integral of the analyte signal, I_{Cal} is the integral of the internal standard peak. N_{Cal} represents the number of calibrant reference material protons. $N_{Analyte}$ is the number of analyte protons. $M_{Analyte}$ and M_{Cal} are the molecular mass of the analyte and calibrant reference standard, respectively. m_{cal} is the mass of reference standard and m_{sample} is the mass of sample. P_{Cal} is the purity of the calibrant peak of internal standard.

3.2.3.2 Vapor sorption analysis

A VTI SGA-100 Symmetric Vapor Sorption Analyzer (TA Instruments) was used to determine the sorption isotherms of the PLA films. The PLA films were dried in a vacuum oven for 24 h to ensure that there was no residual moisture in the film. The sorption capacity of the PLA films in water and D₂O environments at 25 °C was measured by gravimetric analysis. Three replicates were conducted for each test. For each replicate, 15–25 mg samples were put into the tray of the sample chamber. The relative humidity control range was from 0 to 95% RH and with an RH step set as 10%.

3.2.4 Statistical analysis

The statistical significance was determined by a one-way analysis of variance (ANOVA), and the mean differences were determined by Tukey's honest significant difference (Tukey's HSD) test ($\alpha = 0.05$). The software SAS Analysis Software University Edition (SAS Institute Inc., Cary, NC) was used.

REFERENCES

REFERENCES

- [1] Lesikar A. V, On the Self-association of the Normal Alcohols and the Glass Transition in Alcohol-Alcohol Solutions, *Journal of Solution Chemistry*, vol. 6, no. 2, pp. 81–93, 1977, doi: 10.1007/bf00643434.
- [2] Ramos M. A., Calorimetric and thermodynamic study of glass-forming monohydroxy alcohols, *Philosophical Magazine*, vol. 91, no. 13–15, pp. 1847–1856, 2011, doi: 10.1080/14786435.2010.526649.
- [3] Sonchaeng U., Critical and systematic review of poly (lactic acid) mass transfer and evaluation of the *in-situ* changes of its thermo-mechanical properties when immersed in alcohol solutions, PhD thesis, Michigan State University, Michigan, 2019, doi: 10.25335/76kp-yt65.
- [4] Scott E. Denmark C. R. B., Hexamethylcyclotrisiloxane, vol. 3, no. 2, pp. 2–5.
- [5] Meyers M., Ed., *Mechanical Behavior of Materials*, 2nd ed. Cambridge university press, 1999.
- [6] Lindvig T., Michelsen M. L., and Kontogeorgis G. M., A Flory-Huggins model based on the Hansen solubility parameters, *Fluid Phase Equilibria*, vol. 203, no. 1–2, pp. 247–260, 2002, doi: 10.1016/S0378-3812(02)00184-X.
- [7] Hansen C. M., *Hansen solubility parameters: a user's handbook.*, 2nd ed. CRC Press, 2007.
- [8] KA C., *Ludwig's Applied Process Design for Chemical and Petrochemical Plants*, Volume 1. Oxford, UK: Gulf Professional Publishing, 2006.
- [9] Hansen C., Hansen solubility parameters solvent-blends. <https://www.hansen-solubility.com/HSP-science/solvent-blends.php> (accessed Jun. 04, 2021).
- [10] Elangovan D., Nidoni U., Yuzay I. E., *et al.*, Poly(L-lactic acid) metal organic framework composites. Mass transport properties, *Industrial & Engineering Chemistry Research*, vol. 50, no. 19, pp. 11136–11142, 2011, doi: 10.1021/ie201378u.
- [11] Limsukon W., Auras R., and Selke S., Hydrolytic degradation and lifetime prediction of poly(lactic acid) modified with a multifunctional epoxy-based chain extender, *Polymer Testing*, vol. 80, no. September, p. 106108, 2019, doi: 10.1016/j.polymertesting.2019.106108.

- [12] Wu S., 1D and 2D NMR Experiment Methods, Atlanta, GA, 2010. [Online]. Available: http://www.emory.edu/NMR/mysite06/NMR Course/all_book_2010.pdf.
- [13] Basic NMR Concepts: A Guide for the Modern Laboratory. https://www.bu.edu/chemistry/files/cic/nmr/documents/CICNMR_basicconcepts.pdf (accessed Jun. 04, 2021).
- [14] Iniguez-Franco F., Hydrolytic degradation of neat and modified poly(lactic acid) with nanoparticles and chain extenders by water-ethanol solutions, PhD thesis, Michigan State University, Michigan, 2018.
- [15] Gottlieb H. E., Kotlyar V., and Nudelman A., NMR Chemical Shifts of Common Laboratory Solvents as Trace Impurities, *The Journal of Organic Chemistry*, vol. 62, no. 21, pp. 7512–7515, 1997, doi: 10.1021/jo971176v.
- [16] Babij N. R., Mccusker E. O., Whiteker G. T., *et al.*, NMR Chemical Shifts of Trace Impurities: Industrially Preferred Solvents Used in Process and Green Chemistry, *Organic Process Research & Development*, vol. 20, no. 3, pp. 661–667, 2016, doi: 10.1021/acs.oprd.5b00417.
- [17] *1H-NMR Chemical Shift Laboratory Data Guide*, SigmaAldrich, Burlington, MA, 2019.
- [18] Brown D., H-1 NMR spectrum of butan-1-ol. <https://docbrown.info/page06/spectra/butan-1-ol-nmr1h.htm> (accessed Jun. 04, 2021).

CHAPTER 4 Results and Discussion

This chapter presents the effect of alcohol-aqueous solutions and water in PLA films. The thermal properties before and after immersion of PLA films on these solutions were investigated.

The Fox equation (Eq. 3.10) was used to establish a relationship between the amount of alcohol sorbed and the change of T_g in PLA films. The Hansen solubility parameters (HSP) were used to evaluate the solubility of PLA in alcohol-aqueous solutions with different alcohol concentrations. The interaction between the alcohol-aqueous solutions and PLA films were estimated by the Flory-Huggins interaction parameters. The sorption amount of ethanol was measured by qNMR, and the sorption isotherm curves for PLA in water and D₂O were also reported.

4.1 Thermal properties of pre-immersion PLA film

The effect of the alcohol solutions on the in-situ thermal properties of immersed PLA films was assessed, and the thermal properties before and after immersion of the films were compared. **Figure 4.1** shows the DMA results for PLA film as dry samples (i.e., before immersion). According to the peak of the glass transition zone of the $\tan \delta$ curve, the T_g was 62.8 ± 0.4 °C.

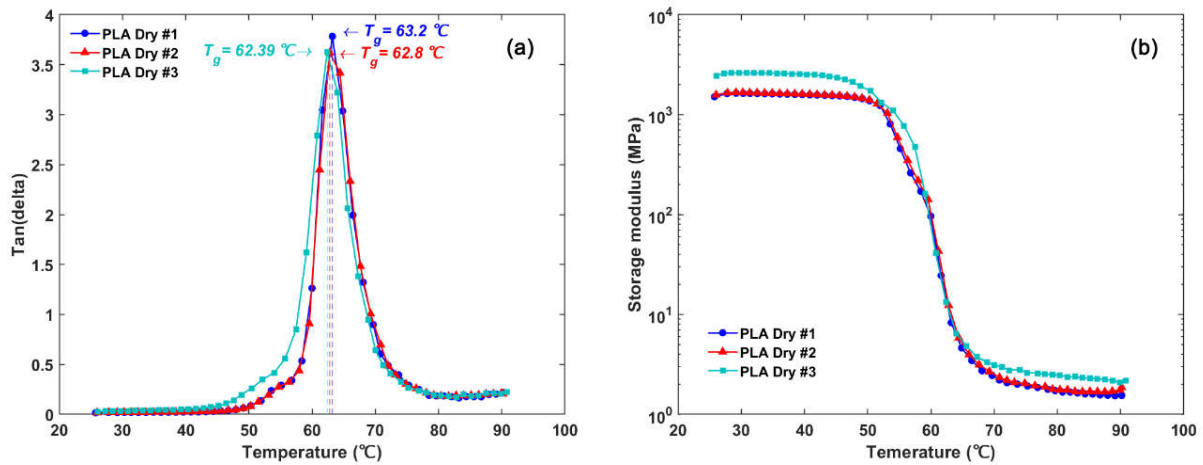


Figure 4.1 DMA test results of PLA pre-immersion samples: (a) Tan δ curves; (b) Storage modulus curves.

The T_g , T_m , the cold crystallization temperature (T_c), and the crystallinity (X_C) of the original PLA films without hot pressing were measured by DSC. The results were $T_g = 58.0 \pm 1.2^{\circ}\text{C}$, $T_m = 149.9 \pm 0.5^{\circ}\text{C}$, $T_c = 123.7 \pm 3.3^{\circ}\text{C}$ and $X_C = 1.3 \pm 0.2\%$ (see **Figure 4.2**).

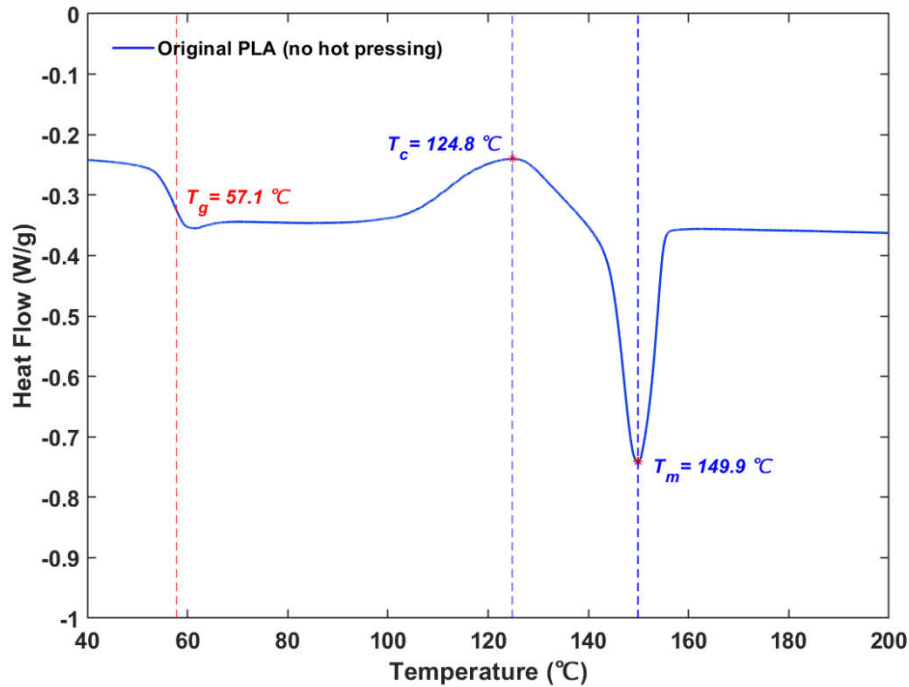


Figure 4.2 DSC test results of original PLA sample (i.e., without hot pressing). T_g , T_c and T_m are 57.1 °C, 124.8 °C and 149.9 °C, respectively.

Compared with the DMA results, the T_g of the original film measured by DSC was lower since the measured T_g depends on the heating rates and frequencies of the different instruments, and each instrument measured different physical properties. DMA measured mechanical changes and DSC measured calorimetric changes. There are reports that DMA has a higher sensitivity to capture the T_g than DSC [1,2].

As mentioned in **Chapter 3**, a hot-pressing process was used to ensure that the PLA films were totally amorphous before DMA testing. According to the results of DSC tests of the pre-immersion PLA sample after the hot pressing process, $T_g = 58.5 \pm 0.6\text{ °C}$. $T_m = 150.6 \pm 0.6\text{ °C}$, $T_c = 125.9 \pm 0.9\text{ °C}$ and $X_c = 0.4 \pm 0.2\%$. **Table 4.1** shows the thermal parameters of the original and hot-pressed PLA films. There is a significant difference

between X_C of the original PLA film and the hot-pressed PLA film, but their T_g , T_m , and T_c are not significantly different.

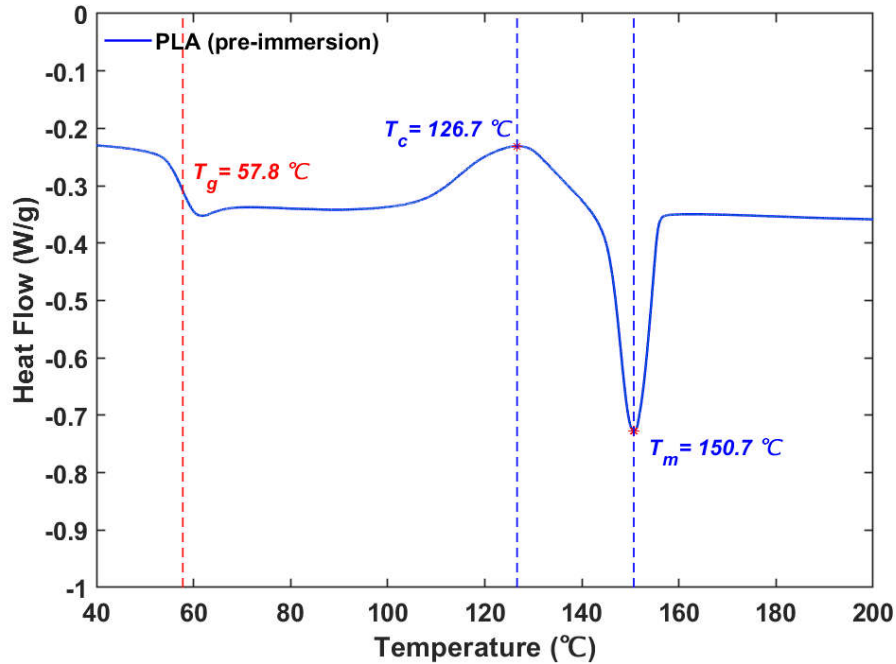


Figure 4.3 DSC test results of pre-immersion hot-pressed PLA sample. T_g , T_c and T_m are 57.8 °C, 126.7 °C and 150.7 °C, respectively.

Table 4.1 Thermal parameters of original and hot-pressed PLA films.

Film type	T_g , °C	T_m , °C	T_c , °C	X_C , %
PLA 2003D (Original)	58.0±1.2 ^a	149.9±0.5 ^a	123.7±3.3 ^a	1.3±0.2 ^a
PLA 2003D (Hot-pressed)	58.5±0.6 ^a	150.6±0.6 ^a	125.9±0.9 ^a	0.4±0.2 ^b

Note: Lowercase superscript letters indicate different comparison based on Tukey's HSD tests at a significance level of 0.05. Values with the same letter(s) are not different.

4.2 Thermal properties of immersed PLA film

In this section, the changes of PLA's T_g immersed in the pure alcohols, alcohol-aqueous and alcohol-D₂O solutions are discussed. Relationships to assess the interaction between the PLA films and the solutions calculated by HSP, Fox equation, and the Flory-Huggins interaction parameters are presented.

4.2.1 T_g reduction of PLA immersed in pure alcohols

The T_g 's of PLA films immersed in different solvents and the reduction of T_g 's (compared with the no immersion sample measured by DMA) are summarized in **Table 4.2** and the DMA results are shown in **Figure 4.4**. There were significant differences between the T_g 's of no immersion PLA film, and PLA films immersed in pure methanol, ethanol, 1-propanol, 1-butanol and water ($\alpha = 0.05$). However, there were no significant difference between the T_g 's of PLA films immersed in 1-propanol and 2-propanol and also between water and D₂O ($\alpha > 0.05$) indicating that the shorter branched chain in 2-propanol has no effect on the T_g of PLA film in comparison to 1-propanol. Also, the difference in the length of the OH/OD bond and the difference in the length of hydrogen bond between water and D₂O has no effect on the T_g of PLA film. For alcohols with small number of carbons, the packing density of the linear alcohol is higher than its branched isomer [3], and although the molecular volume of these alcohol isomers (i.e., 1- and 2-propanol) are different - a difference in the molecular volume of 1.8 mL/mol (1-propanol: 75.1 mL/mol, 2-propanol: 76.9 mL/mol), it may be too small to cause a difference in T_g [1].

Table 4.2 T_g of PLA films immersed in different solvents as tested by DMA.

Solvent	#C	T_g , °C	T_g reduction, %
none (no immersion)	-	62.8±0.4 ^a	-
methanol	1	15.2±0.1 ^b	75.8
ethanol	2	24.3±0.4 ^c	61.3
1-propanol	3	27.7±0.8 ^d	55.9
2-propanol	3	27.9±0.5 ^d	55.6
1-butanol	4	31.8±0.1 ^e	49.4
water	-	51.6±0.3 ^f	17.8
deuterium oxide	-	52.7±0.3 ^f	16.1

Note: Lowercase superscript letters indicate different comparison based on Tukey's HSD tests at a significance level of 0.05. Values with the same letter(s) are not different.

#C is the number of carbon atoms in the main chains of alcohols

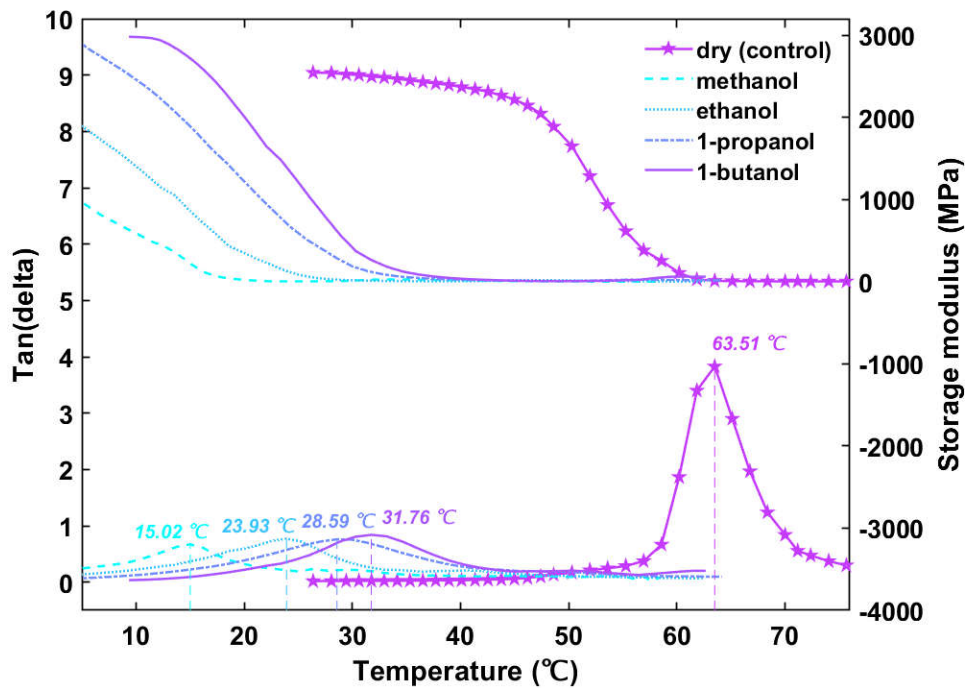


Figure 4.4 Tan δ (bottom) and storage modulus (top) of the PLA films immersed in different alcohols as a function of temperature.

The T_g of the PLA films immersed in water and D₂O decreased but not as much as when compared with the T_g of the PLA films immersed in alcohols. **Figure 4.5** shows the graphical representation between the number of carbon atoms of alcohols and the reduction of T_g . Compared with the PLA films not immersed in the alcohol solution, the T_g of the PLA films immersed in methanol decreased up to 76%. With the increasing of the number of carbon atoms in the main chain of alcohols, the drop of T_g became smaller. T_g is the thermal transition stage indicating the movement of the polymer chains throughout the transition[4]. T_g 's of the PLA films immersed in small molecular weight alcohols were significantly reduced, indicating that these alcohols may plasticize the PLA chains, increasing mobility and the free volume of the system, thereby causing the PLA chains to move and leading to the decreased T_g [1,5]. **Figure 4.5** also shows that the PLA films

immersed in alcohols with higher number of carbon atoms in the main chain have a smaller reduction in T_g , which may indicate that these alcohols have a less plasticizing effect on the PLA matrix. So, alcohols with low number of carbon are easily diffuse through the PLA matrix. Further modeling is needed to fully understand this mechanistic behavior.

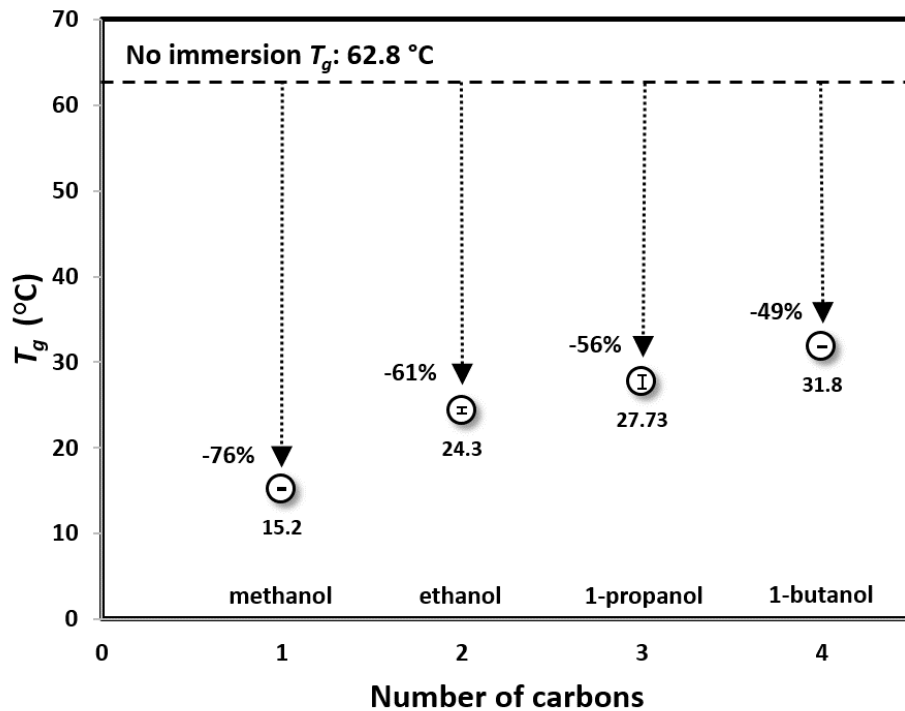


Figure 4.5 Changes in the T_g values (in Celsius) of the in-situ immersed PLA films in aliphatic alcohols (circle markers, showing average values and standard deviation bars) from the T_g of dry PLA (horizontal dash line) as a function of the number of carbons of the solvent chains. Values shown above the circle markers are percent T_g reduction from the T_g of dry PLA.

4.2.2 Modeling relationship between pure alcohols and T_g changes of PLA

The T_g 's of the mixture of the alcohols and PLA film were estimated by using the Fox equation (Eq. 3.10). According to the linear relationship calculated by the equation and the experimental T_g obtained from DMA tests, the weight fraction of alcohols absorbed in PLA films was estimated.

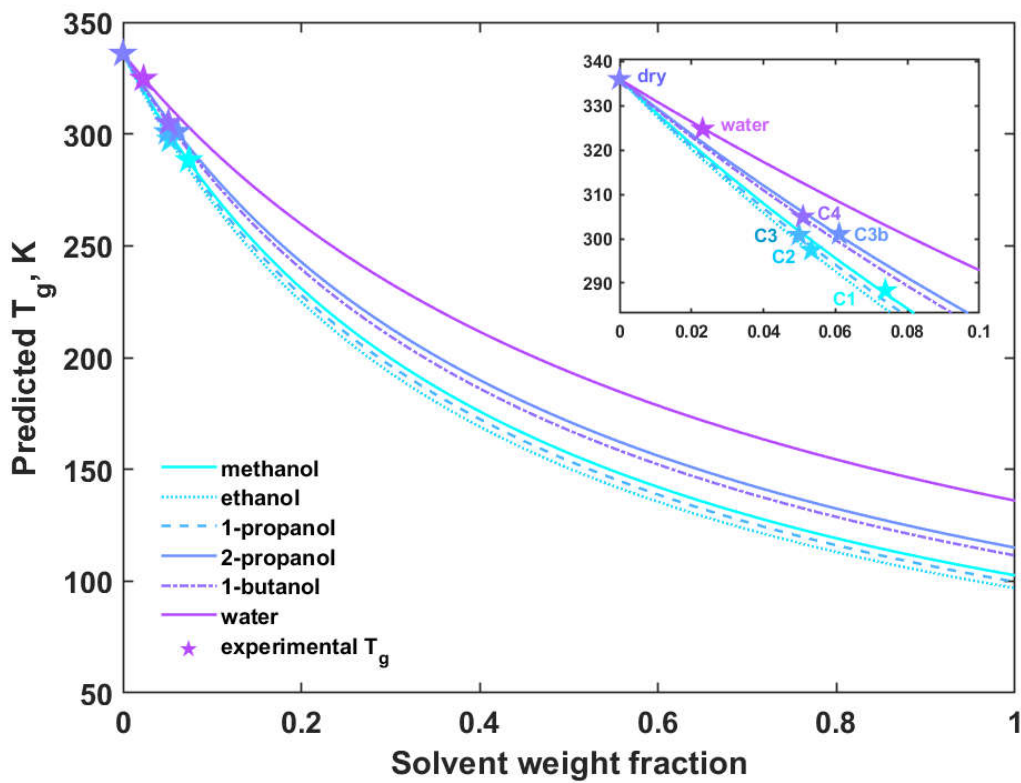


Figure 4.6 Predicted T_g of PLA film immersed in pure alcohols and water versus solvent weight fraction [6]. C1-C4 denote the carbon number in the main chain of alcohols and C3b indicates 2-propanol.

Table 4.3 Fox equation parameters and estimate solvent weight fraction.

Solvent	T_g of solvent used in the Fox equation, K ($^{\circ}\text{C}$)	Experimental T_g of PLA, K ($^{\circ}\text{C}$)	Solvent weight Fraction (w_2), %	w_2/w_1 , %
methanol	102.6 (-170.6)	288.4 (15.2)	7.39	7.98
ethanol	96.9 (-176.3)	297.5 (24.3)	5.33	5.63
1-propanol	99.7 (-173.5)	300.9 (27.7)	4.99	5.25
2-propanol	115.0 (-158.2)	301.1 (27.9)	6.10	6.50
1-butanol	111.5 (-161.7)	305.0 (31.8)	5.10	5.37
dry	-	336.0 (62.8)	0.00	0.00
water	136.0 (-137.2)	324.8 (51.6)	2.31	2.36

Note: w_2/w_1 denotes the estimated amount (wt %) of solvent absorbed into PLA films.

Figure 4.6 shows that the weight fraction of any solvents is no more than 7.4%, corresponding to the weight fraction value of methanol. According to the weight fraction, it can be stated that the amount of solvent absorbed by the PLA films from the highest to lowest amount is methanol, 2-propanol, ethanol, 1-butanol and 1-propanol (C1>C3b>C2>C4>C3). The significant decrease in the T_g of PLA immersed in methanol may be due to a large amount of methanol absorbed into the PLA film. Additionally, experimental work is needed to understand the predicted sorption difference between 2-propanol and 1-propanol. The absorption of alcohols in amorphous PLA films was quantitatively analyzed by qNMR experiments as later explained in **section 4.3 Sorption amounts of alcohols in PLA films**.

4.2.3 Effect of alcohol solution concentrations on T_g

The effect of alcohol solution concentrations on T_g of PLA was determined by *in-situ* DMA tests. The T_g of PLA films immersed in 0% (v/v), 25%, 50%, 75% and 100% methanol-aqueous solutions (an alcohol with 1 carbon atom) are illustrated in **Figure 4.7**. The T_g of PLA was reduced by 8.6 °C per every 25% (v/v) increase of methanol.

The interaction between alcohol molecules and PLA leads to swelling and plasticization of the PLA matrix, resulting in the movement of the PLA segments, thereby reducing the T_g [1]. The extend of the swelling and the reduction of T_g is not yet fully theoretically predicted.

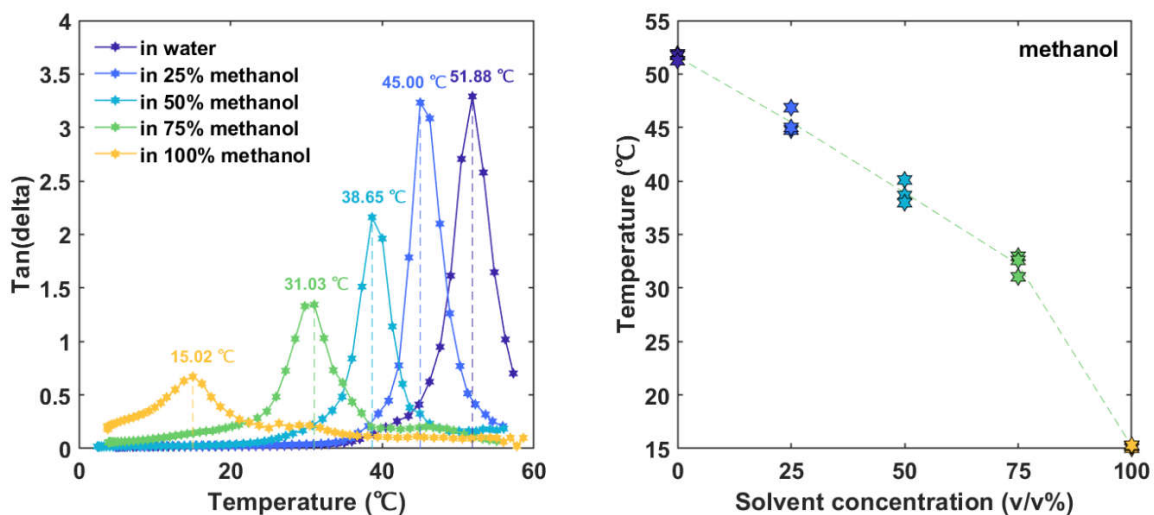


Figure 4.7 (a) $\text{Tan } \delta$ of PLA film in methanol-aqueous solution as a function of temperature (b) T_g of immersed PLA versus the concentration of methanol-aqueous solution.

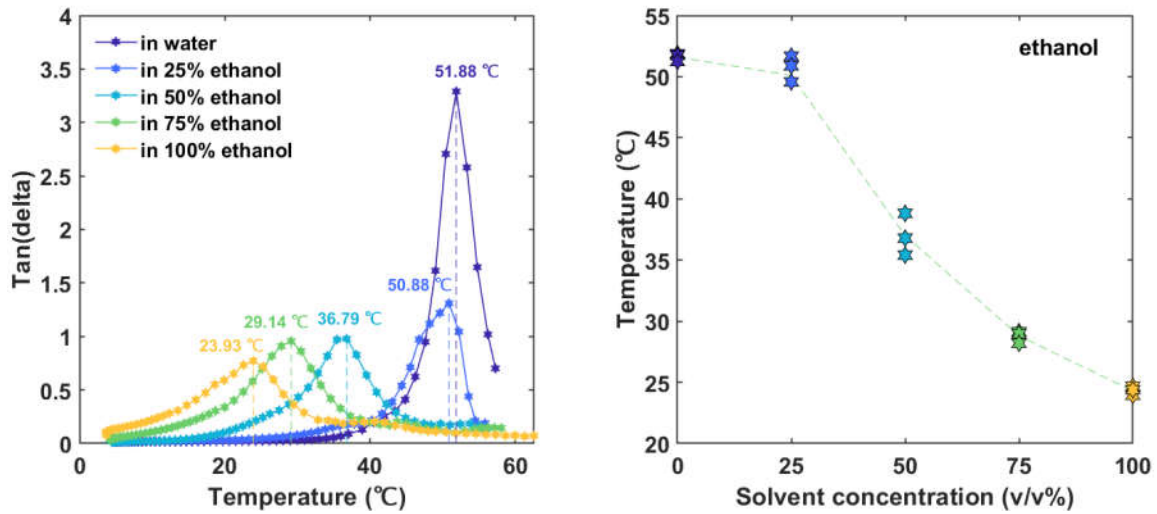


Figure 4.8 (a) Tan δ of PLA film in ethanol-aqueous solution as a function of temperature
 (b) T_g of immersed PLA versus the concentration of ethanol-aqueous solution.

Figure 4.8 shows that the T_g was decreased by 7.6 °C per every 25% (v/v) increase of ethanol (an alcohol with 2 carbon atoms). Compared with methanol, ethanol has a smaller effect on the T_g reduction of PLA, which may be due to the fact that the absorption of ethanol in PLA was less than methanol as predicted by Fox equation (Eq. 3.10) shown in **Table 4.3**, and the larger size molecule of ethanol when compared with methanol.

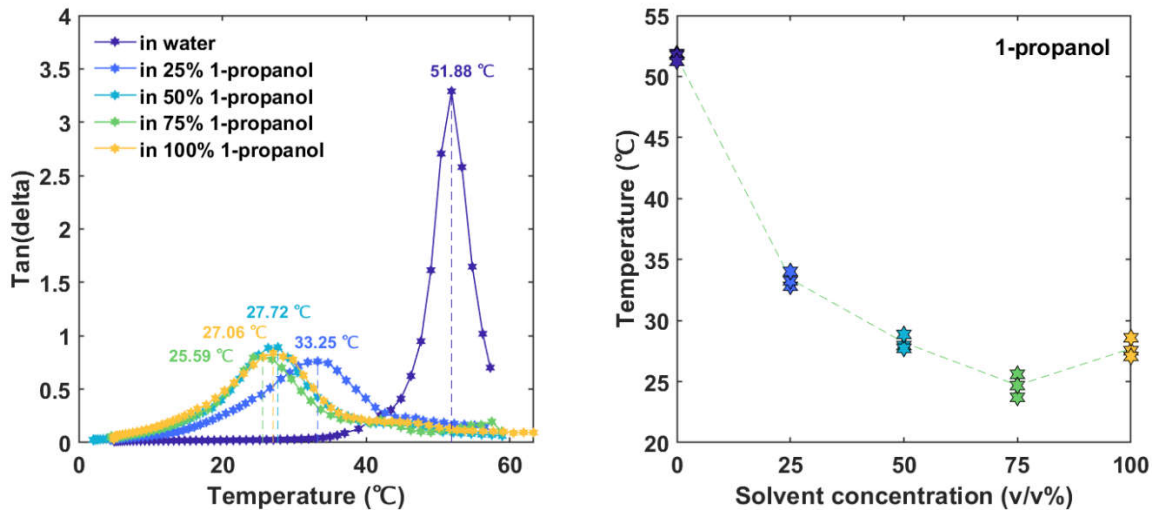


Figure 4.9 (a) $\text{Tan } \delta$ of PLA film in 1-propanol-aqueous solution as a function of temperature (b) T_g of immersed PLA versus the concentration of 1-propanol-aqueous solution.

Figure 4.9 and **Figure 4.10** show that when the PLA films immersed in alcohol solutions with 3 to 4 carbon atoms, the T_g 's decreased until 75% (v/v). T_g 's of 1-propanol and 2-propanol decreased by approximately 8.6 °C and 8.9 °C for every 25% increase in solvent concentration, respectively. Pure 1-propanol and 2-propanol have a similar effect on the PLA films. The different carbon chain structures did not have much effect on the T_g reduction of PLA films. The HSP distance and total HSP of these two structural isomers are also similar, which means they may have similar solubility characteristics with PLA (see later **Table 4.4** and **Table 4.5**).

As the concentration of alcohol increases, the difference between straight-chain alcohols (1-propanol) and alcohols containing branched chains (2-propanol) on the decrease in T_g becomes smaller.

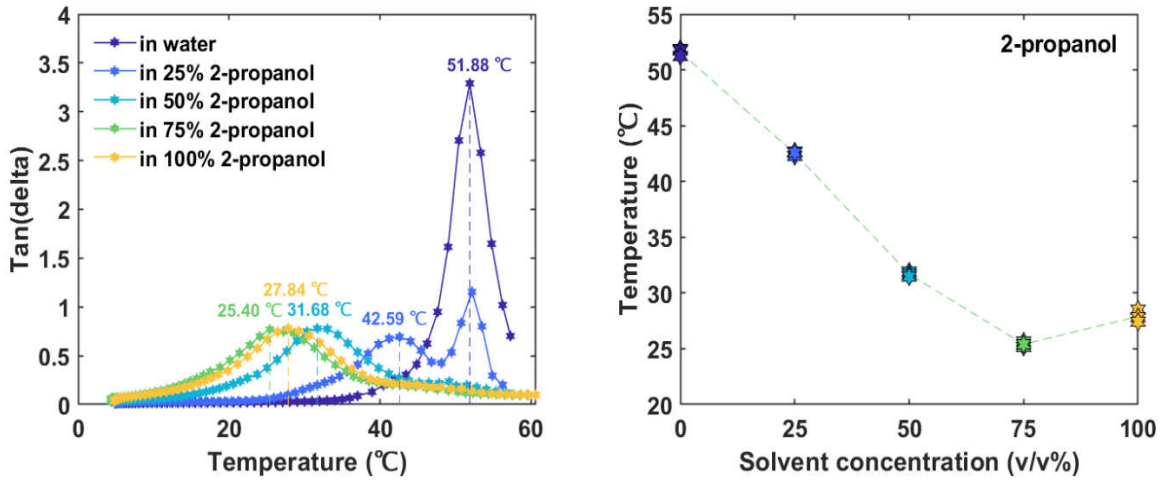


Figure 4.10 (a) $\text{Tan } \delta$ of PLA film in 2-propanol-aqueous solution as a function of temperature (b) T_g of immersed PLA versus the concentration of 2-propanol-aqueous solution.

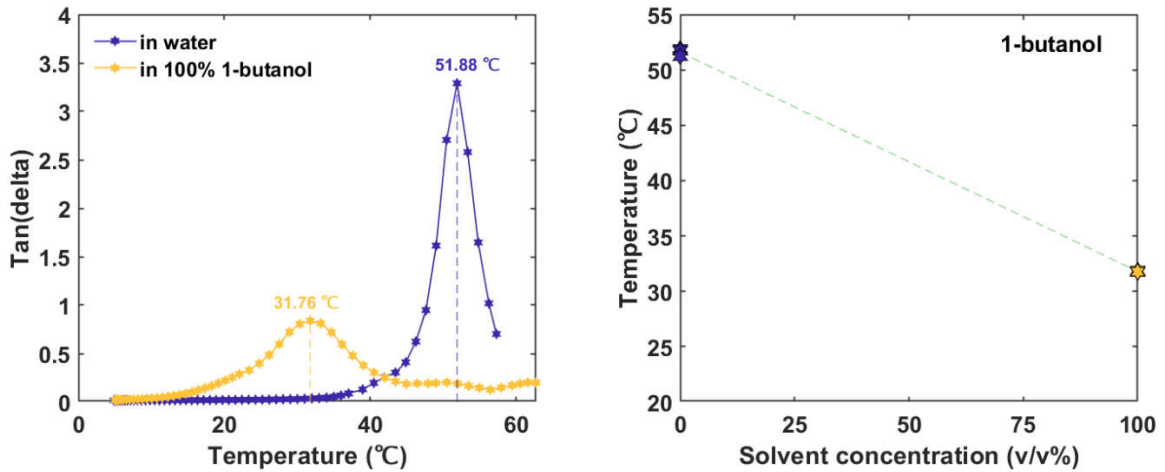


Figure 4.11 (a) $\text{Tan } \delta$ of PLA film in 1-butanol-aqueous solution as a function of temperature (b) T_g of immersed PLA versus the concentration of 1-butanol-aqueous solution.

Since 1-butanol is not miscible with water, we only assessed the concentration of 1-butanol at 100% (v/v). **Figure 4.11** shows that the T_g of PLA immersed in 1-butanol is reduced by about 20 °C compared with PLA immersed in water.

Figure 4.12 shows a comparison of the T_g reduction for PLA immersed in different solutions. The effect of methanol and ethanol concentration on the change of T_g is close to a linear relationship, while 1-propanol and 2-propanol reach the maximum effect on the reduction of T_g at a concentration of 75%.

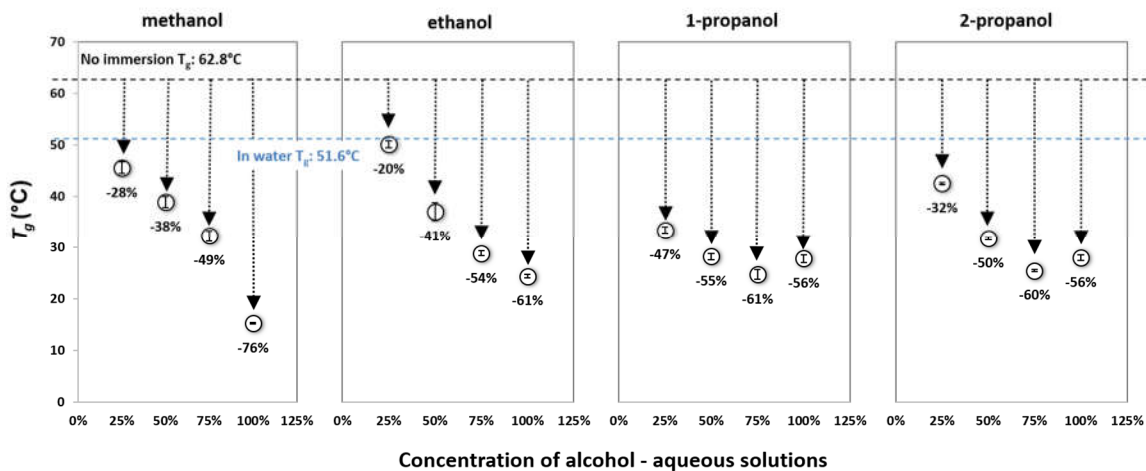


Figure 4.12 Reduction of T_g of PLA immersed in different alcohol-aqueous solutions.

Iñiguez-Franco et al. [7] proposed that when conducting NMR experiments, water from the environment interferes with the experimental results hindering the quantification of water and alcohol sorption in PLA. So, the effect of alcohol-D₂O solutions to T_g of PLA was studied and results are shown as follows. **Figure 4.13** to **Figure 4.17** indicate that the aqueous and D₂O solutions have similar effects on the changes in T_g 's of PLA, which indicates that the plasticization effect of alcohol in D₂O solutions is similar to water. Therefore, D₂O could be used instead of water to configure the solution in a system that

is hard to quantify water. Using D₂O can also avoid the influence of water in the environment when the absorption of alcohol is measured. This will later be explained in **section 4.3 Sorption amounts of alcohols in PLA films.**

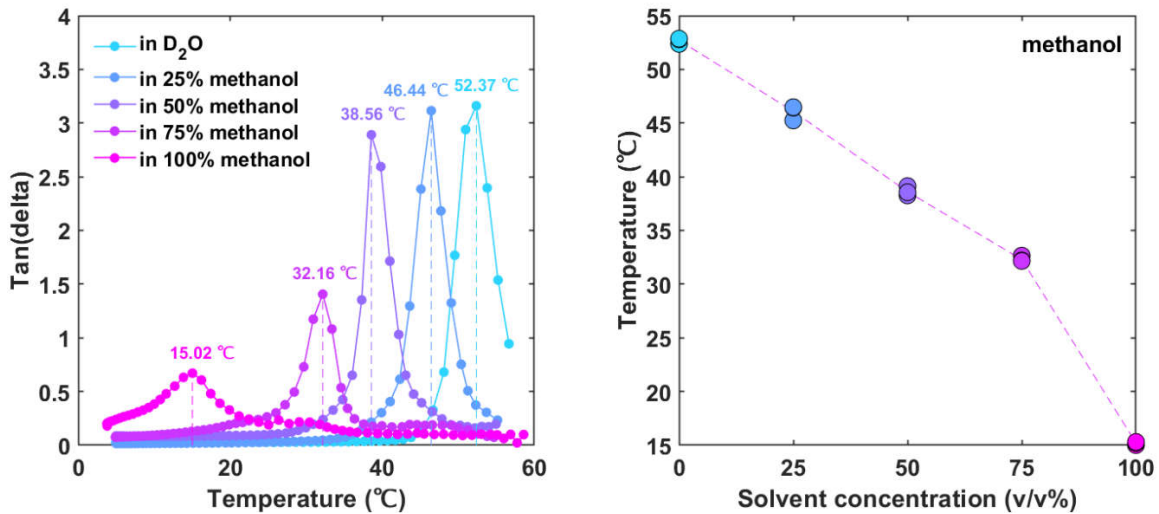


Figure 4.13 (a) Tan δ of PLA film in methanol-D₂O solution as a function of temperature (b) T_g of immersed PLA versus the concentration of methanol-D₂O solution.

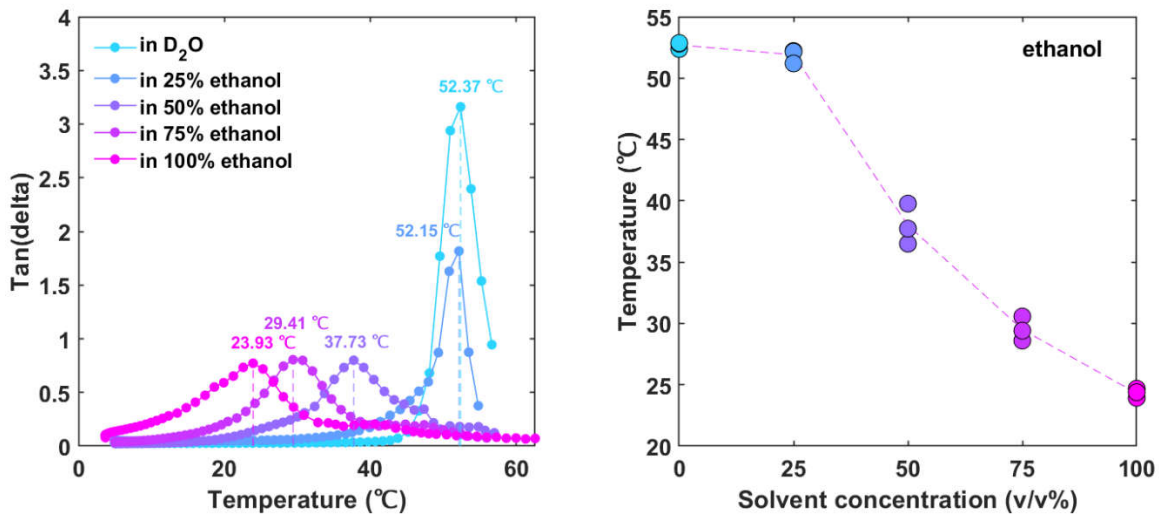


Figure 4.14 (a) Tan δ of PLA film in ethanol-D₂O solution as a function of temperature (b) T_g of immersed PLA versus the concentration of ethanol-D₂O solution.

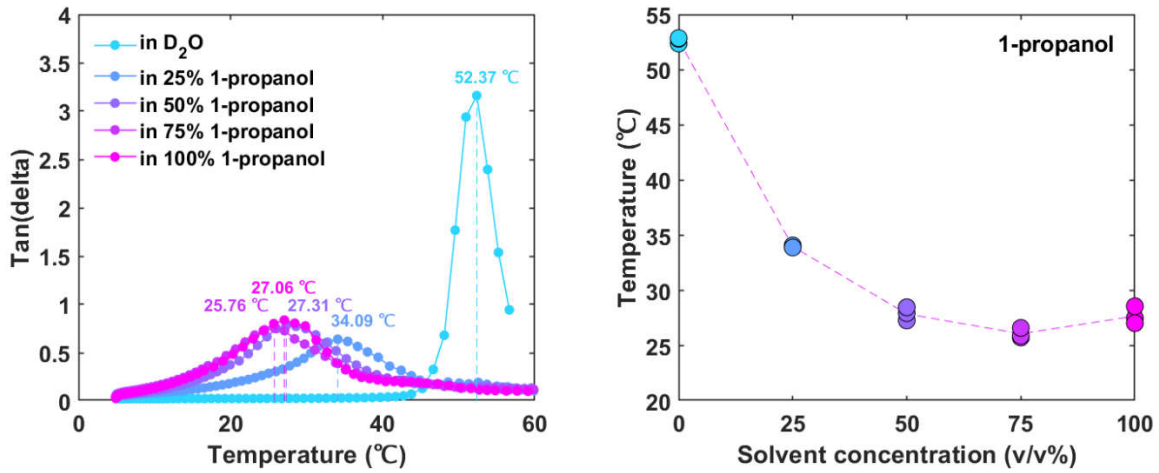


Figure 4.15 (a) Tan δ of PLA film in propanol-D₂O solution as a function of temperature
 (b) T_g of immersed PLA versus the concentration of 1-propanol-D₂O solution.

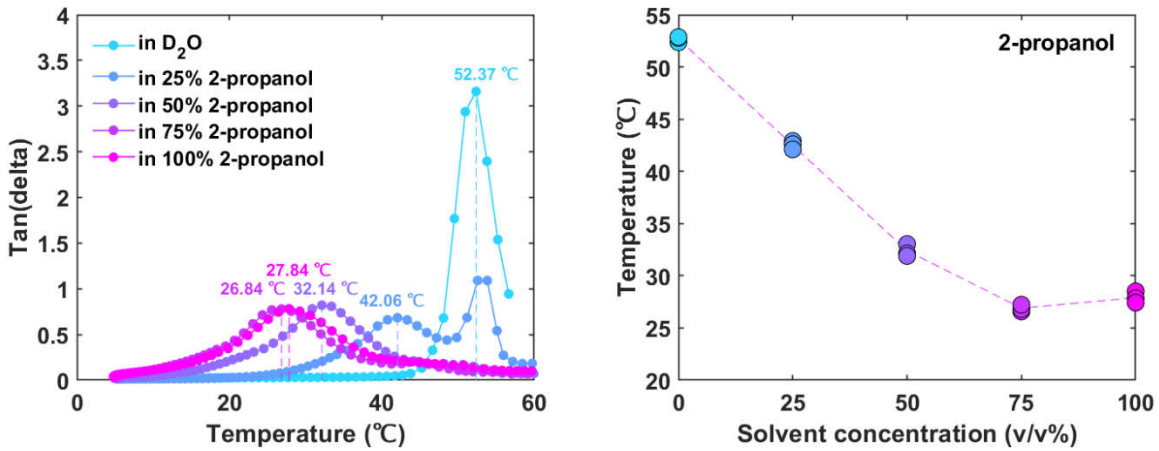


Figure 4.16 (a) Tan δ of PLA film in 2-propanol-D₂O solution as a function of temperature
 (b) T_g of immersed PLA versus the concentration of 2-propanol-D₂O solution.

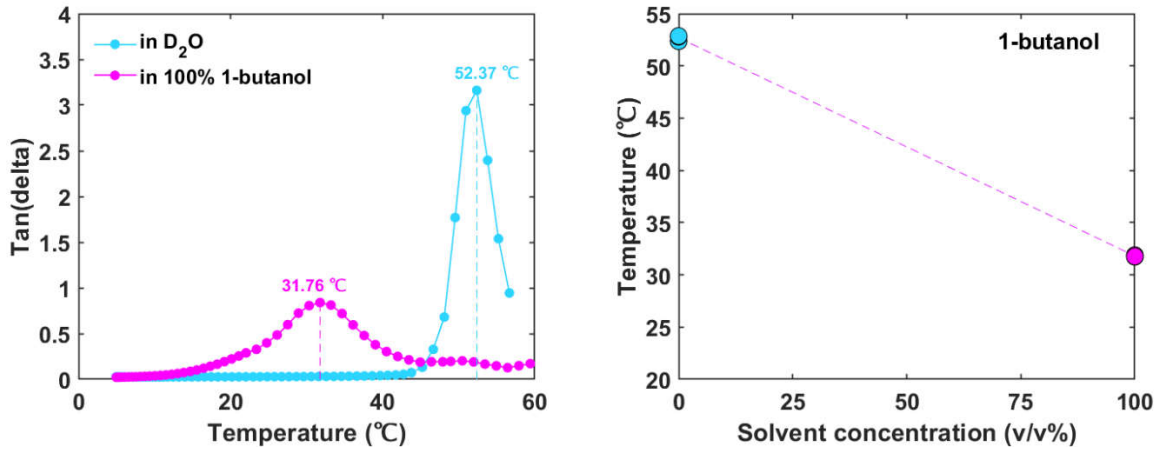


Figure 4.17 (a) $\text{Tan } \delta$ of PLA film in 1-butanol- D_2O solution as a function of temperature
 (b) T_g of immersed PLA versus the concentration of 1-butanol- D_2O solution.

Figure 4.18 and **Figure 4.19** show the summary of T_g of PLA immersed in C1-C4 alcohol-aqueous and alcohol- D_2O solutions as a function of alcohol concentrations.

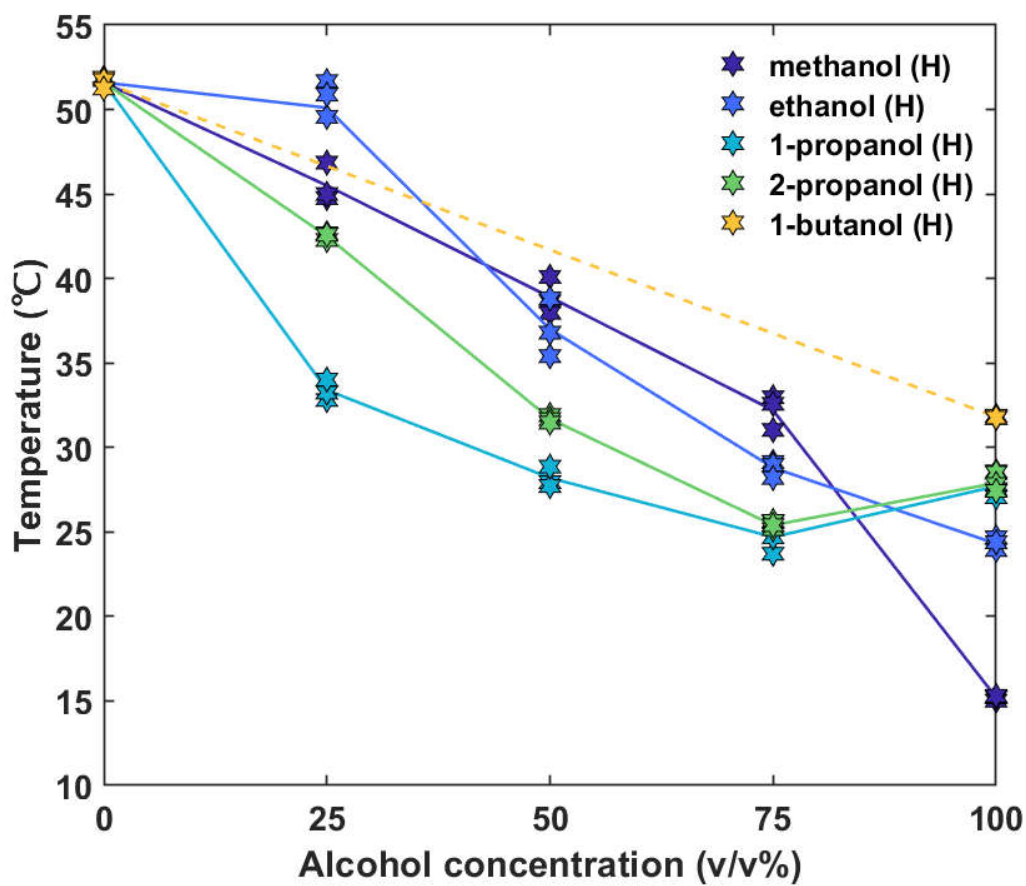


Figure 4.18 T_g of PLA immersed in alcohol-aqueous solutions as a function of alcohol concentration. (H) denotes water. Methanol (H) is methanol-aqueous solution, ethanol (H) is ethanol-aqueous solution, 1-propanol (H) is 1-propanol-aqueous solution, 2-propanol (H) is 2-propanol-aqueous solution and 1-butanol (H) is 1-butanol-aqueous solution.

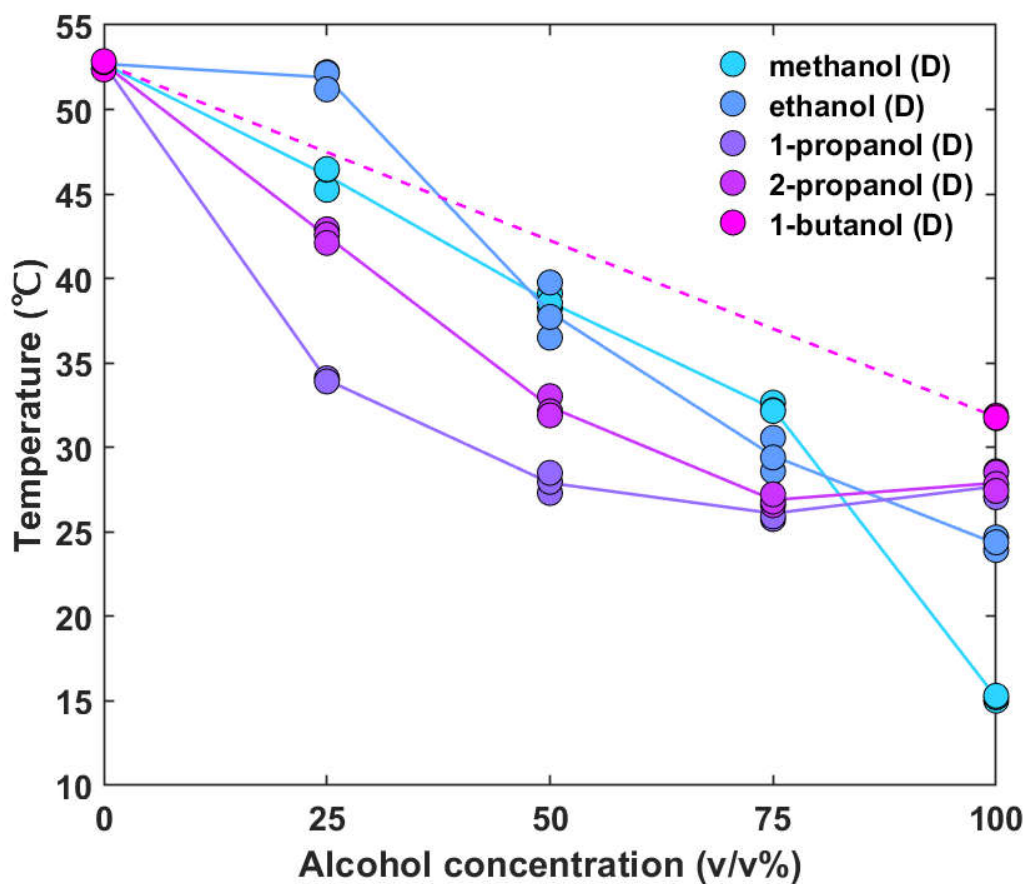


Figure 4.19 T_g of PLA immersed in alcohol-D₂O solutions as a function of alcohol concentration. (D) denotes D₂O. Methanol (D) is methanol-D₂O solution, ethanol (D) is ethanol-D₂O solution, 1-propanol (D) is 1-propanol-D₂O solution, 2-propanol (D) is 2-propanol-D₂O solution and 1-butanol (D) is 1-butanol-D₂O solution.

Although the changes in T_g 's of PLA films immersed in aqueous-alcohol solutions were quantified experimentally, there still lacks theoretical understanding of these behaviors. The next section presents some limit work on this area; however, much focus and additional research will be needed to fully explain these behaviors.

4.2.4 Solubility of PLA in alcohols determined by HSP

The experimental PLA HSP previously measured by our research group were [δ_d = 17.5, δ_p = 5.9, δ_h = 6.1] with a radius of 2.9 [8], as shown in **Figure 4.20**.

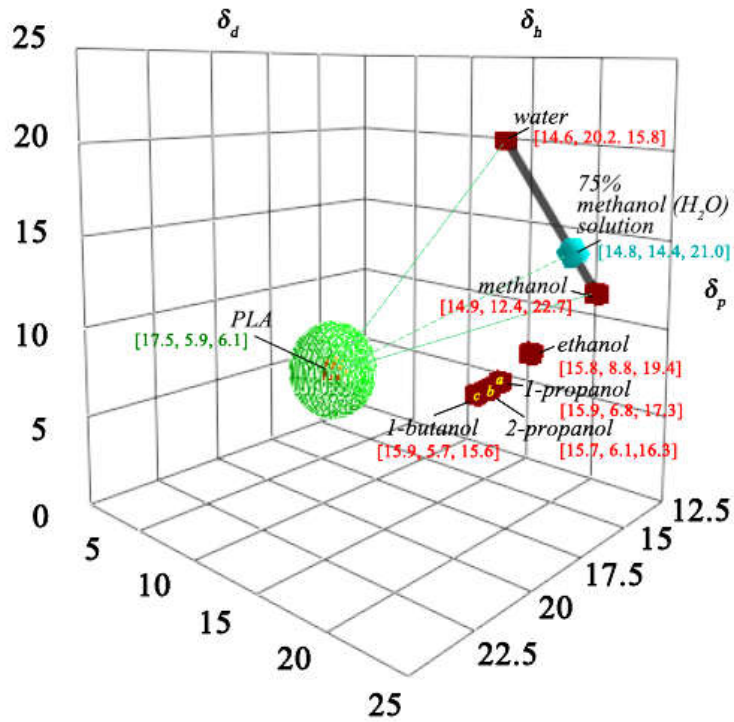


Figure 4.20 Hansen solubility parameters 3D plot of PLA, water and alcohols (C1-C4) at T_g . PLA HSP data adapted from reference [9]. The x-axis, y-axis, and z-axis represent the dispersion (δ_d), polar (δ_p), and hydrogen bonding (δ_h), respectively. The light blue square represents the 75% (v/v) methanol-aqueous solution, and red squares denote the water (1% soluble) and alcohols. Letter a, b and c indicate 1-propanol, 2-propanol and 1-butanol, respectively. The green dash line indicates the HSP distance. The original HSP data of PLA is from reference [9], and it was adjusted to the temperature where the T_g of PLA was observed in the *in-situ* immersion DMA test by using Eq. 3.3 – 3.5.

Figure 4.20 shows that alcohols are at the outside of the interaction sphere [$\delta_d = 17.5$, $\delta_p = 5.9$, $\delta_h = 6.1$], which means they are poor solvents for PLA. However, there may still be some relatively small interactions between alcohols and PLA. The total HSP in **Table 4.4** and **Table 4.5** were calculated by using Eq. 2.8, and the Hansen solubility parameter distance (R_a) was obtained from Eq. 2.9. The adjusted HSP at T_g shown in **Table 4.5** were estimated by Eq. 3.3 – 3.5.

Table 4.4 Hansen solubility parameters and interaction parameters at 25 °C.

Solvent	HSP at 25 °C [δ_d , δ_p , δ_h]	HSP distance (R_a)	Total solubility parameter (δ_t)	Interaction parameter (χ_{12}) at 25 °C
PLA	[17.6, 5.9, 6.4]	-	19.6	-
methanol	[14.7, 12.3, 22.3]	18.1	29.4	0.80
ethanol	[15.8, 8.8, 19.4]	13.8	26.5	0.68
1-propanol	[16, 6.8, 17.4]	11.5	24.6	0.60
2-propanol	[15.8, 6.1, 16.4]	10.6	23.6	0.53
1-butanol	[16, 5.7, 15.8]	9.9	23.2	0.55
water	[15.1, 20.4, 16.5]	18.4	30.3	0.37

Table 4.5 Hansen solubility parameters and interaction parameters at T_g .

Solvent	HSP at T_g [δ_d , δ_p , δ_h]	HSP distance (R_a)	Total solubility parameter (δ_t)	Thermal expansion coefficient (α), 1/°C	Interaction parameter (χ_{12}) at T_g
PLA	[17.5, 5.9, 6.1]	-	19.5	0.00007	-
methanol	[14.9, 12.4, 22.7]	18.6	29.8	0.0012	0.88
ethanol	[15.8, 8.8, 19.4]	14.0	26.6	0.0012	0.71
1-propanol	[15.9, 6.8, 17.3]	11.7	24.5	0.0011	0.62
2-propanol	[15.7, 6.1, 16.3]	10.8	23.5	0.0011	0.54
1-butanol	[15.9, 5.7, 15.6]	10.0	23.0	0.001	0.55
water	[14.6, 20.2, 15.8]	18.2	29.5	0.0009	0.33

Table 4.6 Hansen solubility parameters of mixture at T_g .

Solvent 1	Solvent 2	% of Solvent 1	Mix HSP [δ_d' , δ_p' , δ_h']	HSP distance (R_a)	Total solubility parameter (δ_t)
methanol	water	25%	[14.7, 18.3, 17.5]	17.7	34.2
		50%	[14.8, 16.3, 19.3]	17.6	34.5
		75%	[14.8, 14.4, 21.0]	17.9	35.2
ethanol	water	25%	[14.9, 17.4, 16.7]	16.4	34.7
		50%	[15.2, 14.5, 17.6]	15.1	32.8
		75%	[15.5, 11.7, 18.5]	14.2	31.3
1-propanol	water	25%	[14.9, 16.9, 16.2]	15.7	30.3
		50%	[15.3, 13.5, 16.6]	13.7	30.0
		75%	[15.6, 10.2, 16.9]	12.3	34.7
2-propanol	water	25%	[14.9, 16.7, 15.9]	15.5	31.9
		50%	[15.2, 13.2, 16.1]	13.2	29.7
		75%	[15.4, 9.6, 16.2]	11.5	28.0

The Flory-Huggins interaction parameters (χ_{12}) between pure alcohols and the PLA at different temperatures are shown in **Table 4.4** and **Table 4.5**. Compared with alcohols, χ_{12} of water is closer to zero. A large χ_{12} value indicates a big difference in interaction energy of the solvent molecule immersed in polymer compared with the one in solvent. If χ_{12} is greater than zero, it shows that the solvent “dislike” the polymer, which

means the solvent and the polymer are not similar and generally insoluble in each other [10].

The pure alcohols were found in the region of relatively high dispersion interaction and hydrogen bonding interaction and relatively low polar interaction as shown in **Figure 4.20**. But for alcohol-aqueous solutions, their polar interactions were greater than those of the pure alcohols. Also, lower R_a indicates better solubility. In this case, methanol has the greatest distance from the PLA center sphere, which means PLA has the worst solubility in methanol compared to the solubility in the other solvents in this study.

As mentioned before, liquids with similar solubility parameters are miscible [11]. **Table 4.4** and **Table 4.5** indicate that the difference between the solubility parameters of 1-butanol and water is relatively large, indicating they cannot be mixed very well. Mixing these two liquids cause layering or phase separation. Therefore, for 1-butanol, only 0% (v/v) and 100% concentration data was obtained from the DMA immersion experiment as explained in **section 4.2.3**.

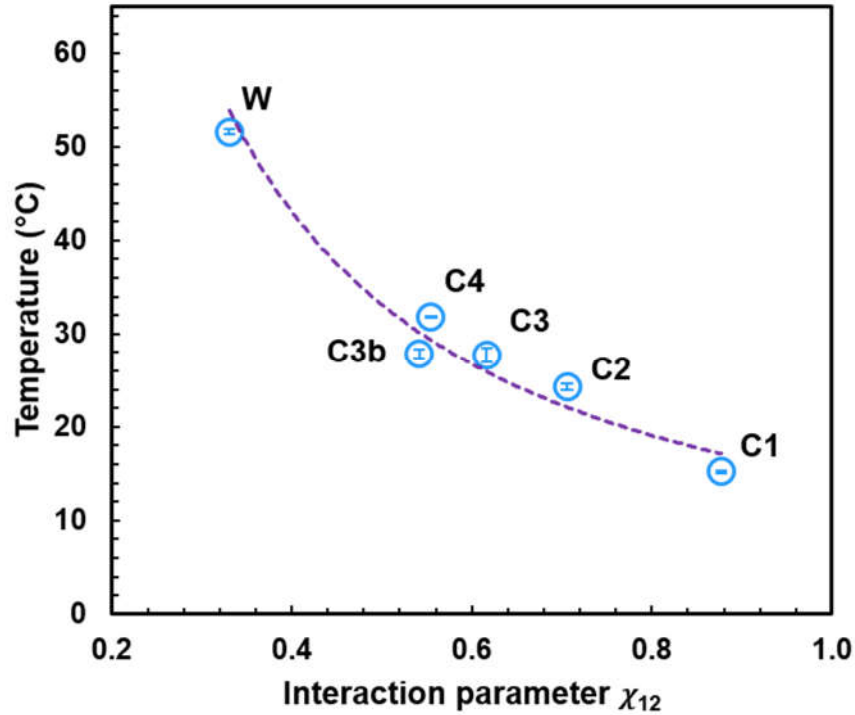


Figure 4.21 T_g of PLA film as a function of Flory-Huggins interaction parameter.

Figure 4.21 shows the relationship between the T_g of PLA films immersed in pure alcohols (C1-C4) and water, and the χ_{12} . The PLA films immersed in pure methanol (C1) has the lowest T_g , highest χ_{12} and largest predicted sorption amount, which is contradictory to what should be expected from χ_{12} where for small solvents χ_{12} is small or negative. If χ_{12} is small or negative, a polymer will expand and/or dissolve in a solvent. In the case of poor solvents, $\chi_{12} > 0$, the polymers will avoid contacts with the solvent; thus, the polymer coils will be much more compact and immiscible with the solvent. Further research of the χ_{12} and the sorption of alcohol in PLA is needed.

HSP indicates that all the tested alcohols are not good solvents for PLA. However, all these alcohols diffuse into PLA and plasticize the polymer matrix reducing PLA's T_g . According to the DMA experiment results, the estimated sorption amount of methanol in

the PLA calculated by the Fox equation (Eq. 3.10) shows almost 8.0% methanol absorbed in the PLA (**Figure 4.6**). PLA immersed in 1-propanol (C3) and 2-propanol (C3b) has similar T_g and the χ_{12} of 1-propanol is a little higher than that of 2-propanol.

For pure (100% concentration) alcohol solutions, alcohols with the total HSP closer to PLA HSP have a greater impact on the reduction of PLA's T_g . This may be because the components with similar solubility parameters are more compatible with each other, as shown in **Figure 4.20**. It can be seen that the total HSP of 1-butanol is the closest to PLA from **Table 4.4** and **Table 4.5**. Although 1-butanol is still some distance away from the PLA sphere (outside, which means it is not a good solvent); it is the closest to PLA sphere compared to other alcohols.

Different types of PLA may have different properties, such as the proportion of L-lactide and D-lactide, and thus have different solubility for alcohols. To calculate the solubility parameters and interaction parameters more accurately, it may be necessary to use multiple solvents to estimate the HSP of PLA, and then calculate the solubility radius of PLA used in the experiment.

Figure 4.20 also shows that even if alcohols and water are poor solvents to PLA, their mixed solutions may have better solubility or compatibility since the mixture's coordinates are on the connecting line of alcohols and water, and the coordinates of the mixture may be closer to the center of the PLA sphere.

4.3 Sorption amounts of alcohols in PLA films

4.3.1 Basic information about $^1\text{H-NMR}$ spectrum of PLA

Figure 4.22 shows the $^1\text{H-NMR}$ spectrum (immersion time: 72h) and the chemical shifts of PLA, ethanol, CDCl_3 and the internal standard. Table 4.7 shows the compound group and their chemical shifts of ethanol in PLA in the $^1\text{H-NMR}$ spectrum.

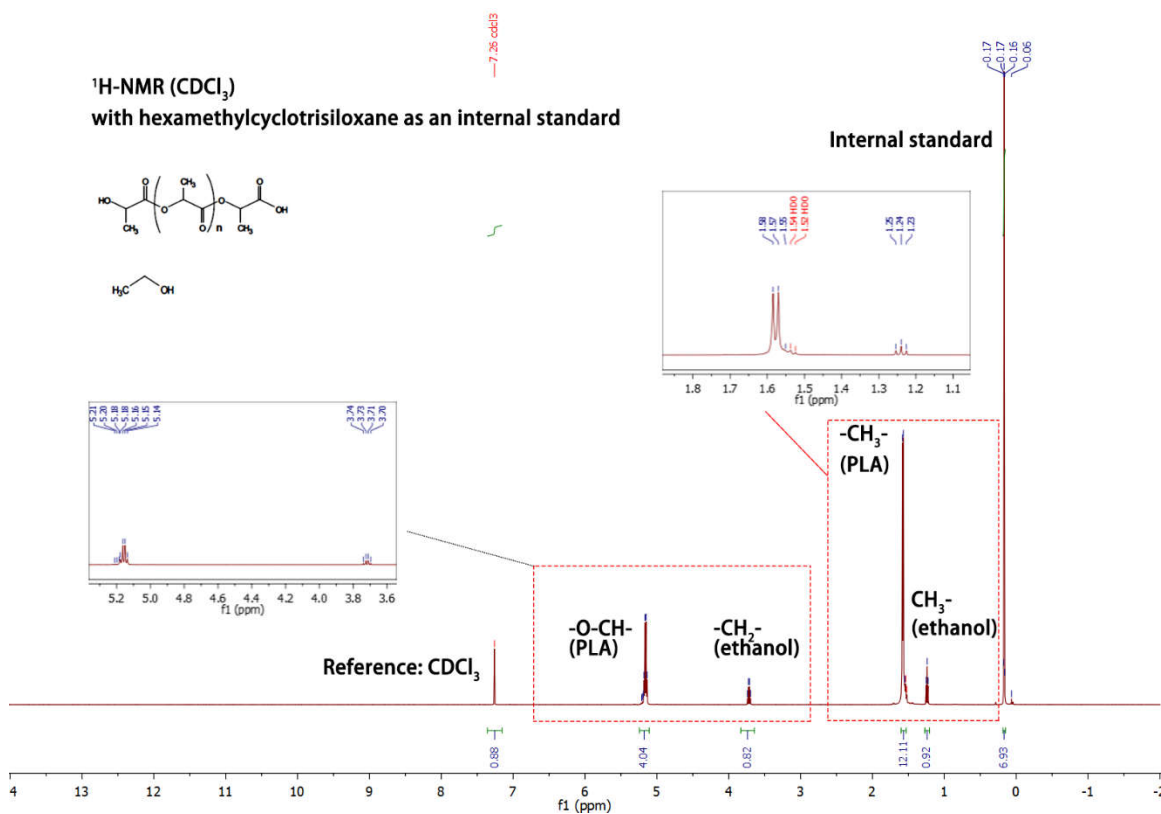


Figure 4.22 The $^1\text{H-NMR}$ result of the PLA film immersed in pure ethanol (Immersion time: 72h).

Table 4.7 ^1H -qNMR compound group and chemical shifts of ethanol in PLA.

Compound	Group	Chemical shifts (ppm)
ethanol	$\text{CH}_3\text{-CH}_2\text{-OH}$	1.22
ethanol	$\text{CH}_3\text{-CH}_2\text{-OH}$	3.70
PLA	$\text{-O-CH-CH}_3\text{-COO-}$	1.56
PLA	$\text{-O-CH-CH}_3\text{-COO-}$	5.14

Data adapted from reference [12].

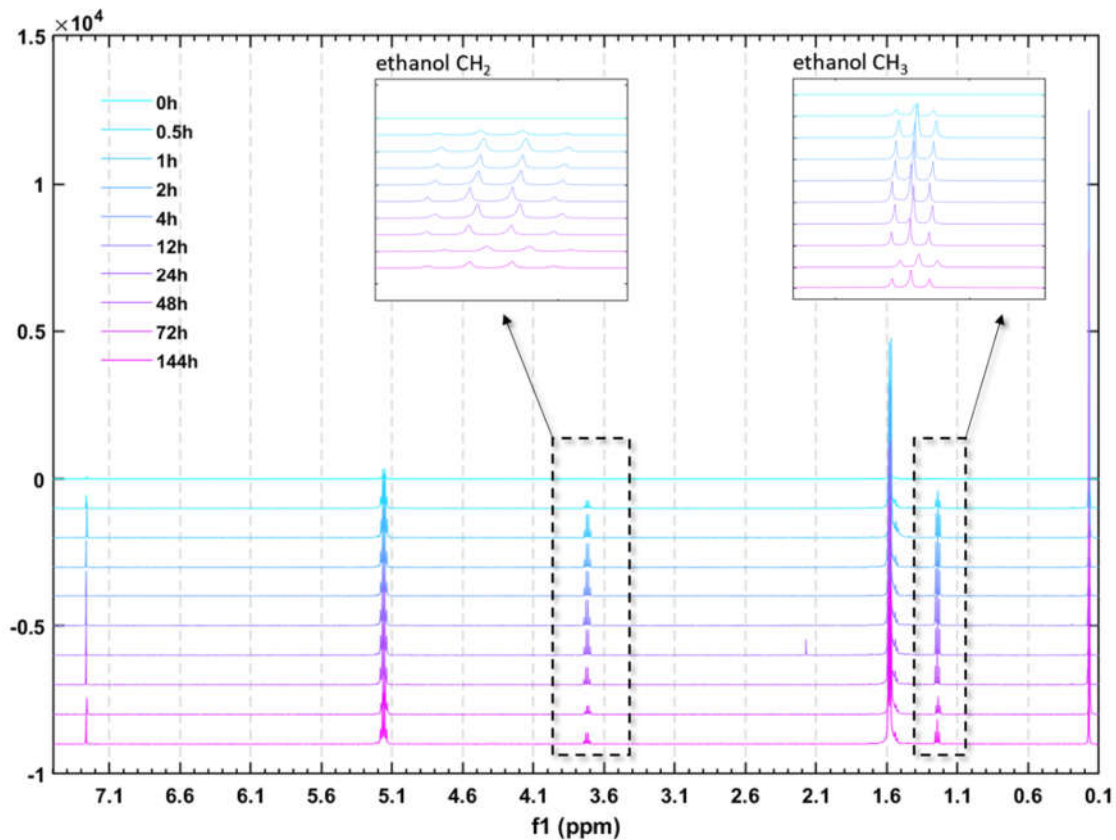


Figure 4.23 ^1H -qNMR results of PLA immersed in pure ethanol for 0h to 144h.

Figure 4.23 shows the ^1H -qNMR results of PLA immersed in pure ethanol for 0h to 144h. The common splitting patterns in the ^1H -qNMR spectrum include singlet, doublet, triplet (intensity ratio = 1:2:1) and quartet (1:3:3:1). **Figure 4.24** shows the commonly observed splitting patterns in an ^1H -NMR spectrum, and according to the N+1 rule (N is the number of neighboring spin-coupled nuclei with the same coupling constant), so the group of compounds can be distinguished.

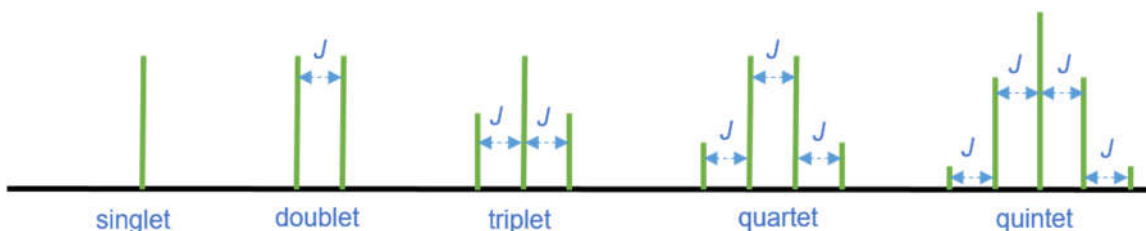


Figure 4.24 Commonly observed splitting patterns in ^1H -NMR spectrum. J denotes coupling constant.

4.3.2 Sorption amount of pure ethanol in PLA films

According to Eq. 3.12, the sorption amount of pure ethanol solvent in PLA films can be calculated from the ^1H -qNMR results. As shown in **Figure 4.25**, when the immersion time reach to 4 h, the maximum amount of ethanol sorbed in PLA samples is approximately 9.16% (g-ethanol/g-PLA \times 100%), which is a little higher than the estimated value of 5.63% obtained from the Fox equation (Eq. 3.10). This maybe because of the quenching treatment of PLA samples for NMR experiment, which leads to less crystallinity (or amorphous) of PLA sample used in DMA experiment. The crystalline parts are arranged regularly, so the PLA film with more crystalline parts may absorb less solution.

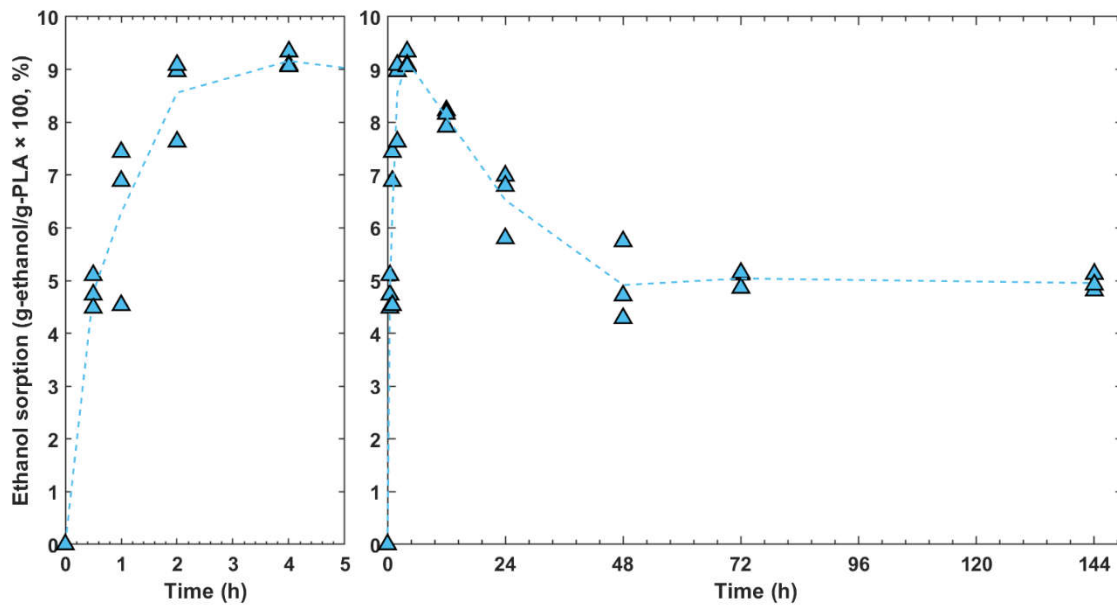


Figure 4.25 Ethanol sorption in PLA samples as a function of immersion time at 25 °C.

According to **Figure 4.25**, after the first 4 h, in the following two days, the amount of ethanol absorbed gradually decreased. This may be due to the increase of crystallization in the PLA film leading to a reduction in amorphous areas (as shown in **Figure 4.26** and **Figure 4.27**). After the immersion time exceeds 48 h, the absorption of ethanol gradually stabilized, reaching about 4.95%.

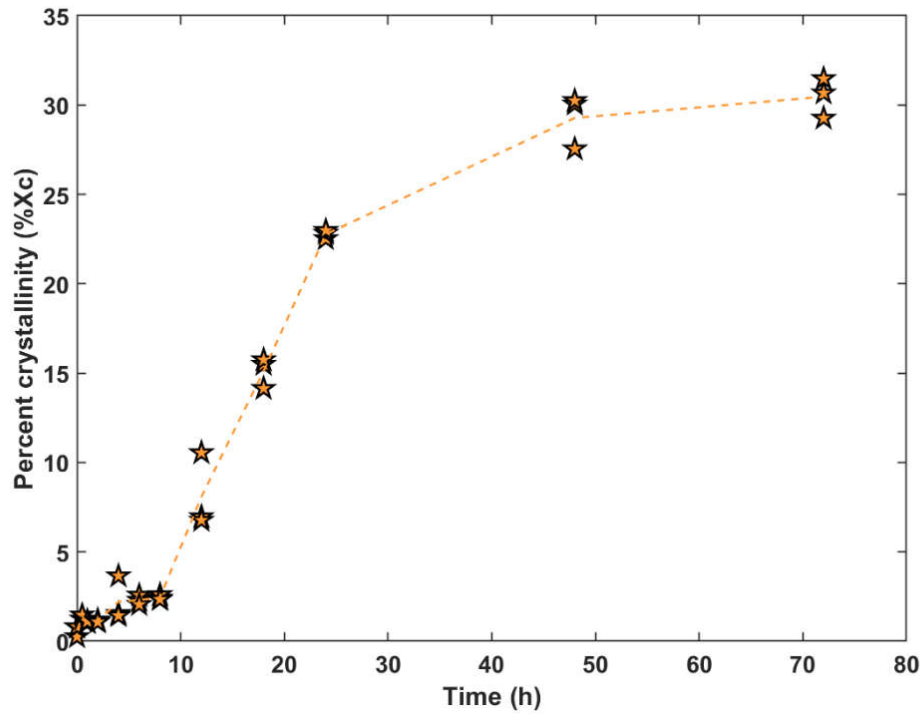


Figure 4.26 Percent crystallinity of PLA film immersed in ethanol versus immersion time at 25 °C.

Table 4.8 shows T_m , T_c and T_g of the PLA films immersed in pure ethanol. PLA films immersed in ethanol for 48h and 72h did not show a cold crystallization peak.

Table 4.8 Results of melting, crystallization and glass transition temperature of PLA film immersed in pure ethanol from DSC tests.

Immersion time (h)	T_m (°C)	T_c (°C)	T_g (°C)	X_c (%)
0	149.9 ± 1.2	121.9 ± 6.9	58.5 ± 0.1	0.2±0.4
0.5	151.8 ± 0.3	101.6 ± 7.2	61.0 ± 2.0	2.6±0.7
1	148.1 ± 0.3	112.8 ± 1.7	60.6 ± 1.0	1.0±0.2
2	149.5 ± 2.4	103.9 ± 7.0	60.9 ± 1.4	2.7±0.6
4	151.8 ± 0.2	100.2 ± 2.3	61.1 ± 1.3	2.9±0.8
6	152.4 ± 0.3	101.1 ± 4.1	59.0 ± 3.7	2.4±1.2
8	152.4 ± 0.1	107.7 ± 0.3	60.2 ± 2.4	2.0±0.1
12	152.4 ± 0.6	100.2 ± 1.9	60.0 ± 4.4	5.2±1.1
18	152.2 ± 0.2	98.9 ± 2.3	62.3 ± 0.3	14.2±1.7
24	151.9 ± 0.2	96.1 ± 0.9	59.8 ± 2.4	23.6±0.4
48	152.3 ± 0.3	-	53.4 ± 2.2	29.4±1.5
72	151.8 ± 0.1	-	59.8 ± 2.3	30.5±0.9

Figure 4.27 shows the relationship between the amount of ethanol sorption and the X_c of the PLA sample. With the increase of X_c , the absorption of ethanol by PLA film decreases. At the initial stage of immersion of the PLA film in ethanol (within 12 h), the X_c change is below 3%. As the immersion time increases, the X_c of the PLA film gradually rises, and it exceeds 20% at 24 h, then stabilizes at approximately 30% after 48 h

immersion. PLA is a slow crystallizable polymer; therefore, it takes approximately 8 h for the induce crystallization of PLA in ethanol to make an effect on the ethanol sorption.

Studying PLA crystallization kinetics when PLA is submerged in ethanol can help to elucidate the crystallization rate and couple these results with ethanol sorption studies. During the immersion in alcohols, the chain scission-induced crystallization can occur. Limsukon et al. [13] studied the hydrolytic degradation of PLA immersed in 50% ethanol-aqueous solution and reported that the X_c increased as the hydrolysis proceeded.

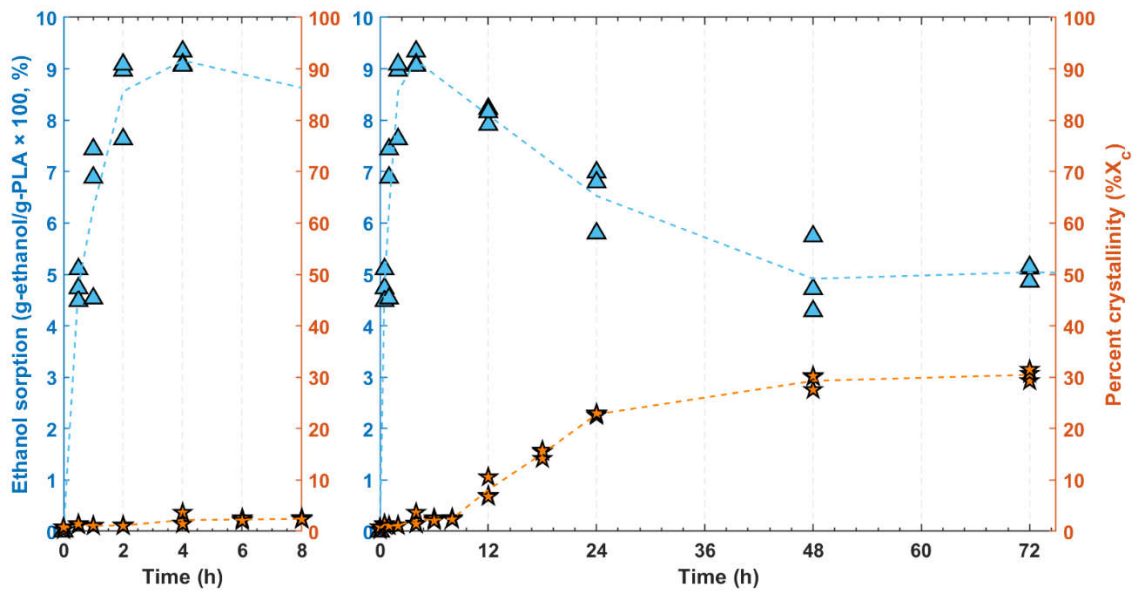


Figure 4.27 Relationship between ethanol sorption amount (left y-axis), percent crystallinity (right y-axis) and the immersion time.

Figure 4.28 shows that in the case of *in-situ* immersion, the T_g of the PLA immersed in ethanol has not changed much from the T_g of dry PLA at 60 °C. As the immersion time increases, the crystallization peak disappears proven that no additionally

crystallization is possible due to the completed crystallization of the PLA film during the immersion process.

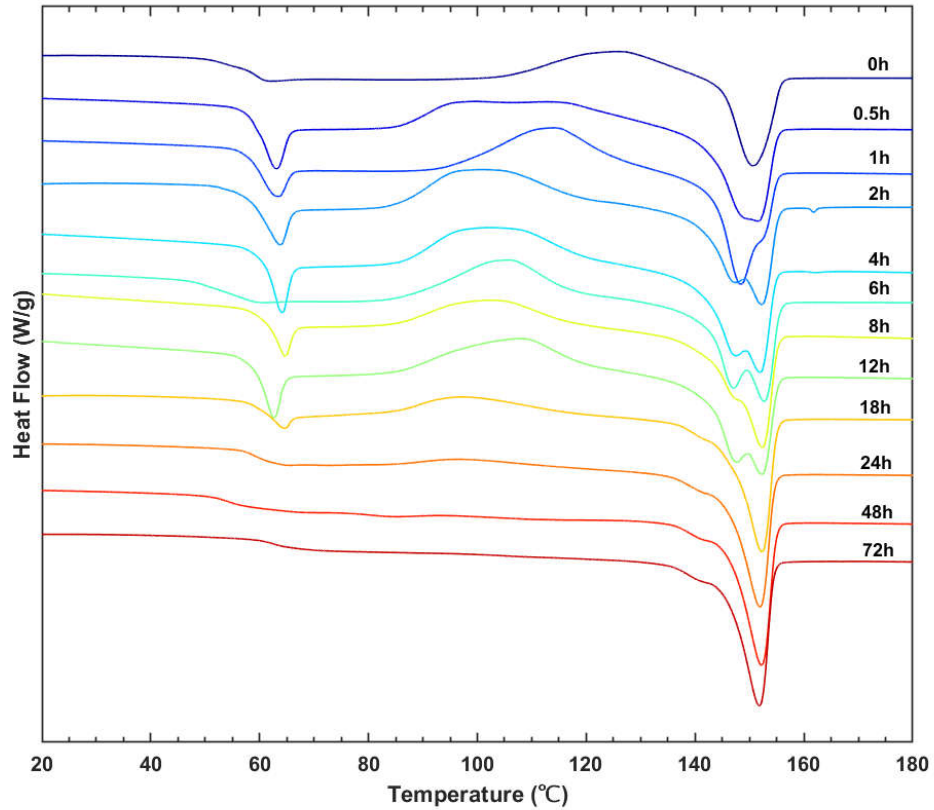


Figure 4.28 DSC results for amorphous PLA with different immersion time in pure ethanol at 25 °C (first heat run).

4.3.3 Sorption isotherm of PLA with water and D₂O

Figure 4.29 and **Figure 4.30** shows the sorption isotherm of PLA in water and D₂O at 25 °C, respectively. The total moisture content at 95% RH are different for PLA in water and D₂O. The moisture content is greater for PLA in D₂O than for PLA in water, which

means at the same temperature, PLA films can absorb more D₂O than water. Additionally, the sorption data for D₂O is more disperse than water.

Iñiguez-Franco et al. [12] measured the sorption isotherm of water and D₂O in PLA films at 40 °C and found that when PLA films were exposed to 80% RH, the moisture content was approximately 0.7 g-water/100 g-dry PLA, which is similar to the results in this thesis. The sorption isotherm of water at 40 °C is shown in the Appendix C ().

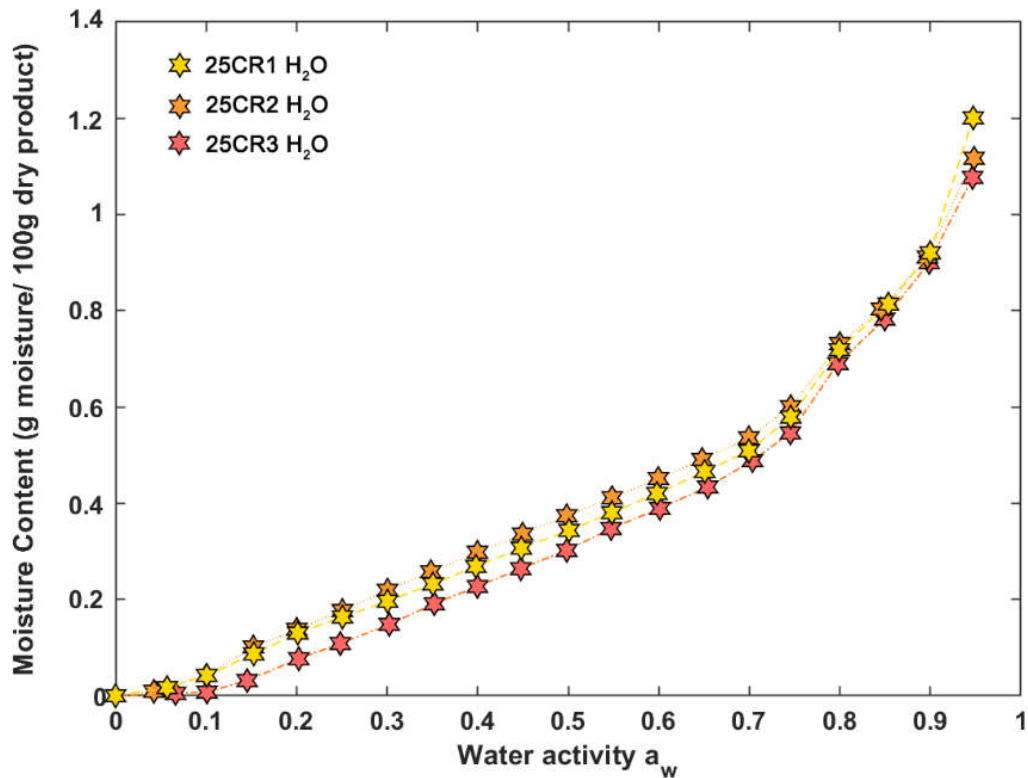


Figure 4.29 Sorption isotherm curve of PLA film in water at 25 °C.

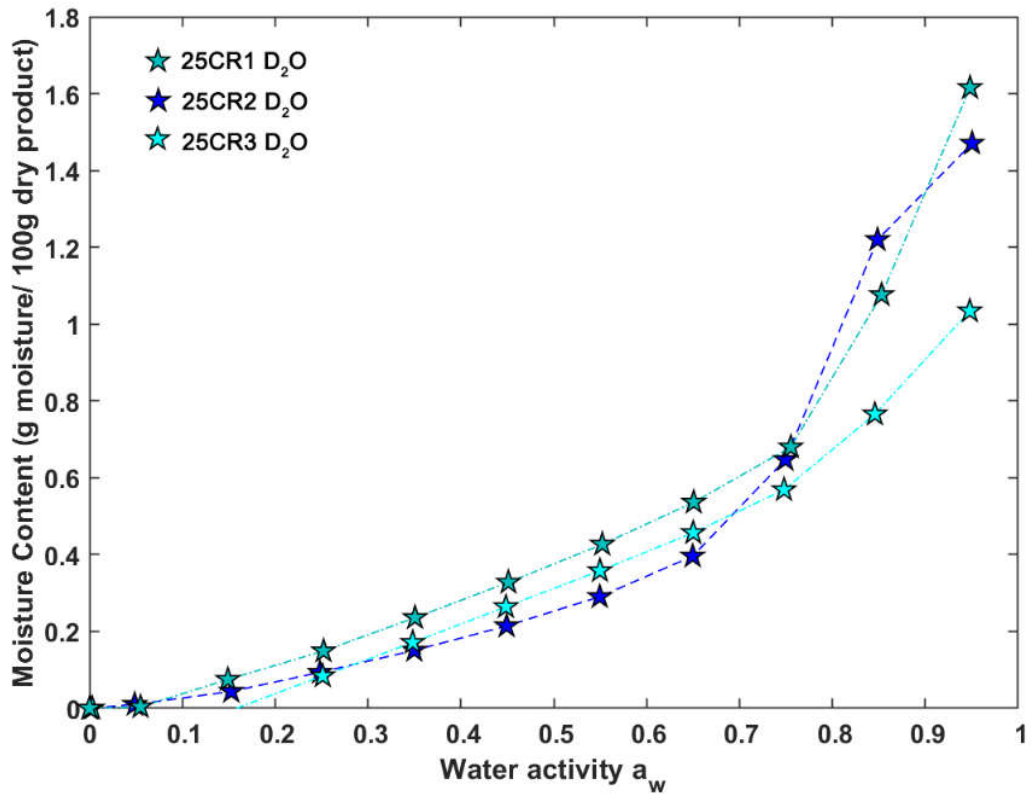


Figure 4.30 Sorption isotherm curve of PLA film in D₂O at 25 °C.

APPENDICES

APPENDIX A: One-way ANOVA results of T_g of PLA immersed in pure alcohols.

One-way ANOVA

Table A1 One-way ANOVA table (The GLM Procedure).

Dependent Variable: T_g

Source	DF	Sum of Squares	Mean Square	F Value	Pr > F
Model	7	5873.745096	839.106442	4591.24	<.0001
Error	16	2.924200	0.182762		
Corrected Total	23	5876.669296			

R-Square	Coeff Var	Root MSE	T_g Mean
0.999502	1.163193	0.427507	36.75292

Source	DF	Type I SS	Mean Square	F Value	Pr > F
alcohol	7	5873.745096	839.106442	4591.24	<.0001

Source	DF	Type III SS	Mean Square	F Value	Pr > F
alcohol	7	5873.745096	839.106442	4591.24	<.0001

Table A2 LS-means of T_g of PLA immersed in pure alcohols.

alcohol	T_g LSMEAN	Standard Error	Pr > t
1-butanol	31.8000000	0.2468215	<.0001
1-propanol	27.7333333	0.2468215	<.0001
2-propanol	27.9000000	0.2468215	<.0001
D ₂ O	52.7000000	0.2468215	<.0001
dry	62.8000000	0.2468215	<.0001
ethanol	24.3233333	0.2468215	<.0001
methanol	15.1666667	0.2468215	<.0001
water	51.6000000	0.2468215	<.0001

Table A3 Tukey grouping results.

Tukey Grouping for alcohol Least Squares Means (Alpha=0.05)					
LS-means with the same letter are not significantly different.					
alcohol	Estimate				
dry	62.8000	A			
D₂O	52.7000	B			
water	51.6000	B			
1-butanol	31.8000	C			
2-propanol	27.9000	D			
1-propanol	27.7333	D			
ethanol	24.3233	E			
methanol	15.1667	F			
alcohol Least Squares Means					
alcohol	Estimate	Standard Error	DF	t Value	Pr > t
dry	62.8000	0.2468	16	254.43	<.0001
methanol	15.1667	0.2468	16	61.45	<.0001
ethanol	24.3233	0.2468	16	98.55	<.0001
1-propanol	27.7333	0.2468	16	112.36	<.0001
2-propanol	27.9000	0.2468	16	113.04	<.0001
1-butanol	31.8000	0.2468	16	128.84	<.0001
water	51.6000	0.2468	16	209.06	<.0001
D₂O	52.7000	0.2468	16	213.51	<.0001

Table A4 Differences of alcohol least square means table.

Differences of alcohol Least Squares Means Adjustment for Multiple Comparisons: Tukey							
alcohol	alcohol'	Estimate	Standard Error	DF	t Value	Pr > t 	Adj P
dry	methanol	47.6333	0.3491	16	136.46	<.0001	<.0001
dry	ethanol	38.4767	0.3491	16	110.23	<.0001	<.0001
dry	1-propanol	35.0667	0.3491	16	100.46	<.0001	<.0001
dry	2-propanol	34.9000	0.3491	16	99.98	<.0001	<.0001
dry	1-butanol	31.0000	0.3491	16	88.81	<.0001	<.0001
dry	water	11.2000	0.3491	16	32.09	<.0001	<.0001
dry	D ₂ O	10.1000	0.3491	16	28.93	<.0001	<.0001
methanol	ethanol	-9.1567	0.3491	16	-26.23	<.0001	<.0001
methanol	1-propanol	-12.5667	0.3491	16	-36.00	<.0001	<.0001
methanol	2-propanol	-12.7333	0.3491	16	-36.48	<.0001	<.0001
methanol	1-butanol	-16.6333	0.3491	16	-47.65	<.0001	<.0001
methanol	water	-36.4333	0.3491	16	-104.38	<.0001	<.0001
methanol	D ₂ O	-37.5333	0.3491	16	-107.53	<.0001	<.0001
ethanol	1-propanol	-3.4100	0.3491	16	-9.77	<.0001	<.0001
ethanol	2-propanol	-3.5767	0.3491	16	-10.25	<.0001	<.0001
ethanol	1-butanol	-7.4767	0.3491	16	-21.42	<.0001	<.0001
ethanol	water	-27.2767	0.3491	16	-78.14	<.0001	<.0001
ethanol	D ₂ O	-28.3767	0.3491	16	-81.29	<.0001	<.0001
1-propanol	2-propanol	-0.1667	0.3491	16	-0.48	0.6395	0.9996
1-propanol	1-butanol	-4.0667	0.3491	16	-11.65	<.0001	<.0001
1-propanol	water	-23.8667	0.3491	16	-68.37	<.0001	<.0001
1-propanol	D ₂ O	-24.9667	0.3491	16	-71.53	<.0001	<.0001
2-propanol	1-butanol	-3.9000	0.3491	16	-11.17	<.0001	<.0001
2-propanol	water	-23.7000	0.3491	16	-67.90	<.0001	<.0001
2-propanol	D ₂ O	-24.8000	0.3491	16	-71.05	<.0001	<.0001
1-butanol	water	-19.8000	0.3491	16	-56.72	<.0001	<.0001
1-butanol	D ₂ O	-20.9000	0.3491	16	-59.88	<.0001	<.0001
water	D ₂ O	-1.1000	0.3491	16	-3.15	0.0062	0.0885

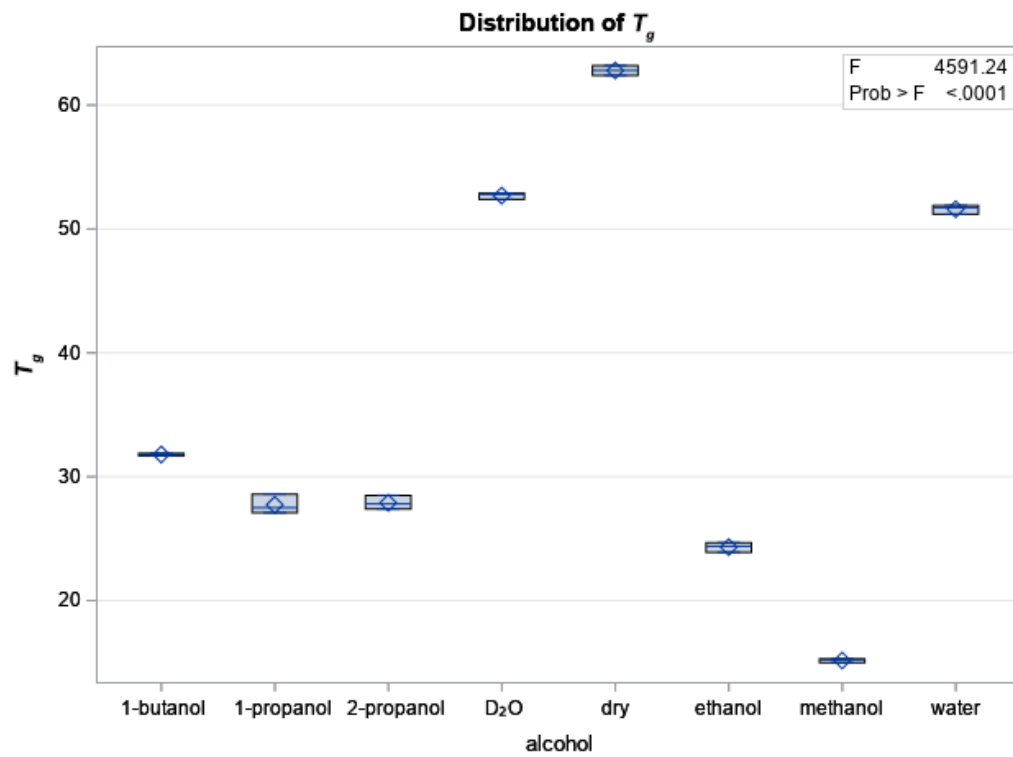


Figure A1 Distribution plot of T_g of PLA.

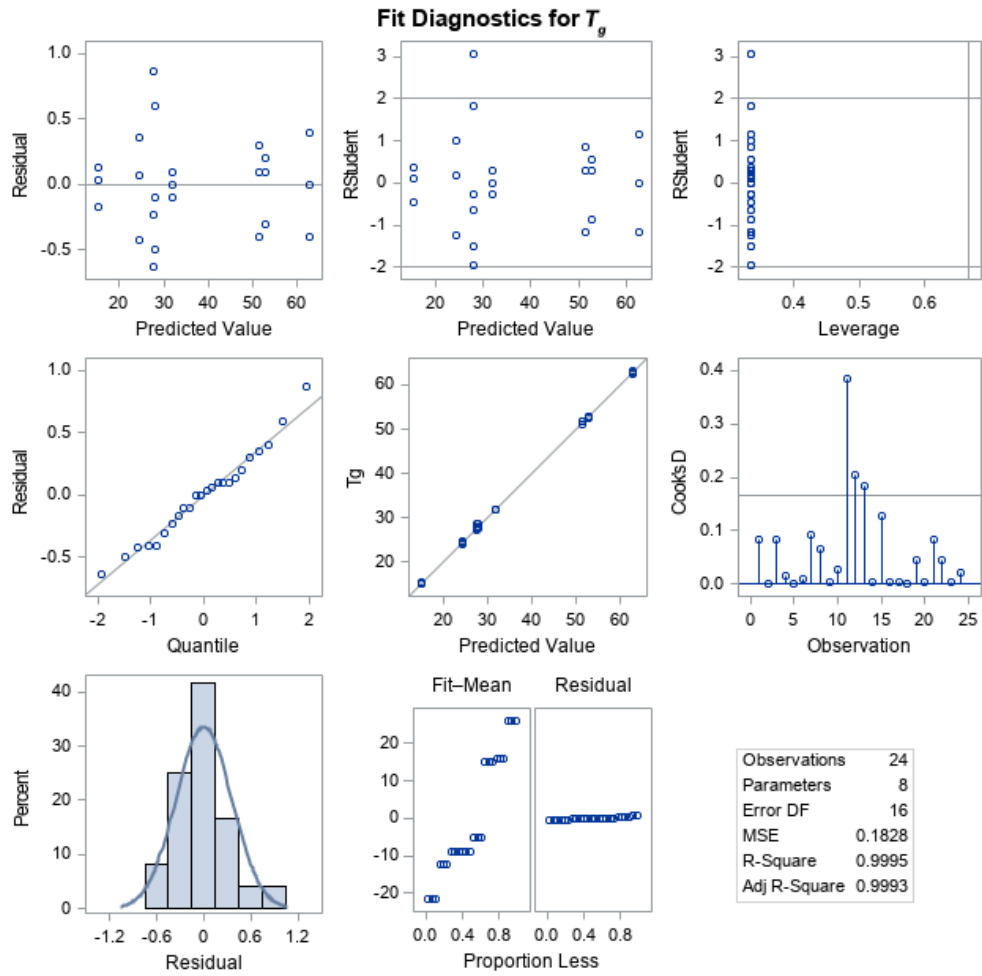


Figure A2 Fit diagnostics plots for T_g of PLA.

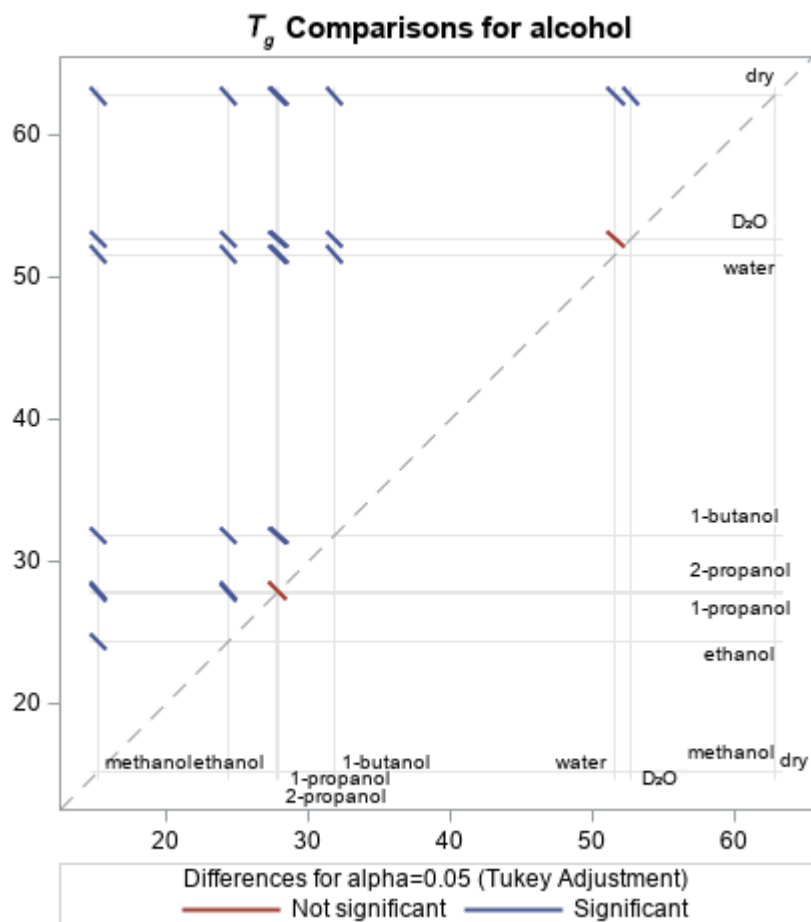


Figure A3 The differences comparisons of T_g for alcohol.

APPENDIX B: T1 measurement for quantitative NMR test.

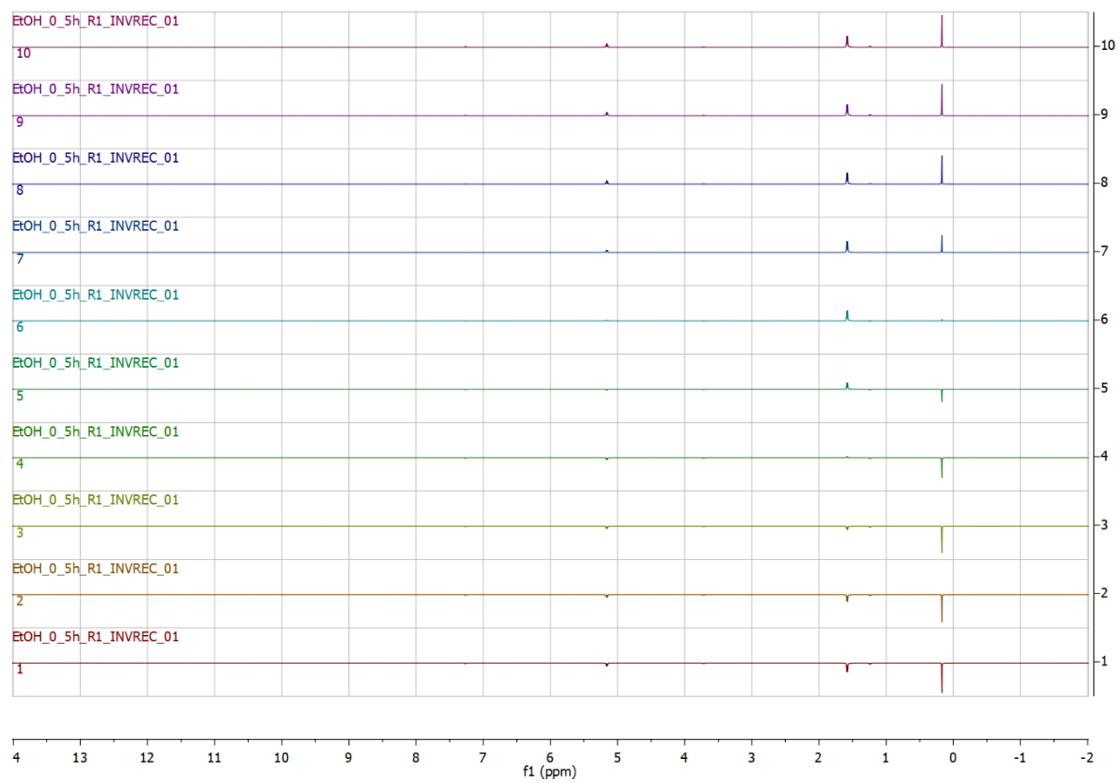


Figure B1 T1 measurement for quantitative NMR experiment.

APPENDIX C: Sorption isotherm for water vapor in PLA films.

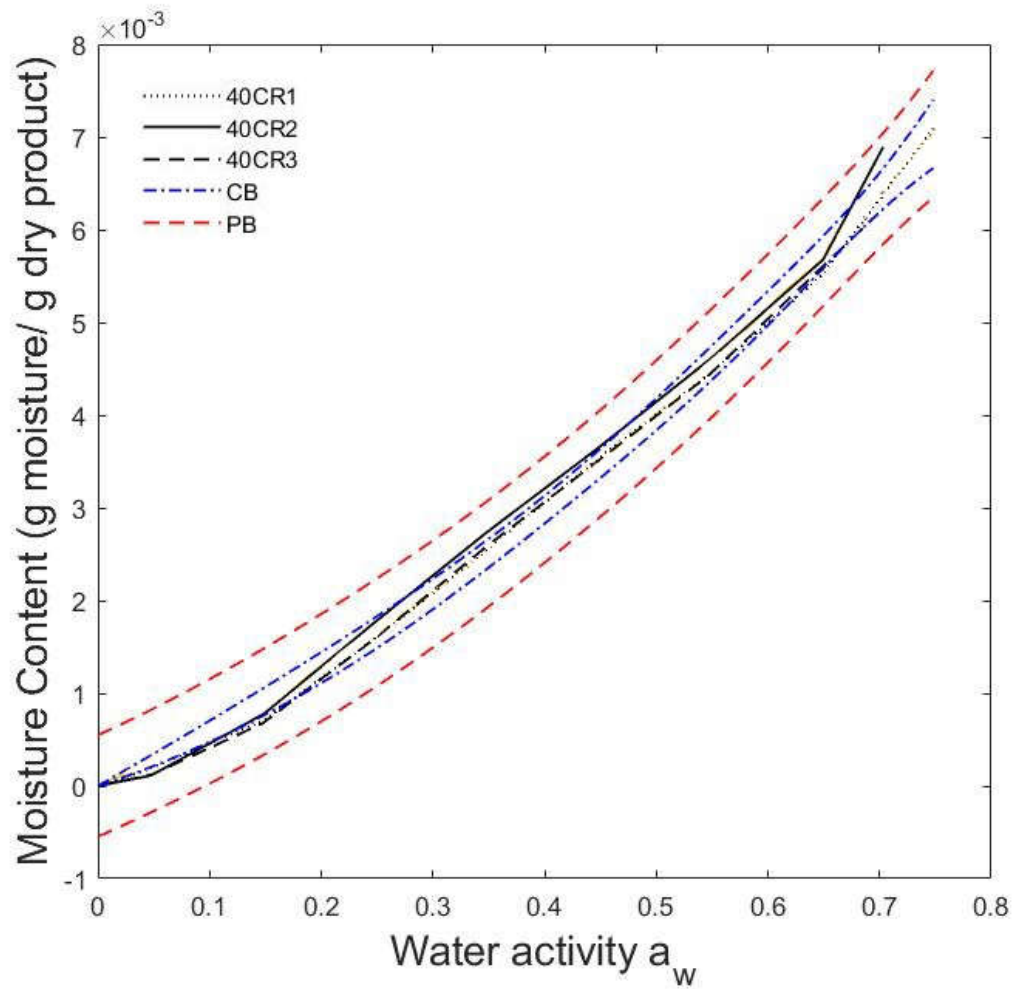


Figure C1 Sorption isotherm for water vapor in PLA films at 40 °C.

REFERENCES

REFERENCES

- [1] Meyers M., Ed., *Mechanical Behavior of Materials*, 2nd ed. Cambridge university press, 1999.
- [2] Sonchaeng U., Critical and systematic review of poly (lactic acid) mass transfer and evaluation of the *in-situ* changes of its thermo-mechanical properties when immersed in alcohol solutions, PhD thesis, Michigan State University, Michigan, 2019, doi: 10.25335/76kp-yt65.
- [3] Yong A. X. H., Sims G. D., Gnaniah S. J. P., *et al.*, Heating rate effects on thermal analysis measurement of T_g in composite materials, *Advanced Manufacturing: Polymer & Composites Science*, vol. 3, no. 2, pp. 43–51, 2017, doi: 10.1080/20550340.2017.1315908.
- [4] Walz M.-M., J. Werner, V. Ekholm, N. L. Prisle G. Ö. and O. B., Alcohols at the Aqueous Surface: Chain Length and Isomer Effects, *Physical Chemistry Chemical Physics*, vol. 18, no. 9, pp. 6648–6656, 2016, doi: 10.1039/c5cp06463e.
- [5] Zhao M., Liu L., Zhang B., *et al.*, Epoxy composites with functionalized molybdenum disulfide nanoplatelet additives, *RSC Advances*, vol. 8, no. 61, pp. 35170–35178, 2018, doi: 10.1039/c8ra07448h.
- [6] MAEDA Y., Effect of Antiplasticization on Gas Sorption and Transport. III. Free Volume Interpretation, *Journal of Polymer Science Part B: Polymer Physics*, vol. 25, no. 5, pp. 1005–1016, 1987, doi: 10.1002/polb.1987.090250503.
- [7] Sonchaeng U., Auras R., Selke S., *et al.*, *In-situ* changes of thermo-mechanical properties of poly (lactic acid) film immersed in alcohol solutions, *Polymer Testing*, vol. 82, 2020, doi: 10.1016/j.polymertesting.2019.106320.
- [8] Mulder M., *Basic Principles of Membrane Technology*. 1996.
- [9] Elangovan D., Nidoni U., Yuzay I. E., *et al.*, Poly(L-lactic acid) metal organic framework composites. Mass transport properties, *Industrial & Engineering Chemistry Research*, vol. 50, no. 19, pp. 11136–11142, 2011, doi: 10.1021/ie201378u.
- [10] Hansen C. M., *Hansen solubility parameters: a user's handbook.*, 2nd ed. CRC Press, 2007.

- [11] Gao J., Using hansen solubility parameters (HSPS) to develop antioxidant-packaging film to achieve controlled release, Master thesis, Michigan State University, Michigan, 2014.

- [12] Iniguez-Franco F., Hydrolytic degradation of neat and modified poly(lactic acid) with nanoparticles and chain extenders by water-ethanol solutions, PhD thesis, Michigan State University, Michigan, 2018, doi:10.25335/M5SN01677.

- [13] Limsukon W., Auras R., and Selke S., Hydrolytic degradation and lifetime prediction of poly(lactic acid) modified with a multifunctional epoxy-based chain extender, *Polymer Testing*, vol. 80, 2019, doi: 10.1016/j.polymertesting.2019.106108.

CHAPTER 5 Conclusions

5.1 Overall conclusions

As one of the main renewable and compostable polymers, PLA has many good attributes such as low carbon footprint and an optional end of life scenario which is composting. However, PLA is susceptible to hydrolysis under environmental conditions such as temperature and humidity which it experiences during its shelf life. Besides, PLA interactions with organic solvents affect its thermal properties and hydrolytic degradation process during its storage [1]. So, the aim of this study was to determine the thermo-mechanical properties of PLA film immersed in alcohol-aqueous solutions and to quantify the sorption amount of alcohols into PLA film.

First, the changes in T_g of PLA films immersed in alcohol-aqueous/D₂O solvents were determined using *in-situ* immersion DMA. According to the results, immersion of PLA in water and alcohol had an effect on the T_g of PLA. Due to plasticization of the PLA matrix by the solvents, the mobility of the polymer system increased so that the PLA's T_g is decreased. Specifically, compared with the PLA film not immersed in the alcohol solution, the T_g of the film immersed in pure methanol decreased up to 76%. Compared to the T_g of dry PLA film, the T_g of PLA film immersed in pure ethanol, 1-propanol, 2-propanol and 1-butanol decreased 61%, 56%, 56%, 49%, respectively.

Furthermore, the PLA films' T_g 's were affected by the concentration of the alcohol solutions. For methanol and ethanol (alcohols with 1 and 2 carbon atoms, respectively), the T_g 's were decreased by 8.6 °C and 7.6 °C per every 25% (v/v) increase of alcohol, respectively. When the PLA films were immersed in solutions of alcohols with 3 to 4

carbon atoms (i.e., 1-propanol, 2-propanol), the PLA T_g 's decreased until 75% (v/v). T_g 's of 1-propanol and 2-propanol decreased by 8.6 °C and 8.9 °C for every 25% (v/v) increase of 1 or 2-propanol, respectively. As the concentration of alcohol (v/v) increased, the difference between straight-chain alcohols (1-propanol) and alcohols containing branched chains (2-propanol) on the decrease in T_g of PLA became smaller. 1-butanol was not as soluble as the shorter chain alcohols (e.g., methanol), so only 100% v/v of 1-butanol could be assessed. The T_g of PLA immersed in pure 1-butanol decreased approximately 20 °C compared with PLA immersed in water.

All the alcohols used in this study are on the outside of the interaction range of the HSP sphere, which means they are poor solvents for PLA. Based on the HSP, the interaction between PLA and alcohols should be relatively small. However, plasticization of PLA by the alcohols was evidenced by the reduction of PLA's T_g . Crystallinity evolution of the PLA films also inferred interactions. For pure (100% concentration) alcohol solutions, the alcohol with the total HSP closer to PLA films has a greater effect on the reduction of PLA's T_g .

Aqueous and D₂O solutions have similar effects on T_g changes, indicating that it is feasible to use D₂O instead of water to measure sorption results of ethanol and D₂O by ¹H-qNMR, in case that water interferes with the experimental results, and hinders the quantification of water and alcohol sorption in PLA.

During the second phase of this study, the amount of ethanol sorbed into the PLA film was investigated by ¹H-qNMR experiments. The sorption amount of ethanol in PLA within the immersion time of 0 h to 144 h at 25 °C was measured. When the immersion time reaches 4 h, the PLA sample has the largest sorption amount of ethanol, which was

about 9.16% (g-ethanol/g-PLA \times 100%), which was slightly higher than the estimated value of 5.63% (g-ethanol/g-PLA \times 100%) by the Fox equation (Eq. 3.10).

In the final phase, the X_c of PLA immersed in pure ethanol during different immersion time at 25 °C was measured by DSC. The results showed that in the first 12 h, the change in X_c was small (< 3%). As the immersion time increased, the X_c of the PLA film increased. When the immersion time reaches 24 h, the X_c exceeded 20%. Since the amorphous region in the film decreased, sorption amount of ethanol decreased. After 48 h of immersion, the X_c was stabilized at around 30%, and the ethanol sorption amount was also stabilized at about 5%.

The water and D₂O sorption of PLA at 25 °C were measured. It was found that in the same %RH, PLA could absorb more D₂O than water.

5.2 Future work

This study provided experimental insights on the interaction of PLA films when it was submerged with organic solvents, specifically alcoholic-aqueous and alcoholic-D₂O solutions. Future work should focus on further understanding the interaction relationship between water, alcohols and PLA. The HSP radius of amorphous PLA as used in this work should be tested experimentally to improve the evaluation for the solubility of PLA film in alcohol-aqueous solution. Also, the sorption amount of other organic solvent (such as methanol, 1-propanol, 2-propanol, etc.) and alcohol-aqueous solutions with different concentrations (volume ratio between alcohol and water) should be investigated by qNMR to understand the effect of different alcohols to PLA matrix. Still, the impact of the alcohol concentrations and the resulting thermo-mechanical properties need much further research.

REFERENCES

REFERENCES

- [1] Sonchaeng U., Auras R., Selke S., *et al.*, *In-situ* changes of thermo-mechanical properties of poly (lactic acid) film immersed in alcohol solutions, *Polymer Testing.*, vol. 82, 2020, doi: 10.1016/j.polymertesting.2019.106320.